8-26-2014 12:00 AM

The Effects of RHAMM on Cell Division, Cell Motility, and Tumorigenesis

Sallie Elhayek, *The University of Western Ontario*

Supervisor: Dr. Eva Turley, *The University of Western Ontario*

A thesis submitted in partial fulfillment of the requirements for the Master of Science degree in Biochemistry

THE EFFECTS OF RHAMM ON CELL DIVISION, CELL MOTILITY, AND TUMORIGENESIS

(Thesis format: Monograph)

by

Sallie Elhayek

Graduate Program in Biochemistry

A thesis submitted in partial fulfillment
of the requirements for the degree of
Master of Science

The School of Graduate and Postdoctoral Studies
The University of Western Ontario
London, Ontario, Canada

Abstract

Overexpression of a RHAMM isoform (RHAMM$^{\Delta 163}$) transforms fibroblasts but the mechanisms underlying this oncogenic function are not well understood. RHAMM$^{\Delta 163}$ binds to the mitotic spindle and centrosomes via a C-terminal leucine zipper; these interactions are predicted to regulate genomic stability and cell polarity and proposed to account for the oncogenic function of RHAMM$^{\Delta 163}$. We hypothesized that RHAMM leucine zipper maintains mitotic spindle integrity and impacts directional cell migration through its interactions with microtubule and centrosome structures. The consequences of a mutated leucine zipper on cell division, cell motility, and tumorigenesis were assessed. Although mutant RHAMM$^{\Delta 163}$ promoted polycentrosomy, it did not alter cell cycle progression and did not strongly affect proliferation or tumorigenesis. However, loss of the leucine zipper function blocked directional movement of fibroblasts without affecting rate of motility. These results suggest that the RHAMM leucine zipper selectively regulates directed migration, which is a centrosome function that contributes to tumorigenesis.

Keywords

RHAMM, leucine zipper, mitosis, microtubules, cell division, centrosomes, cell migration

"You have brains in your head. You have feet in your shoes. You can steer yourself any direction you choose. You're on your own. And you know what you know. And you are the one who'll decide where to go."

-Dr. Seuss

To my loving parents and sisters

Acknowledgments

I want to start by thanking my supervisor, Dr. Eva Turley, for giving me the opportunity to explore my research interests. I have gained valuable experience under your supervision and I thank you for your expertise throughout my time as a graduate student.

Furthermore, I would like to thank my advisory committee, Dr. Eric Ball and Dr. Moshmi Bhattacharya. Thank you both for your invaluable guidance and constructive criticism throughout the duration of my project.

To past and present student members of the Turley lab: Tahereh, Siddika, Sean, Colleen, Steven, Justin, Michal, Aman, Linley, Marie, Cherie, and Mohammad, each one of you has made my time in the lab a memorable one. Thanks for the many laughs, great friendships, and for making it a great environment to work in. To Siddika and Colleen especially, you've both put up with me from day one and I thank you both for your friendship and for making my time at LRCP enjoyable. Colleen, I'll only admit it here that I'll miss you.

To Dr. Patrick Telmer, whose guidance, patience, and support from my undergraduate days have helped shape my understanding of this project and of RHAMM; thank you for answering and putting up with my numerous questions. To Dr. Conny Toelg, thank you for sharing your wealth of knowledge and offering great scientific advice. To Jenny Ma, the (best) lab mom, thank you for caring and supporting me in the completion of this project, I will miss you greatly. To Dr. Vincent Morris, thank you for your assistance in operating the microscope and considerable advice about science and life in general, the Turley lab is lucky to have you around. To Dr. Caitlin Symonette, thank you for encouraging me to keep on "sciencing" and to keep on writing, glad we're at the finish line together. To Pauline Kovacs,

I am thankful for your friendship and support during my time at LRCP and I hope to stay in touch with you wherever life may take me.

On a personal note, I would not be where I am today if it weren't for the love and unconditional support of my family. To my dad, thank you for always pushing me to work hard and to try my best and most of all, thank you for believing in me. To my mom, you have been my rock throughout this entire journey and your support has meant more to me than I could put into words, thank you for being the greatest mom and best friend. To my sisters, thank you for welcoming my rants about lab life over the past couple of years with open arms. I would have no doubt gone crazy if I didn't have you guys by my side to uplift me when I was feeling down and to constantly remind me that laughter is the best medicine. You all are the absolute best sisters and friends anyone could ask for. To Mai particularly, for giving me rides to the lab, whether it was late at night or on weekends or even during snowstorms, just to check up on my cells. We—the cells and I—much appreciated it!

Table of Contents

List of Tables

List of Figures

List of Appendices

List of Abbreviations

ABTS: 2,2'-azino-bis(3-ethylbenzothiazoline-6-sulphonic acid)

ATCC: American Type Culture Collection

aurA/AURKA: Aurora kinase A

BARD1: BRCA1 associated ring domain 1

BRCA1: Breast cancer 1, early onset

C-terminal: Carboxy terminal

CD44: Cluster of differentiation 44

cDNA: Complementary DNA

CMV: Cytomegalovirus

DAPI: 4',6-diamidino-2-phenylindole

DMEM: Dulbecco's Modified Eagle Medium

DNA: Deoxyribonucleic acid

DNase: Deoxyribonuclease

ECL: Enhanced chemiluminescence

ECM: Extracellular matrix

EDTA: Ethylenediaminetetraacetic acid

ELISA: Enzyme-linked immunosorbent assay

ER: Endoplasmic reticulum

ERK1,2: Extracellular signal-regulated kinase 1,2

FACs: Fluorescence-activated cell sorting

FAK: Focal adhesion kinase

FBS: Fetal bovine serum

FSC: Forward side scatter

FW: Forward

G418: Geneticin

GFP: Green fluorescent protein

HA: Hyaluronic acid/Hyaluronan

HAS: Hyaluronan synthase

HCC: Hepatocellular carcinoma

HFF: Human foreskin fibroblasts

HRP: Horseradish peroxidase

HYAL: Hyaluronidase

IgG: Immunoglobulin G

kDa: Kilodalton

Klp2: Kinesin like protein 2

KO: Knockout (Rhamm)

MAPs: Microtubule associated proteins

MAPKs: Mitogen activated protein kinases

MEF(s): Mouse embryonic fibroblasts

MEK: MAP/ERK kinase

MTOC: Microtubule organizing center

N-terminal: Amino terminal

Neo: Neomycin

NOD-SCID: Nonobese/diabetic severe combined immunodeficiency

NSG: NOD scid gamma

p53: Tumor protein p53

PBS: Phosphate buffered saline

PCM: Pericentriolar material

PCR: Polymerase chain reaction

PDVF: Polyvinylidene difluoride

PEG: Polyethylene glycol

PFA: Paraformaldehyde

PI: Propidium iodide

Rb: Retinoblastoma protein

qRT-PCR: Quantitative real-time polymerase chain reaction

RHAMM: Receptor for hyaluronan-mediated motility

$RHAMM^{FL}$: Full length receptor for hyaluronan-mediated motility

$RHAMM^{\Delta 163}$: Oncogenic receptor for hyaluronan-mediated motility lacking the first 163 amino acids

RIPA: Radioimmunoprecipitation assay buffer

RNA: Ribonucleic acid

RNase A: Ribonuclease A

ROS: Reactive oxygen species

RV: Reverse

SAC: Spindle assembly checkpoint

SDS-PAGE: Sodium dodecyl sulfate polyacrylamide gel electrophoresis

SDS: Sodium dodecyl sulfate

SE: Standard error

SMCs: Smooth muscle cells

SSC: Side scatter

TBS-T: Tris-buffered saline with Tween 20

TC: Tissue culture

TME: Tumor microenvironment

TPX2: Targeting protein for XKlp2

XKlp2: *Xenopus laevis* Kinesin like protein 2

Chapter 1

1 Introduction

Constant cell turnover is required for the maintenance of cellular homeostasis and requires a delicate balance between mitogenic growth signals that regulate cell proliferation and anti-proliferative signals that help mediate cell death (1, 2). Proto-oncogenes and tumor suppressors, in part, maintain this regulation. Whereas proto-oncogenes, like Ras and c-Src, are essential for proper cell growth, proliferation, migration and differentiation, tumor suppressors, such as the retinoblastoma protein, Rb, and the transcription factor, p53, repress the cell cycle and promote cellular apoptosis to prevent aberrant cell growth (3). Mutations in these regulatory pathways that disrupt homeostasis, not surprisingly, result in the progression of diseases such as cancer. Cells ignore regulatory cues that normally inhibit cell cycle progression thereby promoting tumor growth (3). Strict regulation of the mechanisms that govern cell division must therefore be tightly regulated.

1.1 Regulation of mitotic cell division

Two main steps characterize cell division: DNA replication during interphase and then the subsequent separation of replicated chromosomes into two daughter cells during mitosis (4). Interphase is comprised up of three phases: G_1, S, and G_2, whereby a cell

prepares for DNA replication (G_1), replicates its DNA (S), and then prepares the cell to undergo mitosis (G_2) (4). DNA replication during S phase is also linked with centrosome replication to ensure that both DNA and centrosomes are only replicated once during each cycle of cell division (5). Centrosome replication involves the duplication of a pair of centrioles and their subsequent separation to spindle poles during prophase of mitosis. Centrioles are linked together through an amorphous mass of coiled coil proteins called the pericentriolar material (PCM) (5). These proteins are recruited to the spindle poles via motor proteins to help carry out centrosome function (6-8). Centrosomes make up the microtubule-organizing center (MTOC) in mammalian cells and function as a major site for microtubule nucleation (7). They also influence a number of cellular functions such as cell polarity and migration, establishment of a bipolar mitotic spindle, and thus proper cell division (9).

Following DNA and centrosome replication, a cell is ready to undergo mitosis. Mitosis is a very brief, yet highly complex and tightly regulated stage of the cell cycle. Mitotic cell division, which is described as the division of the parent cell into two genetically identical daughter cells, occurs in eukaryotic tissues and is critical for development and in maintaining tissue homeostasis (10). The mitotic phase is characterized by five consecutive stages including: prophase, metaphase, anaphase, telophase, and cytokinesis. During this process, centrosomes migrate to opposite poles of the cell and signaling events promote microtubule nucleation from several sources, predominately the MTOC, but also from chromosomes (11). The microtubule network then organizes itself to form a bipolar mitotic spindle. Microtubules emanating from centrosomes in the MTOC attach to protein structures, referred to as kinetochores, on the chromosomes, which then aligns

the chromosomes midway between the two poles and aids in the separation of the sister chromatids to each spindle pole of the developing daughter cell (12, 13).

The mitotic spindle machinery is comprised of microtubules, centrosomes, chromosomes, molecular motors, microtubule-associated proteins, and numerous spindle assembly protein factors that ensure spatial-temporal spindle formation (13).

Amongst other factors, Ran GTPase plays a pivotal role in mitotic spindle formation by creating a Ran-GTP gradient around chromosomes (14, 15). Once a gradient has been established, proteins that promote microtubule nucleation and stability are activated. One target of Ran-GTP is TPX2 (targeting protein for Xklp2), a spindle assembly protein factor that upon activation is released from inhibition by importin-α and initiates microtubule nucleation and activation of downstream targets like Aurora kinase A (AURKA) (16). AURKA is a mitotic serine/threonine kinase that is predominantly activated by TPX2 and whose role is to phosphorylate key proteins to facilitate in the organization of a bipolar spindle (17). Not surprisingly, inhibition of Ran activity results in aberrant mitotic spindles and chromosomal abnormalities (18). Furthermore, molecular motors like dynein, walk along microtubules and carry spindle-associated proteins to their minus ends to ensure proper formation, function and integrity of the mitotic spindle (19). One example of a spindle-associated protein is the receptor for hyaluronan-mediated motility, RHAMM. RHAMM associates with dynein at the spindle poles and it functions to ensure the formation of a bipolar spindle (19). The mechanism by which RHAMM regulates mitotic spindle assembly is not fully understood, however, its genetic deletion results in mitotic defects characterized by multipolar mitotic spindles (20).

Cells employ additional checkpoint mechanisms during spindle assembly to monitor and regulate proper spindle formation. Assembly of the mitotic spindle is controlled by two linked checkpoints: the kinetochore attachment checkpoint and the spindle assembly checkpoint (SAC). The kinetochore attachment checkpoint ensures that all chromosomes are stably attached by their kinetochores to mitotic spindle microtubules from either spindle pole (21). The cell then relays the status of the kinetochore-microtubule attachment to the SAC. If all chromosomes are attached properly to the spindle poles, chromosome segregation commences. If, however, chromosomes are not attached properly, it signals the intact SAC to halt the cell cycle and delay anaphase until all chromosome kinetochores are properly attached to the microtubule spindles (22). Failure to attach can lead to chromosomal missegregation and thus this regulatory mechanism is essential in maintaining genomic stability within a cell. When proteins that regulate the SAC become mutated, the fidelity of chromosome segregation becomes compromised as the SAC becomes defective and cells ignore the checkpoint and continue cell division (22, 23). Segregation defects can result in a gain or loss of part or whole chromosomes leading to chromosomal instability, which is a major driving force in cancer progression(10). Changes to chromosome number can result in a state of aneuploidy and changes to chromosome structure can lead to loss or translocation of critical genomic DNA, both contributing to genomic instability, which then has the potential to drive these premalignant cells cancerous (22).

1.2 Cancer Development

Cancer development is a complex, multi-step process that arises as a result of multiple genetic alterations that drive the transformation of normal cells to malignant cancer cells. During cancer initiation, oncogenes become hyperactivated and acquire gain-of-function mutations, whereas mutations in tumor suppressors accumulate and cause their loss-of-function (24, 25). These mutations give rise to numerous types of human cancers all governed by disruption of a subset of key cellular processes. Hanahan and Weinberg (26) identified several key hallmarks of cancer that promote a cell's progression from a normal state to a malignant transformed phenotype. Based on this, a cancer cell must initially acquire the ability to autonomously grow, resist anti-growth cues, and ignore signals for programmed cell death (26).

Cells normally require mitogenic factors that bind to their respective receptors and stimulate a signaling cascade to promote cell proliferation. Conversely, transforming cells do not rely on exogenous growth signals to propagate, but rather have the ability to synthesize their own mitogenic factors to sustain their proliferation(26). Furthermore, these cells overexpress cell surface receptors that become overly responsive to growth factors and this results in a deregulation of downstream signaling pathways, such as that of the mitogenic Ras-Raf-MAP kinase cascade(26). Cancer cells may acquire mutations that induce constitutive expression of the Ras oncogene and enables them to bypass signaling through their upstream receptors (27).

Tumor cell proliferation is often linked with resistance to anti-growth signals that is otherwise associated with normal cells. Normal cells receive cues from their environment to halt the cell cycle and enter a state of quiescence in G_0 or enter into a post-mitotic state in order to maintain homeostasis (26). This regulation is achieved through tumor suppressors such as Rb and p53 (26, 28, 29). Rb helps to regulate cell cycle progression and apoptosis by controlling the function of E2F transcription factors and thus the progression from G1 to S phase of the cell cycle (30). p53 is essential during the DNA damage response in cells and arrests the cell cycle or initiates apoptosis if the damage cannot be repaired (28). When mutated or inactivated, these tumor suppressors lose their function and cells are not able to respond to anti-growth signals, thus promoting tumorigenesis.

Not only do cancer cells resist anti-growth cues, but also become insensitive to signals promoting programmed cell death, which in turn disrupt cell homeostasis. Signals that typically activate the apoptotic machinery include defects in cell division, either DNA replication or during mitosis as well as cellular stresses arising from DNA damage, accumulation of ROS species, or hypoxia (26). Conversely, cancer cells acquire mechanisms to evade apoptosis by up-regulation of anti-apoptotic factors, such as Bcl-2, or by inactivation of the tumor suppressor p53 (26, 31). This attribute allows cancer cells to thrive and become resistant to cancer therapies (26).

While these hallmarks are all critical for the primary transformation of normal cells into malignant phenotypes, arguably the deadliest characteristic of cancer cells, which accounts for more than half of cancer related deaths (32), is their ability to metastasize to distant tissues and form secondary lesions. In order to metastasize, cancer cells acquire

increased migration and invasion abilities. Therefore, the events regulating cell migration and invasion must be finely tuned to prevent triggering a cell's metastatic potential.

1.3 Cell Migration

Cell migration is essential during many cellular processes including embryogenesis, tissue regeneration, wound healing, and immune surveillance (33, 34). Migratory events are generally tightly regulated and when they are perturbed can play a causative role in numerous diseases such as chronic inflammation, autoimmune diseases, and tumor progression and metastasis (35-37).

Several biochemical pathways are involved in the initiation of cell migration and are predominantly regulated by the Rho family GTPases, including Rac1, Cdc42, and RhoA (34, 36). The Rho family of GTPases is a subset of the Ras superfamily and these proteins play a vital role in cell migration by regulating the actin network, microtubule dynamics, and several signal transduction pathways (33, 35, 38, 39). They function as molecular switches cycling between an inactive GDP-bound form, where they reside in the cytosol, and upon activation to their GTP-form they translocate to specific membranes or the actin cytoskeleton where they interact with target proteins and generate a downstream signal (33, 34).

During cell migration, specific Rho family GTPases, Cdc42 and Rac1, interact with their targets and first polarize the cell and orient it towards the migration front end (34). Activated Cdc42 and Rac1 stimulate actin polymerization to form finger-like projections

or protrusions, filopodia and lamellipodia, respectively, at the leading edge which are used to establish stable adhesions to the substratum (33-35). To initiate cell migration, RhoA regulates the assembly of actin and myosin bundles, which facilitate the contraction of the cell body and the rear end of a cell to detach rear adhesions and translocate toward the leading edge (40). Migratory events require adhesion sites at the leading and rear end of the cell to alternatively assemble and disassemble via actin reorganization in a spatiotemporal manner to propel a migratory cell forward (33-35).

The role of microtubules during cell motility is not well established, but a dynamic microtubule network is required (40). Microtubules are present in both the leading and trailing edges, but are more dynamic at their tails. Inhibition of microtubule dynamics blocks cell migration due to an inability of cells to retract their trailing edges (40). Loss of the microtubule network via treatment of cells with high concentrations of nocodazole inhibits directional cell migration and as a result cells move more randomly (40).

Directed cell migration depends on the polarization of microtubules and the reorientation of the MTOC towards the direction of migration. During migration, microtubules function as tracks for motor proteins to transport cellular cargo towards the leading edge and for regulating cell polarity and shape (41). Microtubule minus ends emanate from the MTOC, where they are nucleated from and are dynamically unstable at their plus ends. Stabilization of the plus ends during cell migration enables the MTOC to reorient itself towards the direction of migration at the leading edge (33, 41). The major component of the MTOC is the centrosome and centrosomes are known to play an integral role in cell polarization as its damage/loss disrupts directed motility (42). Regulation of these pathways are dependent on Rho GTPases, particularly Cdc42, which acts through its

effectors to control the position of the nucleus relative to the MTOC and also plays a role in microtubule orientation (34, 38).

De-regulation of migratory pathways is seen in a number of metastatic cancers. Cell migration of cancer cells is augmented via communication between the cell and its local microenvironment, which constitutes the extracellular matrix (ECM) and other cells such as stromal cells, fibroblasts, and immune cells (39, 41, 42). These cells begin to overexpress growth factors and chemokines, which bind to cancer cell receptors and elicit pro-migratory pathways (43, 44). An enhanced migratory ability allows cancer cells to invade into the ECM and local microenvironment and travel on ECM fibers to blood vessels. Carcinoma cells then intravasate into the blood stream where they travel via the vasculature to distant sites, extravasate and form secondary tumors (43).

1.4 Extracellular Matrix

The ECM is an intricate network of macromolecules that provides structural and functional support to the surrounding cells within a tissue (38, 45). Cells interact with the ECM through the integrin family of transmembrane receptors as well as other cell surface receptors, such as RHAMM (46-48). The attachment of these cell receptors to the ECM elicit a variety of biochemical signal transduction pathways that in turn regulate numerous cellular functions including, cell growth, migration, differentiation, and maintaining tissue homeostasis (47). Abnormalities in ECM proteins are seen in a wide variety of human diseases (49). In particular, aberrations in ECM components give

cancer cells the ability to promote tumor proliferation, migration and invasion. As well, deregulation of the ECM components impacts the surrounding cells in the local microenvironment, including stromal cells, immune cells, and fibroblasts, and together help promote disease progression (48, 50, 51). Therefore, understanding the role of ECM proteins and how they affect signaling pathways can provide insight into how cancer is initiated.

Two main classes of macromolecules make up the ECM: fibrous proteins and glycosaminoglycans (GAG). Fibrous proteins present in the ECM include collagen, fibronectin, and elastin, just to name a few, and they help to maintain the ECM's structure by providing tensile strength, protecting against stretches in the tissue, and in mediating cell adhesion to the ECM (45). Conversely, GAGs are large, extremely hydrophilic polysaccharides and their ability to form hydrogels serves an essential role in resisting compressive forces (45). GAGs have a wide variety of other functions that are molecule and tissue-specific.

1.4.1 Hyaluronan

One GAG of interest, hyaluronic acid/hyaluronan (HA), is found widely distributed throughout the ECM of all vertebrates. Its negative charge at neutral pH and hydrophilic nature attracts water molecules within the ECM, giving it an essential lubrication and hydration function(52). HA is a high molecular weight GAG with an average molecular

mass of $4x10^6$ Da and it is composed of alternating disaccharide units of D-glucuronic acid and D-N-acetylglucosamine (53, 54).

Hyaluronan is synthesized by hyaluronan synthases (HASes), of which there are three conserved genes—*HAS1*, *HAS2*, *HAS3*—each with a unique spatial and temporal expression pattern (52). During embryonic development, HAS2 synthesizes the majority of hyaluronan present (52) and its expression is also unregulated during tumor progression in a number of cancers, including breast cancer, mesothelioma, and colon cancer (52, 55-57).

Conversely, hyaluronan is degraded by a number of hyaluronidases (HYALs), with the two most prominent HYALs being HYAL1 and HYAL2. Aberrant expression of either has been seen in invasive ductal carcinoma (52, 58, 59).

Hyaluronan also functions as a signaling molecule in a number of cellular processes including cell migration, proliferation, and during wound healing (52). In particular, HA synthesis is consistently and transiently increased immediately after tissue injury and in sites of rapid tissue turnover, including embryogenesis, inflammation, and neoplasia (52). The vast functions of HA are dependent on its molecular weight (48)—degradation of HA gives rise to bioactive molecules that function differently than full-length forms. For example, full-length hyaluronan is antiangiogenic and immunosuppressive, whereas hyaluronan fragments promote angiogenesis and inflammation (48, 60-62).

HA mediates its effects through interactions with a class of proteins referred to as the hyaladherins. This class of hyaluronan-binding proteins differs in their cellular distribution, either within subcellular compartments or on the cell surface, and the

sequences by which they interact with HA and thus the effects they exert are hyaladherin-specific (63). One hyaladherin of interest is RHAMM, which interacts with HA both intracellularly and at the cell surface and their interactions regulate a number of cellular functions including cell proliferation and cell migration (64, 65).

1.5 RHAMM structure and function

RHAMM was first isolated and purified from subconfluent migrating cardiac fibroblasts as a cell surface hyaluronan binding protein (66, 67). It is largely an acidic coiled-coil protein with a basic amino-terminal globular head (68, 69). RHAMM binds to hyaluronan via two carboxyl terminal coiled domains that are rich in basic amino acids and are commonly referred to as $B(X)_7B$ motifs (70, 71). This region partially overlaps with one of two microtubule-binding sites of RHAMM—an N-terminal sequence for associating with interphase microtubules and a C-terminal binding region for interacting with mitotic spindle microtubules, the latter of which overlaps with the HA binding site (20, 69). RHAMM also contains a highly conserved D-docking site common to many ERK binding substrates (Figure 1.1B) (20).

RHAMM protein contains a number of leucine zipper domains and along with its coiled coil structure predicts that it can form homodimers or heterodimers with its binding partners (71, 72). One particular leucine zipper domain of interest is located within the C-terminal microtubule-binding region and this sequence presumably functions in and regulates RHAMM and mitotic spindle interactions/integrity (Figure 1.1C) (19, 20, 73).

RHAMM protein is found in many species and is predominantly studied in humans, mice, and *Xenopus laevis*, where the protein sequences are most homologous at their N- and C-termini (74). The RHAMM gene is comprised of 18 exons and is located on chromosome 5 in humans; its mRNA transcript encodes an 84-kDa protein (Figure 1.1 A) (75). In mice, the RHAMM gene is localized to chromosome 11 and its mRNA transcript encodes a 95-kDa protein. Furthermore, the RHAMM gene in *Xenopus* encodes a 150-kDa protein and it is 45% and 65% identical to human and mouse RHAMM, respectively (74).

RHAMM expression is tightly regulated and is absent or present at low levels in most homeostatic human tissues. Protein and mRNA levels of RHAMM, however, are transiently and strongly up-regulated during tissue repair (64, 76). Surprisingly, genetic deletion of RHAMM in mice displays no visible defects during embryonic development, albeit with slow healing of skin wounds, owing to its essential role during wound repair (64).

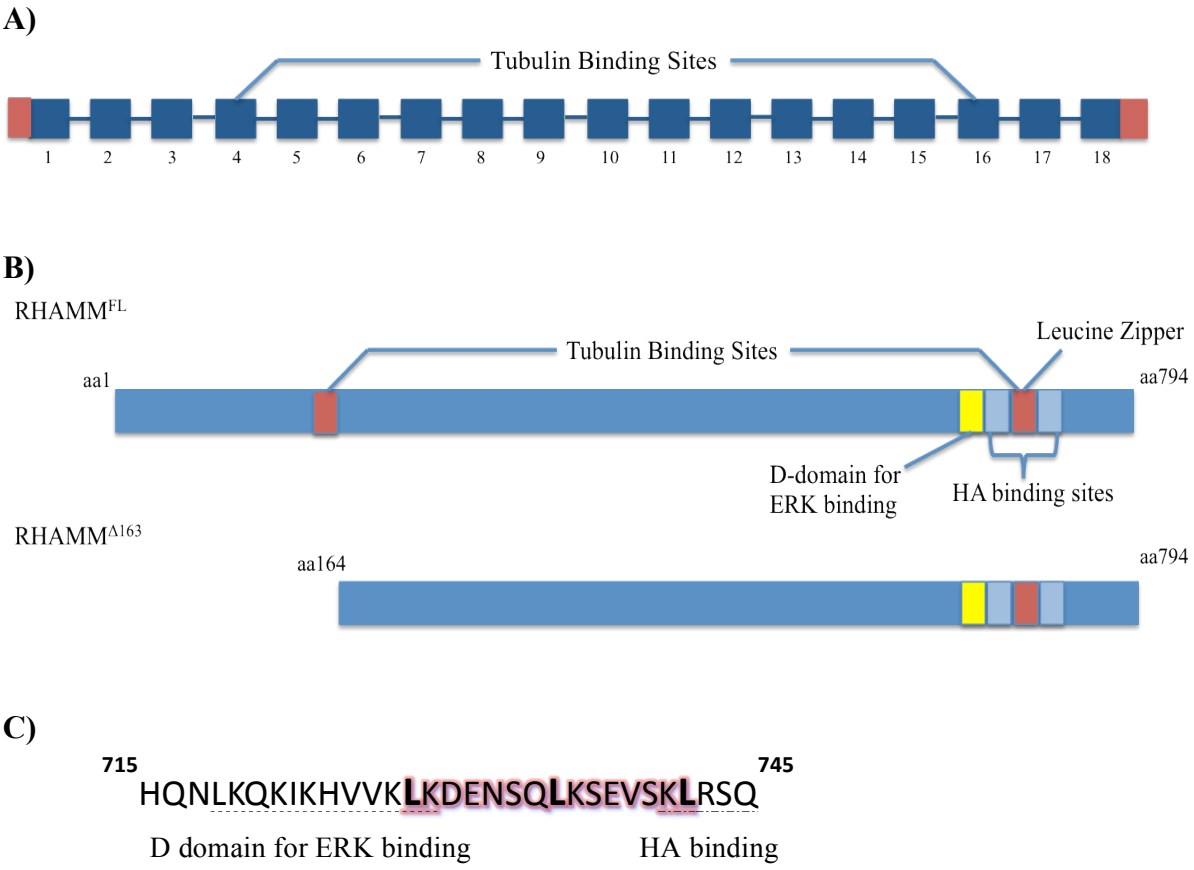

Figure 1.1 Schematic Representation of RHAMM

A) The RHAMM gene is comprised of 18 exons. Exons 4 and 16 contain tubulin-binding sequences, for binding to interphase and mitotic spindle microtubules, respectively. **B)** Full-length RHAMM encodes a 794 amino acid protein sequence. RHAMM^{FL} contains two tubulin-binding sites, at the N-terminus and C-terminus. The C-terminal end of RHAMM contains HA and ERK binding sites that overlap with the leucine zipper motif. RHAMM$^{\Delta 163}$ is an oncogenic isoform and only contains the C-terminal tubulin binding sequence. **C)** Amino acid sequence of a C-terminal RHAMM fragment containing the leucine zipper motif (highlighted in pink) with overlapping HA and ERK binding sites

Furthermore, elevated RHAMM expression is associated with several pathologies, including arthritis, diabetes, and several human cancers (77-81).

RHAMM is present in many cell types, including: fibroblasts, smooth muscle cells, immune cells, and endothelial cells, just to name a few (20, 82-84).

It is a multifunctional protein with extracellular and intracellular functions that affects cell motility/invasion and mitotic spindle integrity/genomic stability, respectively. RHAMM is part of a heterogeneous group of cell surface proteins that lack an N-terminal signal peptide and is therefore not exported through the classic Golgi/ER route (85). This class of proteins is nonetheless released to the extracellular compartment via poorly characterized unconventional export mechanisms and in response to specific stimuli (85). For example, during cell transformation in multiple myeloma and in highly invasive breast cancer cell lines, the putative oncogene RHAMM is unconventionally exported to the cell surface, where it contributes to tumor formation (85, 86). Other stimuli that induce RHAMM export include cell stress, during cell transformation or wounding (87). Extracellular RHAMM is not integrated into the plasma membrane by membrane spanning sequence or by GPI tail. At the cell surface, it functions as a co-receptor, binding hyaluronan and a number of tyrosine and non-tyrosine kinase receptors, including PDGFR, RON, CD44, and TGFβR (48, 76, 88-90).

RHAMM binding to CD44 and HA promotes cell migration through activation of the ERK1,2 MAP kinase pathway (64). RHAMM also interacts with and mediates activation of Src and focal adhesion kinase (FAK) and these interactions are essential for focal adhesion turnover during cell motility (65). Furthermore, extracellular RHAMM

regulates cell cycle progression; blocking cell surface RHAMM results in a slower progression of cells through G2/M, a stage in the cell cycle where RHAMM mRNA is up-regulated (91).

In addition to its localization on the cell surface, RHAMM is also present in several subcellular compartments, where it plays a prominent role in cell proliferation events. RHAMM localizes to the cell nucleus, on interphase microtubules, centrosomes, podosomes, and on mitotic spindle microtubules (20, 69, 72, 85). Furthermore, intracellular RHAMM interacts with MEK1/ERK1,2 complexes and targets them to microtubules, where they control the stability of interphase and mitotic spindle microtubules (20), and to the cell nucleus (20, 76), where they play a role in regulating mitotic spindle integrity, cell cycle progression, cell proliferation, and likely centrosome function (19, 20, 81). Deregulation of these functions not only result in defected mitotic spindle assembly, but also disrupt centrosome structure (19, 81, 85). RHAMM-regulated ERK activity is required for maintaining a bipolar mitotic spindle and defects due to RHAMM loss can be rescued by mutant active MEK1 (20). The complete mechanisms by which intracellular RHAMM carries out these functions are still being characterized.

The complex subcompartmentalization of RHAMM is not well understood, but is likely attributed to specific targeting of isoforms within the cell. Several isoforms of RHAMM exist in cell lines, some of which are generated via alternative mRNA splicing and others are through alternative start codons resulting in N-terminal truncated isoforms (72, 92). Full-length RHAMM most often localizes to microtubules, whereas targeting of RHAMM to the nucleus requires either N-terminal truncations or alternative splicing (69, 93). The N-terminal truncated forms of RHAMM appear typically after cells are plated in

culture as well as following tissue injury (94). One isoform, termed RHAMM$^{\Delta 163}$, is an N-terminal truncation of the full-length protein and represents the oncogenic form of RHAMM found in many human cancers (95). In experimental models, overexpression of RHAMM$^{\Delta 163}$ transforms 10T1/2 and 3T3 mesenchymal cell lines, which form metastatic tumors in NOD/SCID xenograft mouse models (95). The mechanisms by which RHAMM mediates MEF transformation, however, have not been fully elucidated. Aberrant RHAMM regulation of mitotic spindle integrity has been predicted to contribute to tumor progression by promoting genomic instability, but neither an effect on genomic stability or if this is relevant to progression has been directly demonstrated (73, 78). Thus an understanding of how RHAMM is involved in the regulation of microtubule and centrosome structures/function can help us better understand the oncogenic roles of RHAMM$^{\Delta 163}$.

1.6 The role of RHAMM in mitosis

1.6.1 The role of RHAMM in microtubule and mitotic spindle regulation

The microtubule network is composed of polymers of α- and β-tubulin heterodimers that make up one constituent of the structurally important cytoskeleton. A dynamic microtubule network with rapid turnover is necessary for cellular events such as formation of the mitotic spindle during mitosis. Microtubule stability is regulated in part

by a group of microtubule-associated proteins (MAPs), including RHAMM, that bind to tubulin and either directly or indirectly contribute to its polymerization and stability by decreasing disassembly rate (10, 41).

Many proteins make up the microtubule-associated proteome (MTAP) and RHAMM is one known component (96). Its functions during mitosis are dependent on its interactions with and regulation of microtubules. Full length RHAMM consists of two conserved microtubule-binding sequences, one located in exon 4 and the other in exon 16 (Figure 1.1A), for binding to interphase and mitotic spindle microtubules, respectively, and these interactions are seen in numerous cell backgrounds (20, 69, 81).

The N-terminal microtubule binding sequence of RHAMM located in exon 4 is essential for binding to interphase microtubules and deletion of this region results in a loss of RHAMM localization from interphase microtubules and rather a diffuse distribution throughout the cytoplasm, as well as in the cell nucleus (19, 69).

Furthermore, RHAMM is localized to microtubules throughout the mitotic phases of the cell cycle. During prophase, in both adherent, (HeLa cells), and suspension cell lines, (RPMI 8226 and Raji cells) RHAMM is found distributed at the center of microtubule asters emanating from the centrosphere (81).

In prometaphase and metaphase, intracellular RHAMM localizes to mitotic spindle poles and along the length of microtubules through a carboxyl terminal region (19). Additionally, throughout anaphase and telophase, RHAMM is localized at the midbody and microtubule spindles at the midzone, respectively, where it functions during cytokinesis (19). Genetic deletion of RHAMM in fibroblasts results in aberrant

chromosome alignment/segregation and inappropriate cell division during mitosis, giving rise to multinucleated cells(20). Consistent with its role during cytokinesis, RHAMM has been shown to interact with supervillin—a gelsolin family member of proteins that functions in mysoin II mediated contractility during the early stages of cytokinesis (97-99).

Although RHAMM functions throughout the stages of mitosis, it has largely been studied for its role in organizing and maintaining mitotic spindle integrity. During cell division, the formation of a bipolar mitotic spindle ensures fidelity of chromosome segregation and maintains genomic stability (20). Forced high expression or genetic deletion of RHAMM results in multi-pole mitotic spindles (19, 20, 73, 74), the former of which has been linked to genomic instability in multiple myeloma(81). Consistent with these data, siRNA knockdown of RHAMM in neointimal smooth muscle cells (SMCs) and HeLa cells resulted in multipolar spindles and disorganized spindles, further confirming RHAMM's role in spindle assembly (84, 100). siRNA knockdown of RHAMM in HeLa cells also resulted in a delay in spindle assembly and a delay in the time required to complete mitosis, suggesting a role for RHAMM in microtubule nucleation (100). These defects can collectively be rescued by re-expression of RHAMM confirming the aberrations to be a particular result of the loss of RHAMM (19, 20, 73, 74, 100). Levels of RHAMM must thus be tightly regulated as an abundance or loss results in aberrant mitosis.

Although the mechanism by which RHAMM regulates mitotic spindle integrity is not well established, previous work has highlighted an important role for the highly conserved leucine zipper located in exon 16 (19, 20, 73) in mediating RHAMM/mitotic spindle interactions (Figure 1.1C). Previous mutational analysis of the leucine zipper

motif demonstrated an essential role for it in maintaining spindle pole organization and recruitment of key spindle protein factors (73, 100). Tubulin binding assays also confirmed that RHAMM binds to tubulin heterodimers via its C-terminal domain and this interaction can be abolished by a synthetic peptide containing the leucine zipper (20). Furthermore, in *Xenopus*, binding of RHAMM to tubulin is essential for Ran-driven, chromatin-induced (noncentrosomal) spindle assembly (73, 74) and depletion of RHAMM results in defects in microtubule assembly (74). The latter two studies thus suggest that tubulin and mitotic spindle binding regions of RHAMM overlap, though direct analysis of this has not been previously published.

The C-terminal leucine zipper motif of RHAMM partially overlaps with the hyaluronan and ERK1 binding sites (Figure 1.1C). It is therefore not surprising that RHAMM's role in mitotic spindle integrity is in part attributed to RHAMM's interactions with HA and MEK1/ERK1, 2 complexes.

1.6.1.1 RHAMM and HA interactions in mitosis

HA binds to intracellular RHAMM and has been shown to play a role in mitotic functions (101). During mitosis, HA synthesis is increased and is present in abundance (102), where it is found to associate with microtubules in the perinuclear area as well as more peripherally in the cytoplasm of human arterial smooth muscle cells(101). RHAMM also closely associates with microtubules and endogenous HA-positive vesicular structures;

these interactions are confirmed following uptake of fluorescein-labeled HA and excess unlabeled HA can competitively abolish the binding of HA to RHAMM (101).

HA is also found to intimately colocalize with RHAMM in and around mitotic spindle microtubules of SMCs, both endogenously and following uptake of fluorescein-HA, suggesting a role for both in the organization of astral and spindle microtubules. In later stages of mitosis, HA staining is present in abundance throughout telophase and HA is localized to the microtubules of the midbody during cytokinesis (101).

In support of RHAMM/HA interactions during mitosis, both RHAMM mRNA expression and expression of hylauronan synthases, in particular HAS2 is elevated at the G2/M boundary during cell cycle progression (67). Elevated HA synthesis during G2/M is necessary for cell rounding as a result of cytoskeletal reorganization (101). Furthermore, when HAS and RHAMM expression are inhibited, prostate cancer cell lines arrest at mitosis (103). Given that both HA and RHAMM decorate the mitotic spindle and that RHAMM and HAS mRNA are elevated at the G2/M boundary supports the hypothesis that intracellular RHAMM/HA interactions play an integral, yet unclear, role in a cell's progression through mitosis. Studies hypothesize that these interactions are essential for RHAMM's role in regulating microtubule stability and spacing within a cell (48, 101).

1.6.1.2 RHAMM-dependent ERK regulation during mitosis

ERK decorates interphase and mitotic spindle microtubules in both non-transformed and transformed cells (41, 104, 105) and has been shown to have an extensive effect on microtubule stability by regulating the ability of these proteins to control tubulin polymerization (41).

H-ras transformed cells, however, have higher levels of active ERK bound to interphase microtubules and these microtubules are less stable—indicative of constant turnover—in comparison to non-transformed fibroblasts. The effect of ERK regulation on these processes is mediated by the upstream kinases Ras-Raf-MEK (41). Inhibition of ERK-activated signaling results in increased microtubule stability, which has been shown to result in multi-pole mitotic spindles (20, 41).

RHAMM promotes interphase microtubule instability indirectly through MEK1/ERK1,2 activity (20). Overexpression of RHAMM has been shown to constitutively activate ERK and expression of a dominant negative mutant form of RHAMM blocks activation of ERK by mutant active Ras, thus providing a role of RHAMM in ERK regulation (88). Intracellular RHAMM directly binds with ERK1 through a highly conserved D-docking site, which partially overlaps with the C-terminal leucine zipper motif (20). This binding site is common to many ERK binding substrates and contains both hydrophobic and positively charged basic residues (106). Conversely, intracellular RHAMM indirectly complexes to ERK2 and MEK1, as well as ERK1,2 substrates (20). Mutations in the D-docking site of RHAMM results in a decreased binding of ERK1 *in vitro* and in cultured

cells (20). Furthermore, expressing RHAMM mutated in the D-docking site in 10T1/2 H-ras transformed fibroblasts resulted in decreased total cellular levels of phosphorylated ERK1,2 (p-ERK1,2) as well as reduced detectable p-ERK1,2 from tubulin (20). In terms of microtubule dynamics, expression of this mutant RHAMM form promoted microtubule stability (20), as evidenced by an increase in the levels of acetylated tubulin (20). Additionally, RHAMM regulation of microtubules through MAPKs appears to be important in maintaining mitotic spindle formation/integrity as mitotic spindle defects seen in RHAMM$^{-/-}$ fibroblasts are not only rescued by re-expression of RHAMM, but also to a similar extent by mutant active MEK1 (20). This proposes a model in which RHAMM functions as a scaffold protein that binds ERK1 and ERK2/MEK1 complex and recruits them to microtubules, via RHAMM's interactions with tubulin, to phosphorylate and activate other microtubule associated proteins, which then regulate microtubule dynamics/stability (Figure 1.2) (20, 107). With respect to the mitotic spindle, RHAMM controls targeting of ERK to microtubule-associated substrates and hence an absence of RHAMM would result in compromising spindle integrity, while overexpression of RHAMM could sequester ERK1, 2 from its key target substrates and result in aberrant localization/activation (107).

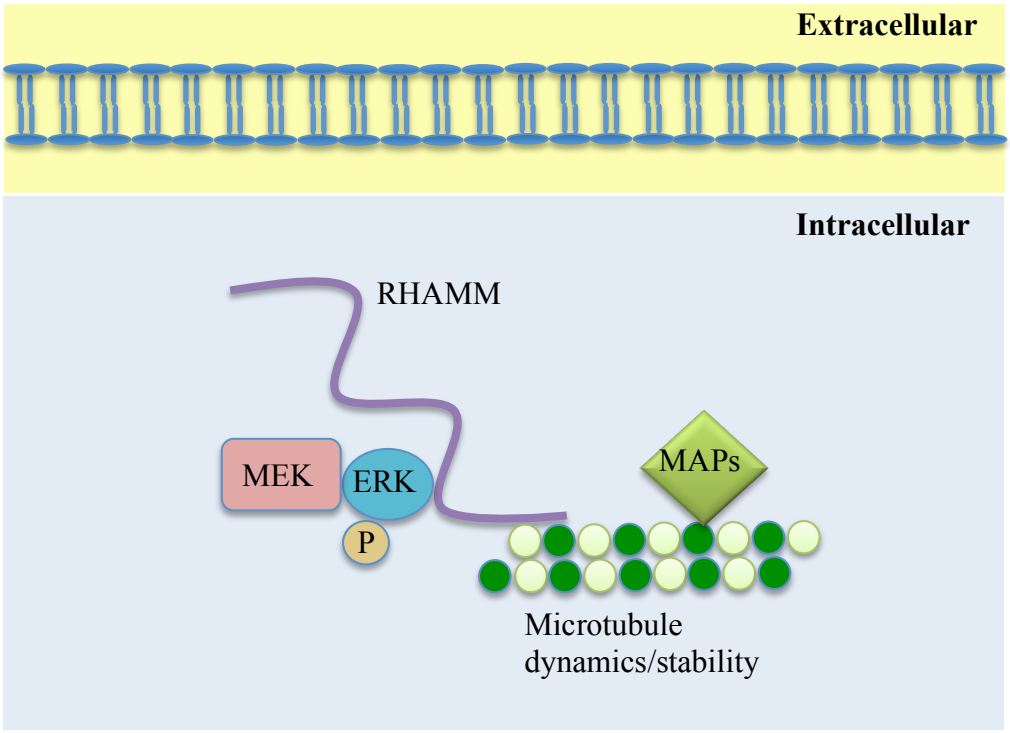

Figure 1.2 RHAMM/ERK interactions in microtubule regulation

RHAMM functions as a scaffold protein, binding ERK1 directly and MEK1 indirectly, recruiting them to microtubules, via RHAMM's interactions with tubulin, which then regulates microtubule dynamics/stability

1.6.2 RHAMM and spindle assembly binding partners

Apart from microtubules, RHAMM binds to many other structures in the context of cell division/mitosis, which in particular assist in the regulation of proper spindle assembly.

One critical organelle of interest is the centrosome. Centrosomes make up the microtubule-organizing center and are the major sites of microtubule assembly. They are comprised of two centrioles surrounded by an amorphous pericentriolar material (9). The PMC is made up of numerous coiled coil proteins that are directed to centrosomes via motor proteins and assist in microtubule nucleation (7). Given RHAMM's role in microtubule regulation, it is not surprising that RHAMM localizes to centrosomes and this interaction helps to maintain both centrosome and spindle integrity during mitosis (19). RHAMM binds to centrosomes via its conserved C-terminal leucine zipper (19) and this association is seen in meiotic *Xenopus* extracts (74) and in mammalian cell lines (19). Deletion constructs of RHAMM fusion proteins lacking the leucine zipper inhibit the targeting of RHAMM to centrosomes (19). However, the leucine zipper alone is not sufficient for targeting to centrosomes as GFP-tagged C-terminal RHAMM fragments of 100 amino acids containing the leucine zipper did not associate with centrosomes, but did with spindle poles (19).

Furthermore, unregulated RHAMM expression leads to centrosome defects. Elevated RHAMM expression in multiple myeloma plasma cells resulted in structural, but not numerical, centrosomal abnormalities (81). Similarly, overexpression of RHAMM five-fold in RPMI 8226 cells in culture results in excess PCM volume (81). Knockdown of

RHAMM in SMCs results in premature centrosome replication and the presence of fragmented and detached centrosomes (84). Not surprisingly, expression of mutant RHAMM in neointimal SMCs also resulted in less RHAMM being concentrated around centrosomes, suggesting a critical role in maintaining division fidelity at least in neointimal SMCs (84). Structural centrosome defects are typically seen in human cancers as a result of aberrant mitosis that consequently contributes to genomic instability (81).

During mitosis, the division of the centrosome and its subsequent polar separation helps assemble the critical bipolar mitotic spindle. Mutating the carboxyl terminal centrosomal binding domain of RHAMM resulted in an increase in the number of spindle pole defects (84). Thus RHAMM's localization to centrosomes provides a putative mechanism by which RHAMM regulates spindle assembly during mitosis and accordingly helps maintain genomic stability (79).

Like many other proteins found at centrosomes, a subset of intracellular RHAMM is targeted to centrosomes via a complex with the molecular motor protein, dynein. In general, the dynein/dynactin motor complex is responsible for transporting cellular cargo to microtubule minus ends (19). RHAMM antibodies bind to dynein during interphase and a slightly higher fraction of RHAMM binds to dynein in mitotic *Xenopus* extracts (19). Co-localization studies also confirm the interaction between endogenous RHAMM with dynein in mammalian mitotic HeLa cells (19) and neointimal SMCs, particularly at the spindle poles and co-immunoprecipitation studies reveal that they are part of a complex (84). Whether this interaction with dynein is direct or indirect remains unknown, but RHAMM's association with dynein at the spindle poles is essential in maintaining

mitotic spindle organization and also helps orient the mitotic spindle during metaphase (19, 84, 93, 100).

Consistent with RHAMM's role in maintaining spindle integrity, the carboxyl terminal leucine zipper of RHAMM shares 72 percent structural homology with that of the Kinesin-like protein 2 (Klp2) family (19). Klp2 proteins are plus-end associated kinesin-like proteins whose leucine zipper domain is responsible for localizing to centrosomes via an indirect interaction with the dynein/dynactin motor complex(108). Xklp2, the *Xenopus laevis* Klp2 member, is crucial for the polar separation of centrosomes and in maintaining spindle bipolarity (19, 108) and functions via its interactions with targeting protein for Xklp2, TPX2 (108). TPX2 is a spindle assembly protein factor that assists in microtubule nucleation and assembly by activating AURKA, which recruits a number of key proteins required for mitotic spindle formation (74, 81, 84, 100, 109). The structural similarities between RHAMM and the Klp2 family of proteins would suggest that RHAMM functions in a similar manner to maintain spindle assembly and integrity. Not surprisingly, TPX2 is one binding partner of RHAMM. These interactions are cell cycle dependent and the majority of RHAMM, at least 40-60%, associates with TPX2 during mitosis in human cells (81, 100, 110). There is no evidence in the literature to suggest that these proteins interact with each other at other times during the cell cycle. RHAMM's interaction with TPX2 is essential for targeting TPX2 to the spindle poles and activation of AURKA during spindle formation (100). Immunodepletion of RHAMM in *Xenopus* meiotic cell extracts or siRNA knockdown of RHAMM in mitotic HeLa cells both results in the loss of TPX2 at the spindle poles (74, 100). RHAMM binds to TPX2 via its conserved carboxy terminal leucine zipper region and this interaction is observed

in many cell types, including both *Xenopus* and human cells (19, 74). Mutation of the three leucines in the leucine zipper sequence to arginines abolishes TPX2 binding to RHAMM (100). Furthermore, an alteration in this sequence results in aberrant spindle formation and also disrupted localization of TPX2 in *Xenopus laevis* extracts and thus impacted AURKA phosphorylation/activation (19, 74). Interestingly, RHAMM's interaction with TPX2 in human cementifying fibroma cells only occurs in the presence of HA (109). Note that HA production is highest during G2/M when RHAMM and TPX2 interact, suggesting critical roles for these interactions in mitotic functions.

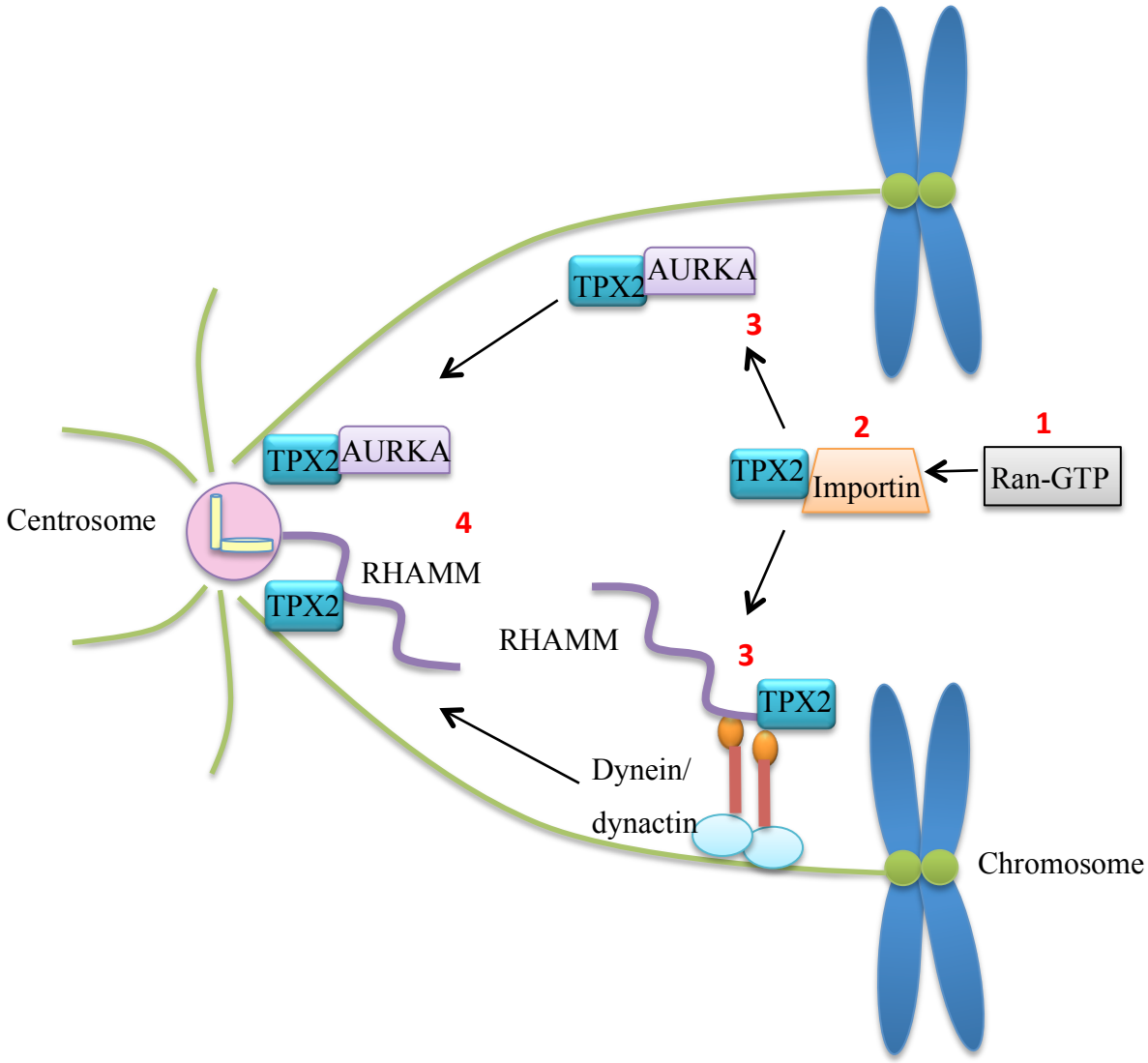

Figure 1.3: Schematic representation of RHAMM function at the mitotic spindle

During mitotic spindle assembly, a (1) Ran-GTP gradient is established around chromosomes and allows for the release of TPX2 from inhibitory importins (2). TPX2 is free to interact with and activate AURKA (3;top), which assists in spindle pole assembly (4). TPX2 can also form a complex with RHAMM and dynein/dynactin (3;bottom), which travel along microtubules to recruit TPX2 and RHAMM to the spindle poles and centrosomes where they both play a role in regulating mitotic spindle integrity (4) (Adapted from Maxwell *et al* 2008 (85))

1.6.3 RHAMM and cell cycle progression

Consistent with RHAMM's role during mitosis, RHAMM expression in mammalian cells is tightly regulated during the cell cycle, both *in vitro* and *in vivo* (79).

Quantitative real-time PCR analysis of cultured HeLa cells synchronized at the G1/S phase and released from the block at various times after showed that the level of human RHAMM transcripts was predominantly activated at G2/M (79). This induction of RHAMM expression at the G2/M phase of the cell cycle coincides with the expression of a hallmark G2/M regulatory protein, cyclin B (79). Briefly, cyclin B expression is cell cycle regulated, its expression peaks during mitosis, and it is necessary for cells to progress through mitosis by forming a complex with the regulatory cyclin dependent kinase 1 (Cdk1) (4).

RHAMM expression is also elevated at G2/M *in vivo* in the liver of BALB/c mice that were subjected to a 70% partial hepatectomy (79). Generally, the liver is a highly differentiated organ and is not a suitable for examining cell division except in the case where a hepatectomy was subjected where the regeneration of a liver exhibits normal cell cycle regulated gene expression. BALB/c mice showed elevated RHAMM expression after 48 hours during liver regeneration and this coincided with cyclin B expression at the G2/M phase (79).

In line with these findings, Sohr *et al* (111) demonstrated that expression of both RHAMM mRNA and proteins are cell cycle regulated in human foreskin fibroblasts (HFF). Whereas RHAMM mRNA and protein follow the same expression patterns in the

early stages of the cell cycle, mRNA expression peaks at G2/M, however, protein levels peak and begin to decrease during S phase of the cell cycle (111).

Consistent with RHAMM's role in G2/M regulation, ectopic overexpression of RHAMM in human 293T cells results in the accumulation of a population of cells in G2/M as demonstrated by FACs analysis (79). This suggests that overexpression of RHAMM affects cell cycle G2/M progression by arresting cells during mitosis. Similarly, overexpression of GFP-RHAMM in RPMI 8226 and HeLa cells results in a metaphase block during mitosis and a significant decrease in the number of mitotic cells (19, 81). Conversely, the knockdown of RHAMM in HCF cells results in a decrease in the percentage of cells at G2/M, as detected by flow cytometry (109). These results suggest that a tight regulation of RHAMM expression levels is essential for normal cell cycle progression.

Not surprisingly, RHAMM mRNA and protein levels are indirectly downregulated by the tumor suppressor, p53 (48). p53 is a transcription factor that controls the expression patterns of many genes involved in cell-cycle regulation and apoptosis. Furthermore, the levels of many cell cycle regulators are controlled by degradation through ubiquitin E3 ligases (112). The anaphase-promoting complex (APC) is one ubiquitin ligase that helps regulate the turnover of several spindle assembly factors, including RHAMM (113). This regulatory mechanism appears to be important in keeping RHAMM levels in check for binding to other spindle assembly factors, like TPX2, and promoting proper spindle assembly (107, 113). RHAMM levels are also presumably regulated by ubiqutination through a complex with another ubiquitin E3 ligase, BRCA1/BARD1 and this interaction helps to keep RHAMM levels in check to maintain a bipolar mitotic spindle (73).

The precise reason why and when cells need RHAMM for the progression of the cell cycle are not yet clear, however, RHAMM functions in this process are likely dependent on its interaction with, and regulation of, microtubules and centrosomes and thus its role in maintaining mitotic spindle and centrosome integrity.

It is surprising, however, given RHAMM's functions in these processes, that RHAMM-/- mice are not embryonic lethal and there are no obvious defects in these viable mice (76). This suggests that there are redundant mechanisms that help compensate for RHAMM loss and perhaps RHAMM is not compensated for only during specific pathologies such as wound repair and cancer progression.

1.7 RHAMM and cell proliferation

Given RHAMM's interactions with cytoskeletal elements and proteins that are involved in regulating mitosis, it is not surprising that RHAMM functions during cell proliferation. This role, however, is often non-essential and largely cell type specific.

RHAMM promotes cell growth in several cell backgrounds via phosphorylation and activation of ERK1/2 kinases (114). RHAMM loss in J82 bladder cancer cells resulted in reduced cell proliferation and an increase in the percentage of cells in G_1 of the cell cycle as a result of their anti-proliferative effects; this was not due to an increase in cell death as no induction of apoptosis was observed after RHAMM knockdown (115). Furthermore, knockdown of RHAMM by siRNA in immortalized human cementifying fibroma cells from the jawbone resulted in a decrease in cell proliferation and an

inhibition of ERK1,2 phosphorylation (109). Consistent with these results, RHAMM overexpression in MC3T3-E1 osteoblast cell line promotes cell proliferation and induces ERK1,2 phosphorylation directly. Inhibiting activation of ERK1, 2 by using an inhibitor, PD98059, resulted in a decrease in cell proliferation of MC3T3-E1 RHAMM overexpressing cells (114). Similarly, blocking RHAMM function with an anti-RHAMM antibody abolished cell growth of Kv562 human leukemic cells (116). The effects of proliferation on these cells were mediated through RHAMM and were dependent on the presence of HA and activation of the PI3K pathway (116).

Conversely, pancreatic islet tumor N134 cells ectopically expressing RHAMM showed that RHAMM promotes tumor growth independent of cell proliferation(117). Staining of uninfected cells and RHAMM-expressing tumor cells with a proliferation marker, Ki67, demonstrated that RHAMM-expressing cells were less proliferative than controls suggesting an inhibitory affect of RHAMM overexpression on cell growth (117).

In certain cell backgrounds, however, RHAMM was shown to have no effect on cell proliferation. Overexpression of RHAMM is known to promote breast cancer progression (94, 118). RHAMM knockdown studies in an aggressive breast cancer cell line, MDA-MB-231 show no effect of RHAMM loss on cell proliferation, however, it does inhibit cell migration and invasion (119). This suggests that RHAMM functions in breast cancer progression is unrelated to cell proliferation, but rather is essential during migration and invasion. Likewise, stable expression of shRNA to RHAMM in 2884 malignant peripheral nerve sheath tumor (MPNST) cell line had no effect on cell proliferation in comparison to controls (120).

Taken together, this data suggests that RHAMM's role during cell proliferation is context and cell type dependent.

1.8 RHAMM and cell migration

Given RHAMM's role in regulation of microtubule structures and centrosomes, it is not surprising that RHAMM also plays an essential role during non-mitotic functions, such as cell motility. Similar to its role in mitosis, RHAMM functions during cell migration are mediated by its interactions with its binding partners, including ERK1,2, HA, and centrosomes.

ERK1,2 signaling pathway has been shown to play extensive roles during cell migration and in regulating cell protrusion, both initiation and speed (64, 121). RHAMM is required to sustain activation of ERK1,2 and thus its localization and function (88). $RHAMM^{-/-}$ fibroblasts exhibit defects in cell migration characterized by failure to resurface scratch wounds due to slower speeds and loss of directionality compared to RHAMM expressing fibroblasts, and these effects have been shown to be due to loss of ERK activation (64). Genetic deletion of RHAMM also resulted in decreased activation of ERK1,2 in the nucleus and cell lamellae, which is required for cell protrusion (64). Defects in ERK1,2 activity and cell migration can be rescued by expression of full length RHAMM or by an activated form of MEK1. Consistently, a MEK inhibitor blocks serum-induced motility of RHAMM expressing fibroblasts (64). These results

collectively suggest a role for RHAMM-MEK/ERK interactions in regulating cell migration.

RHAMM/HA interactions also play a role in directing cell migration of both transformed and non-transformed cells including endothelial cells and bovine aortic SMCs (122, 123). HA stimulation increases cell migration of *ras* transformed fibroblasts and arterial smooth muscle cells (ASMCs) in a dose dependent manner and this effect is independent of cell proliferation (122, 123). Cell migration in HA-induced ASMCs is dependent on RHAMM as knockdown of RHAMM via siRNA inhibits cell motility. Mutation of the HA-binding site of RHAMM also reverted the Ras-induced transformation of 10T1/2 fibroblasts (95). Furthermore, studies using RHAMM function blocking antibodies have inhibited HA-stimulated motility in a number of cell lines (64, 67). RHAMM/HA interactions also mediate activation of Rac1 via a PI3K dependent mechanism, which promote the formation of actin rich lamellipodia and stress fibers that promote membrane protrusions and contraction, respectively, during cell motility (123).

Furthermore, centrosomes are known to play an integral role during cell migration as they help polarize the cytoskeleton (84). Centrosome loss or damage disrupts directed cell motility due to loss of cell polarization (42), and thus strict control of the number, structure, and position of the centrosome is critical. RHAMM localizes to centrosomes via a carboxyl terminal leucine zipper domain (19). RHAMM plays a role in controlling the position and function of centrosomes and accurate rear polarization during cell migration in neointimal smooth muscle cells (SMCs) (124), the latter of which is dependent on PKCα activity (124). Silencing of RHAMM via siRNA treatment in neointimal SMCs results in a shift from rear polarization to front polarization of the

MTOC and slow migrating cells compared to control treated cells (slow closing of the scratch wound) (124). RHAMM also plays a role in the organization of the actin and microtubule network during cell migration; silencing of RHAMM results in fragmented lamellipodia and an increase in the number of stable microtubules in the perinuclear region (124). Dynamic microtubules are required for cell locomotion as they assist in the retraction of the rear end of the cell (40). Furthermore, removal of the centrosome from a polarized cell results in changes in the actin and microtubule cytoskeletal networks, which give rise to a non-polarized phenotype (42). These results suggest that RHAMM plays a role in regulating centrosome function during cell migration via organization of cytoskeletal components to give rise to a polarized cell. These results further hypothesize that RHAMM regulation of centrosome function could attribute to the defects seen in migration in RHAMM$^{-/-}$ fibroblasts (64).

1.9 The role of RHAMM in cancer

RHAMM overexpression has been implicated in a number of human cancers, including breast cancer, multiple myeloma, prostate cancer, hepatocellular carcinomas, colorectal cancer, ovarian cancer, and acute myeloid leukemia (79, 92, 118, 125-128). RHAMM is a novel breast cancer susceptibility gene and high protein and mRNA expression of RHAMM have been correlated with increased peripheral metastasis and poor outcome in breast cancer patients (118).

In experimental models, RHAMM overexpression is required for maintaining Ras transformation through an HA dependent manner. Mutation of the HA binding region of RHAMM reverts H-ras transformation (95) suggesting that RHAMM effects on transformation are in part mediated through HA. As well, overexpression of RHAMM$^{\Delta 163}$ isoform transforms 10T1/2 mesenchymal cell lines and these form metastatic tumors in xenograft models, strongly suggesting that RHAMM is an oncogene (95). Consistent with its oncogenic potential, RHAMM mRNA and protein levels are downregulated by the tumor suppressor, p53 (48).

RHAMM functions during tumorigeneis, however, are not fully elucidated. This is in part due to the multifunctional roles of RHAMM regulation on the cell surface and within intracellular compartments and both play a role in cancer progression.

Cell surface RHAMM functions as a co-receptor for CD44 and upon binding hyaluronan mediates sustained activation of ERK1,2 kinase in MDA-MB-231 breast cancer cell lines (94). HA-dependent ERK activation results in increased cell migration and invasion, contributing to the oncogenic effects of this protein (94).

Intracellular RHAMM regulation of mitotic spindle integrity and centrosome function provides a putative mechanism by which RHAMM overexpression promotes genomic instability and contributes to tumorigenesis. Consistent with this hypothesis, unregulated RHAMM expression has been shown to correlate with genomic instability in multiple myeloma (92)

Furthermore, RHAMM functions in mitotic spindle integrity are regulated in part by the BRCA1/BARD1 complex (73, 78). RHAMM and BRCA1/BARD1 interactions are seen

in numerous mammalian cell lines and together they regulate centrosome amplification (78). BRCA1/BARD1 complex regulates the levels of RHAMM via its ubiquitin E3 ligase activity (73, 78). Overexpression of RHAMM in the absence of BRCA1/BARD1 results in disrupted mitotic spindle assembly (73).

It is well established that a loss-of-function mutation in BRCA1 increases susceptibility to breast and ovarian cancers (78). Taken together, BRCA1 mutations along side RHAMM overexpression thus have the potential to promote genomic instability and contribute to breast cancer progression.

1.10 Hypotheses and Objectives

Given the importance of RHAMM in binding to and regulating mitotic spindle integrity, microtubules, and centrosome structures, I hypothesized that RHAMM leucine zipper maintains mitotic spindle integrity through its direct interactions with tubulin heterodimers.

Furthermore, I hypothesized that RHAMM regulation of centrosome structures controls cell polarity and impacts directional migration via its leucine zipper motif.

The objectives for this dissertation were as follows:

1) Examine the role of the leucine zipper of RHAMM in direct binding to tubulin, *in vitro*

2) Determine the consequences of a mutated leucine zipper motif of RHAMM$^{\Delta 163}$ on mitotic spindle functions and tumorigenesis
3) Determine the effects of a mutated leucine zipper motif of RHAMM$^{\Delta 163}$ on directed cell migration and centrosome function

Chapter 2

2 Materials and Methods

Cell culture

The 10T1/2 mouse embryonic fibroblast (MEF) cell line was purchased from American Type Culture Collection (ATCC; Manassas, VA, USA). RHAMM knockout (-/-) primary mouse embryonic fibroblasts (MEFs) were isolated as described by Tolg *et al.*, 2003 and 2006 (64, 76). Cell lines were grown as monolayers in low glucose Dulbecco's Modified Eagle Medium (DMEM) (Wisent BioProducts, Montreal, QC, Canada) supplemented with 10% fetal bovine serum (FBS) (Wisent BioProducts) and 1x antibiotic-antimycotic (Invitrogen, Life Technologies, Burlington, ON, Canada) in a humidified atmosphere of 5% CO_2 at 37°C. Cells were grown to 80% subconfluency prior to passage and were released from tissue culture plastic with 0.25% trypsin-EDTA (Invitrogen, Life Technologies).

RHAMM$^{\Delta 163}$ mutant constructs

Mouse RHAMM$^{\Delta 163}$ isoform (aa163-794) was used for this dissertation. A RHAMM $^{\Delta 163}$ with a C-terminal leucine zipper mutation was previously constructed in our lab by altering the three leucine amino acids in the leucine zipper region using site directed mutagenesis. The following mutations were made: Mutation 1—L735R/L742R and Mutation 2—L728A/L735R/L742R. Wildtype and mutant RHAMM$^{\Delta 163}$ were amplified

by PCR with a 5'Sal I site (FW primer: 5' GGATCAGTCGACATGAGAGCTCTAAGCCTGGAATTGATGAACT 3') and a 3' Bam HI site (RV primer: 5' CCCGGATCCTCAGCAGCAGTTTGGGTTGCC 3') using Phusion High Fidelity DNA polymerase (New England Biolabs, Whitby, ON, Canada) as recommended by the manufacturer. Blunt PCR products were then purified using DNA Gel Extraction Kit (Bio Basic Inc, Markham, ON, Canada) and cloned into pCR-Blunt vector using Zero Blunt PCR Cloning Kit (Invitrogen, Life Technologies), as per the manufacturer's instructions. After enzymatic digestion of both cDNA and vector with Sal I and Bam HI restriction enzymes (New England Biolabs), cDNA was ligated into pHβApr-1-neo expression vector under the control of the β-actin promoter. The construct was sequenced at Robarts Sequencing Facility (Western University, London, ON, Canada) and transfected into 10T1/2 MEFs.

RHAMM expression in 10T1/2 and RHAMM$^{-/-}$ MEFs

Untagged wildtype and mutant RHAMM$^{\Delta 163}$ constructs were transfected in 10T1/2 and RHAMM$^{-/-}$ (KO) MEFs using jetPrime transfection reagent (jetPrime Polyplus, New York, NY, USA), as per the manufacturer's instructions. Immortalized 10T1/2 and KO MEFs were grown in a 6-well plate to a confluency of 70-80% in DMEM supplemented with 10% FBS and 1x antibiotic-antimycotic. The plasmid DNA was diluted with jetPrime buffer (jetPrime Polyplus) and incubated with transfection reagent at a ratio of 3 μg DNA: 7 μl transfection reagent. The transfection mix was then slowly added to the cells and incubated for 4 hours, after which the media was replaced and incubated

overnight. Stable cell lines were established in 10T1/2 and KO fibroblasts by selecting for a mixed pool of transfectants with 1-5 mg/ml G418 (Sigma-Aldrich, St. Louis, MO, USA).

DNA isolation

Wildtype and mutant 10T1/2-RHAMM$^{\Delta 163}$ cells were harvested by trypsin, washed twice with PBS, and then digested overnight at 56°C at 1000rpm on a thermomixer with 18µl of 10mg/ml proteinase K in 500 µl of lysis buffer containing 1M Tris (pH 8), 0.5M EDTA (pH 8), 10% SDS, and 5M NaCl. After overnight incubation, the cells were suspended thoroughly by vortexing and subsequently centrifuged for 10 min at 13000rpm. Supernatant was collected and added to a new eppendorf tube containing 500µl isopropanol to precipitate the DNA. Following thorough mixing, the cells were centrifuged for 5 min at 13000rpm and supernatant was discarded. The DNA pellet was washed with 500µl of 70% ethanol and then centrifuged for 5 min at 13000rpm. The supernatant was discarded and the DNA was left to air dry at room temperature overnight and then resuspended in 50µl ddH_2O for further analysis. DNA from a sample of tumor tissue from xenograft studies weighing ~200mg was also obtained using the same method.

DNA sequencing

DNA was isolated as above and amplified by PCR using primers spanning an intron-exon boundary to amplify ~200 bp region of exogenous RHAMM. The following RHAMM primers were used: FW: 5' AAACCTTTTCAGCAACTGGAT 3' and RV: 5' AGATCGGAGTTTTGACACCTC 3' and PCR was carried out using Phusion High Fidelity DNA polymerase (New England Biolabs) as recommended by the manufacturer. PCR products were then purified using DNA Gel Extraction Kit (Bio Basic Inc.) and cloned into pCR-Blunt vector using Zero Blunt PCR Cloning Kit (Invitrogen, Life Technologies), as per the manufacturer's instructions. The samples were then sent to Robarts Sequencing Facility (Western University, London, ON, Canada) to be sequenced using M13 forward and reverse primers.

Direct and competitive tubulin ELISA

Biotinylated and unlabeled C-terminal RHAMM peptides (aa720-750) containing the leucine zipper, both wildtype and L735R mutant, were synthesized by CanInc Peptide (Montreal, QC). Interactions between RHAMM peptides and >99% purified bovine α/β-heterodimeric tubulin protein (Cytoskeleton, Denver, CO, USA) were detected using a direct and competitive tubulin ELISA assay (Figure 2.1). Wells of a 96-well microplate (non-TC treated) (Sigma-Aldrich) were coated with 10 µg/ml of α/β-heterodimeric tubulin protein (Cytoskeleton) diluted in PBS overnight at 4°C. Control wells with no tubulin were coated with PBS. Wells were washed 3-10 minutes with 0.01% Tween-20 in PBS and blocked with 5% skim milk in PBS for 2 hours at room temperature. After

washing 3 times with 0.01% Tween-20 in PBS, wells were incubated with 5-40 μg/ml of either wildtype or L735R mutant biotinylated RHAMM peptides diluted in sterile dH_2O for 2 hours at room temperature. After two hour incubation with labeled peptides, for competitive ELISA assay, 100 μg/ml of unlabeled wildtype RHAMM peptide (diluted in water) was mixed into the wells containing 10 μg/ml biotinylated peptides and incubated overnight at 4°C. After thorough washing, wells were incubated with streptavidin conjugated with horseradish peroxidase (HRP) (Abcam, Cambridge, MA, USA), diluted at 1:2000 in PBS for 1 hour at room temperature. Wells were washed for a final 3-10 min with 0.01% Tween-20 in PBS and the interaction was detected by incubation with 1-STEP ABTS (2,2'-azinobis [3-ethylbenzthiazoline-6-sulfonic acid] diammonium salt) solution (Thermo Scientific, Waltham, MA, USA) for 20 min, as per the manufacturer's instructions. The reaction was halted by the addition of 1% SDS and absorbance readings were measured at 405 nm using the Wallac 1420 VICTOR^2 plate reader (PerkinElmer, Waltham, MA, USA). Three biological replicates were used per treatment. Control wells with no tubulin and no peptide served as the background control.

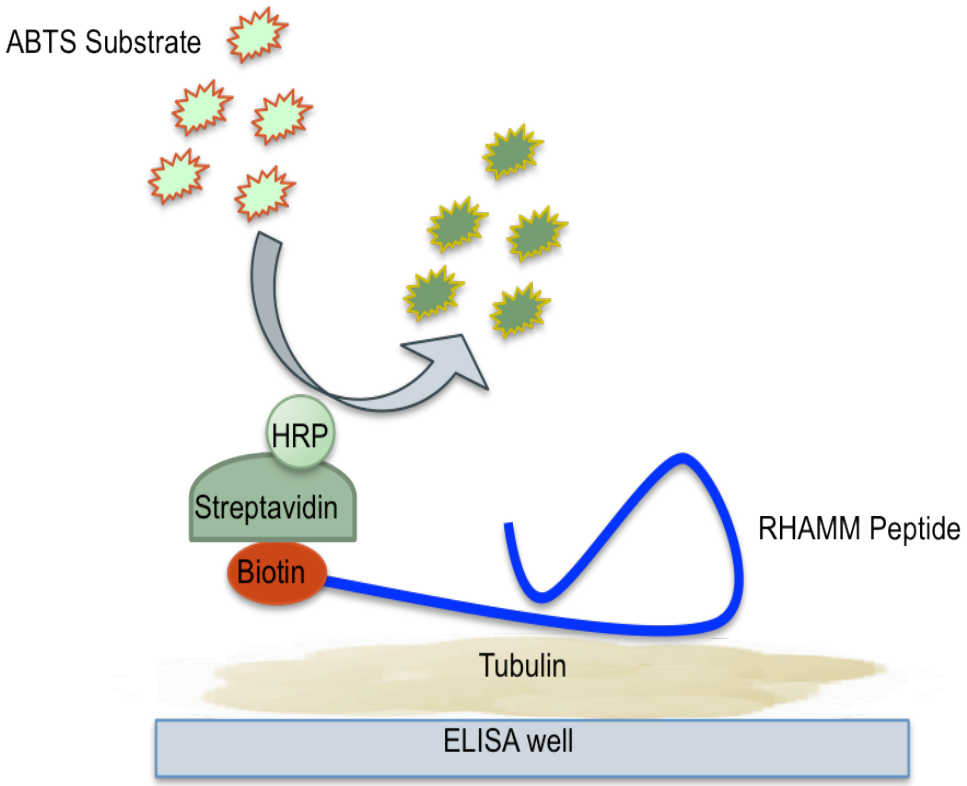

Figure 2.1: Direct tubulin ELISA-assay

Schematic representation of the novel tubulin ELISA assay generated for testing direct RHAMM peptide and tubulin interactions in vitro. Wells were coated with 10µg/ml of tubulin heterodimers and incubated with biotinylated RHAMM peptides, either wildtype or mutant. Binding was detected via direct interactions between biotin and streptavidin, the latter of which is HRP conjugated to allow for the subsequent enzymatic conversion of ABTS substrate into a measurable fluorescent product

RNA isolation

10T1/2 parental fibroblasts, as well as stably transfected wildtype and mutant RHAMM$^{\Delta 163}$-fibroblasts were plated on 10 cm tissue culture plastic in DMEM supplemented with 10% FBS. When plates reached 80% subconfluency, total RNA was isolated from cells using TRIzol Reagent (Invitrogen, Life Technologies) as per the manufacturer's instructions, and RNA concentrations were determined by absorbance at 260nm.Three biological replicates were used.

cDNA synthesis and quantitative real-time PCR

Quantitative real-time PCR (qRT-PCR) was used to verify the overexpression of wildtype and mutant RHAMM$^{\Delta 163}$ that are stably expressed in 10T1/2 fibroblasts. 1 µg of total RNA was used to prepare a 20µl reaction volume of cDNA using Random Primers (Invitrogen, Life Technologies) in a first strand cDNA synthesis reaction using Superscript II Reverse Transcriptase (Invitrogen, Life Technologies) as per the manufacturer's instructions. Primers for qPCR were designed to amplify a 200 bp region of mouse RHAMM and were synthesized by Invitrogen (Pleasanton, CA, USA) and amplification of 28S RNA was used for normalization. The following primers were used: RHAMM FW: 5' GTTTCAATAGAGAAAGAAAAGATC 3'; RHAMM RV: 5' CCTCAAGAGACTGCTTAAGAC 3'; 28S FW: 5' TCATCAGACCCCAGAAAAGG 3;; 28S RV: 5' GATTCGGCAGGTGAGTTGTT 3'. qPCR amplification was performed on a Stratagene Mx3000P instrument (Agilent Technologies, Mississauga, ON, Canada) with SYBR Green QRT-PCR Master Mix (Agilent Technologies) and the reactions were

set up as per the manufacturer's instructions provided for the master mix. The following cycle conditions were used: 3 min at 95°C, 20 sec at 95°C, 20 sec at 60°C, 1 min at 95°C, 30 sec at 60°C, and 30 sec at 95°C. Relative expression levels were calculated by the standard curve method and analyzed using Stratagene Mx3000P software as well as Microsoft Excel.

Western blot of RHAMM protein expression

Parental 10T1/2 MEFs and wildtype or mutant 10T1/2- RHAMM$^{\Delta 163}$ cells were washed twice with cold PBS and then lysed with RIPA Buffer (Sigma-Aldrich) as per the manufacturer's instructions. Cells were detached from the dish with a cell scraper and collected via centrifugation at 8000xg for 10 min at 4°C. Protein concentration from the cell supernatant was measured using Pearson's Modification of Micro Lowry Total Protein Kit (Sigma-Aldrich). 10µg of protein were loaded and separated onto 10% SDS-PAGE gels and transferred to a PDVF membrane (Millipore, Billerica, MA, USA). Membrane was subsequently blocked for 1 hr at room temperature in 10% skim milk in TBS-T (50mM Tris base pH 7.5, 150mM NaCl and 0.05% Tween-20). After washing once with TBS-T, membrane was incubated with rabbit anti-RHAMM monoclonal antibody (Epitomics, Burlingame, CA, USA) at a dilution of 1:500 in TBS-T containing 0.5% skim milk overnight at 4°C. Membrane was then washed 4-10 minutes with TBS-T followed by an incubation with anti-rabbit horse radish peroxidase conjugated (HRP) secondary antibody at a dilution of 1:100000 in TBS-T containing 0.5% skim milk for 1 hour at room temperature. After thorough 3-30min washes with TBS-T, the membrane

was developed using the Enhanced Chemiluminescence (ECL) detection kit (GE Healthcare, Mississauga, ON, Canada). Levels of endogenous full length RHAMM ($RHAMM^{FL}$) served as the loading control as the RHAMM antibody detects both $RHAMM^{FL}$ and $RHAMM^{\Delta 163}$ forms.

Quantification of cell proliferation

Parental 10T1/2 and KO MEFs and those stably expressing untagged wildtype or mutant $RHAMM^{\Delta 163}$ cells were seeded at 1000 cells/well in a 96-well plate. Cells were incubated overnight in DMEM supplemented with 10% FBS. After 24 hours, $1/10^{th}$ of alamarBlue reagent (Invitrogen, Life Technologies) was added to wells per cell line and incubated for 5 hours in a humidified atmosphere of 5% CO_2 at 37°C. Cell proliferation was assessed over the duration of 96 hours using this method. Fluorescence readings were measured at 580nm on the Wallac 1420 $VICTOR^2$ plate reader (PerkinElmer). Nine biological replicates were used per cell line.

Flow cytometry

Parental 10T1/2 MEFs and 10T1/2 MEFs stably expressing wildtype and mutant $RHAMM^{\Delta 163}$ were seeded at 10^6 cells in 10 cm culture plates and allowed to adhere overnight in DMEM supplemented with 10% FBS. Cells were released from tissue culture plastic with 0.25% trypsin-EDTA (Invitrogen, Life Technologies) and harvested at 1500 rpm for 5 minutes. Cell pellets were then suspended in 500 µl cold PBS and fixed

by drop wise addition of 1.5 ml of 90% ethanol while vortexing at a slow speed setting. After incubating fixed cells on ice for an hour, cells were centrifuged at 1500 rpm for 5 min and supernatant was discarded. Cells were then suspended in 1 ml of 2N HCl/0.5% Triton X-100 dropwise with gentle vortexing and incubated at room temperature for 30 min. Cells were pelleted at 1500 rpm for 5 min and then resuspended in 1 ml of 0.1M sodium tetraborate (NaB_4O_7) (pH 8.5). After pelleting cells at 1500 rpm for 5 min and washing with PBS, cells were stained with 1 ml of PBS with 1% FBS and 200 µl of 1mg/ml stock of propidium iodide (Sigma-Aldrich) with 100 µl of 20mg/ml stock of DNase-free RNase A (Invitrogen, Life Technologies) and stored overnight at 4°C. Stained cells were detected using a flow cytometer (Beckman Coulter, Mississauga, ON, Canada) using FACS Calibur with Cell Quest acquisition. Viable cells were gated based on forward and side scatter (FSC and SSC, respectively) to eliminate cell debris. Cell cycle analysis was then conducted on single cell populations at 20,000 events per sample after gating out doublets. Analysis was performed on FlowJo software (Treestar, Ashland, OR, USA) and percentages of cells at different stages of the cell cycle were calculated using the Watson (Pragmatic) model on FlowJo.

Quantification of cell apoptosis

10T1/2 MEFs stably expressing wildtype and mutant RHAMM$^{\Delta 163}$ (L735R and L728A/L735R) were seeded at 5000 cells/well in a 96-well plate and allowed to adhere overnight in DMEM with 10% FBS. Apoptosis was detected by the presence of mono- and oligonucleosomes in the cytoplasmic fraction of cell lysates using the Cell Death

Detection ELISA^{PLUS} kit (Roche Applied Science, Indianapolis, IN, USA) as per the manufacturer's instructions. The kit detects apoptosis in cell lysates using anti-histone and anti-DNA antibodies. Absorbance readings were measured at 405 nm using the Wallac 1420 VICTOR^2 plate reader (PerkinElmer) and four biological replicates were used per cell lysate.

Tumor xenografts

10T1/2 MEFs stably expressing wildtype or mutant RHAMM$^{\Delta 163}$ were seeded in tissue culture plates to reach 80% confluency in complete DMEM supplemented with 10% FBS. Cells were released from tissue culture plastic with 0.25% trypsin-EDTA (Invitrogen, Life Technologies) and resuspended in complete DMEM supplemented with 10% FBS prior to cell counting via a hemocytometer. After cell counting, 2 million cells, per mouse to be injected, were resuspended in a 50µl total volume of low glucose DMEM with 50% volume of Matrigel Basement Membrane Matrix (BD Biosciences, Mississauga, ON, Canada). Cells were then subcutaneously injected in the flank of 5-week-old female NSG mice ordered from The Jackson Laboratory (Bar Harbor, Maine, USA). Mice were monitored for tumor growth for 6 weeks and tumors were excised and weighed. Three replicate mice were used per cell line to be injected.

Cell migration

KO- RHAMM$^{\Delta 163}$ and KO- RHAMM$^{\Delta 163}$-L735R cells were grown to confluent monolayers overnight in 12.5cm^2 tissue culture flasks (Falcon®, VWR, Mississauga, ON, Canada). Cell monolayers were scratched with a sterile 1250µl pipette tip and media was replaced with fresh DMEM supplemented with 10% FBS and allowed to recover in a humidified atmosphere of 5% CO_2 at 37°C for 30 min. Wound closure was filmed on a Nikon TE300 Inverted Microscope (Nikon, Melville, NY, USA) overnight and time-lapse images were captured every 5 min. Number of cells that migrated in the wound post-scratch were counted using ImageJ grid analysis software and the average number of cells of three wounded areas were quantified.

Pericentrin immunofluorescence

KO MEFs and those stably expressing RHAMM$^{\Delta 163}$ and RHAMM$^{\Delta 163}$–L735R were seeded to confluency at 55000 cells/well on coverslips in a 24-well plate and allowed to attach overnight. After overnight culture, cell monolayers were scratched with a sterile 1250µl pipette tip and media was replaced with fresh DMEM supplemented with 10% FBS and incubated in a humidified atmosphere of 5% CO_2 at 37°C for 6 hours. Coverslips were then fixed gently with fresh 3.5% paraformaldehyde for 7 min at room temperature. After washing 3 times with 1X buffer (10X buffer: 0.1M Tris pH 7.5, 1.5M NaCl, 1% BSA), cells were permeabilized with 0.2% Triton X-100 in 1X buffer for 5 min at room temperature and then blocked with 1X buffer for 5 min at room temperature. Cells were then incubated with rabbit polyclonal anti-pericentrin antibody (Abcam)

diluted at 1:1200 in 1X buffer for 30 min in a humidified atmosphere of 5% CO_2 at 37°C. After washing once in 1X buffer for 5 min, cells were incubated with anti-rabbit Alexa Fluor 488 IgG diluted at 1:1000 in 1X buffer for 1 hour at room temperature. Cells were washed once with 1X buffer and coverslips were then mounted using Prolong Gold DAPI antifade reagent (Invitrogen, Life Technologies) and imaged on the Nikon A1R Confocal Laser Microscope (Nikon).

The percentage of cells with greater than one centrosome at the wound edge were quantified; mitotic figures as determined by DNA staining with DAPI, were excluded from the count. Furthermore, the location of the centrosome relative to the cell nucleus was determined by monitoring the directional movement of cells into the wounded area; the percentage of cells with centrosomes behind the nucleus was quantified.

Statistical analysis

Statistical differences between groups were assessed using two-tailed Student's t-test. P-values <0.05 were considered statistically significant.

Chapter 3

3 Results

3.1 Objective 1: Examining the role of the leucine zipper motif in RHAMM-microtubule interactions

Site directed mutagenesis of a leucine zipper interaction motif: Rationale for mutations

Site-directed mutagenesis is routinely used to study the functional consequences of a single, point mutation in a protein of interest. To gain a better understanding of the C-terminal leucine zipper of RHAMM$^{\Delta 163}$, mutations were constructed by altering the following leucine amino acid residues in the leucine zipper motif: Mutation 1—L735R/L742R and Mutation 2—L728A/L735R/L742R (Table 3.1-Initial mutations). Mutated RHAMM$^{\Delta 163}$ cDNAs were prepared and cloned into the pHβ-APr1 mammalian expression vector with a neomycin selection marker (Figure 3.1) and mutations were confirmed by DNA sequencing. Cloned plasmids containing mutant RHAMM$^{\Delta 163}$ cDNA were expressed in 10T1/2 MEFs and a pool of mixed transfectants were selected in G418 to generate stable cell lines. Genomic DNA from 10T1/2 MEFs expressing mutant RHAMM$^{\Delta 163}$, L735R/L742R or L728A/L735R/L742R, were isolated and sequenced. Sequencing results of both mutants revealed a R742L reversion (Table 3.1-Reverted mutations) suggesting that this leucine residue is functionally important, yet its significance warrants further investigation. Despite the apparent reversion under selection pressure, mutation of one hydrophobic leucine residue to a charged arginine residue

should be sufficient to abolish leucine zipper dimerization function. Since stable cell lines express the reverted sequences, experiments throughout this dissertation were based on the reverted RHAMM mutations and referred to as L735R and L728A/L735R.

Table 3.1: RHAMM Leucine Zipper Sequences

Wildtype Sequence	^{728} **L**KDENSQ**L**KSEVSK**L** ^{742}
Initial Mutations	**L735R/L742R→** ^{728} **L**KDENSQ**R**KSEVSK**R** ^{742}
	L728A/L735R/L743R→ ^{728} **A**KDENSQ**R**KSEVSK**R** ^{742}
Reverted Mutations	**L735R→** ^{728} **L**KDENSQ**R**KSEVSK**L** ^{742}
	L728A/L735R→ ^{728} **A**KDENSQ**R**KSEVSK**L** ^{742}

Sequences represent the carboxyl terminal leucine zipper region of RHAMM from amino acid 728 to 742 of the full-length protein. This region of RHAMM is proposed to facilitate RHAMM-mitotic spindle interactions in cell culture. Initial mutations, L735R/L742R and L728A/L735R/L742R, represent mutations that were generated by site-directed mutagenesis to alter the leucine zipper function; mutated amino acid residues are outlined in red. Reverted amino acids, obtained after selection for expression of initial mutations, are indicated in blue

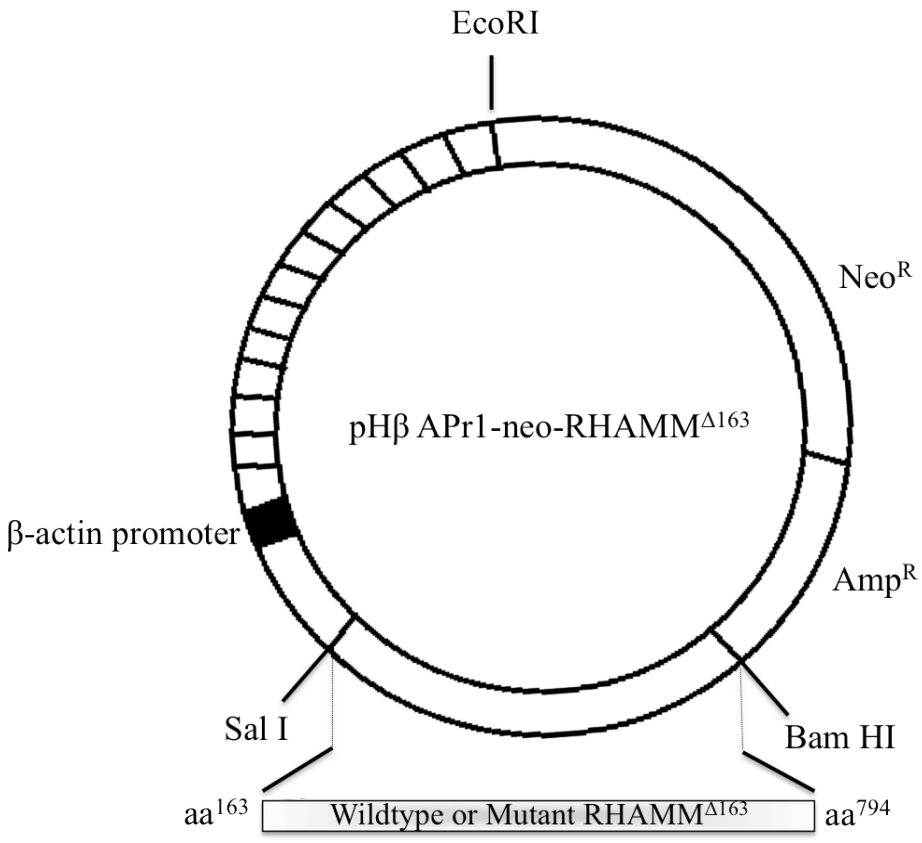

Figure 3.1 RHAMM$^{\Delta 163}$ Constructs

Wildtype and mutant RHAMM$^{\Delta 163}$ cDNA were amplified by PCR and cloned into the mammalian pHβ-APr1 expression vector in the Sal I and Bam HI sites. The vector is driven by the β-actin promoter and contains a neomycin resistant gene for selection of stable transfectants in 10T1/2 and RHAMM$^{-/-}$ MEFs

RHAMM sequence containing the leucine zipper binds directly to tubulin in vitro

During mitotis, RHAMM localizes along the length of microtubules and this interaction occurs via its carboxyl terminus. Within the C-terminal microtubule binding region is a conserved leucine zipper that is thought to mediate RHAMM/mitotic spindle interactions. Deletion of RHAMM fragments lacking the leucine zipper disrupts proper spindle formation, thus owing to its essential role in maintaining mitotic spindle integrity (19, 73, 74)

Our lab has demonstrated that C-terminal RHAMM fragments bind to tubulin heterodimers, *in vitro*, and this interaction can be disrupted by the addition of a synthesized peptide containing the leucine zipper motif. To identify the mechanism by which RHAMM associates with the mitotic spindle, we aimed to determine whether RHAMM directly interacts with microtubules [tubulin heterodimers] via the leucine zipper sequence. Direct interactions between commercially purified α/β-heterodimeric tubulin and a C-terminal biotinylated wildtype RHAMM peptide (Table 3.2) containing the leucine zipper were tested using an ELISA assay (Figure 2.1). Wildtype RHAMM peptide showed specific binding to tubulin heterodimers in a concentration dependent manner (Figure 3.2A); background binding was low, and these interactions were abolished by competition with excess competitive RHAMM peptide (Figure 3.2B). Furthermore, a scrambled peptide of the same amino acid residues showed positive, yet nonspecific weak binding as this interaction could not be competed off with excess competitive RHAMM peptide (Figure 3.2B). These results support the hypothesis that RHAMM-tubulin interactions occur through the conserved C-terminal domain of RHAMM and most importantly that these interactions occur directly.

Table 3.2: RHAMM Peptide Sequences

Peptide	Sequence
Wildtype	Biotin-AEEA-QKIKHVVK**L**KDENSQ**L**KSEVSK**L**RSQLVKRK-NH2
L735R	Biotin-AEEA-QKIKHVVK**L**KDENSQ**R**KSEVSK**L**RSQLVKRK-NH2
Scrambled	Biotin-AEEA -LDRLKHVQKNKLSKSQKIVKSKVELRSQEVK-NH2
Competitive	Ac- QKIKHVVK**L**KDENSQ**L**KSEVSK**L**RSQLVKRK-NH2

3.5 kDa RHAMM peptide sequence representing 31 amino acids of the C-terminal domain of RHAMM (aa720-750), including the underlined leucine zipper proposed to function in binding to the mitotic spindle. Three peptides were biotinylated at the N-terminus via a short PEG linker (AEEA) to allow for specific binding to streptavidin in tubulin ELISA assay. The mutated amino acid residue in the leucine zipper of L735R is highlighted in red. Scrambled peptide was generated by randomly rearranging the amino acids of the wildtype peptide. Competitive peptide was used for a competitive ELISA assay and was unlabeled but acetylated at the N-terminus end

A)

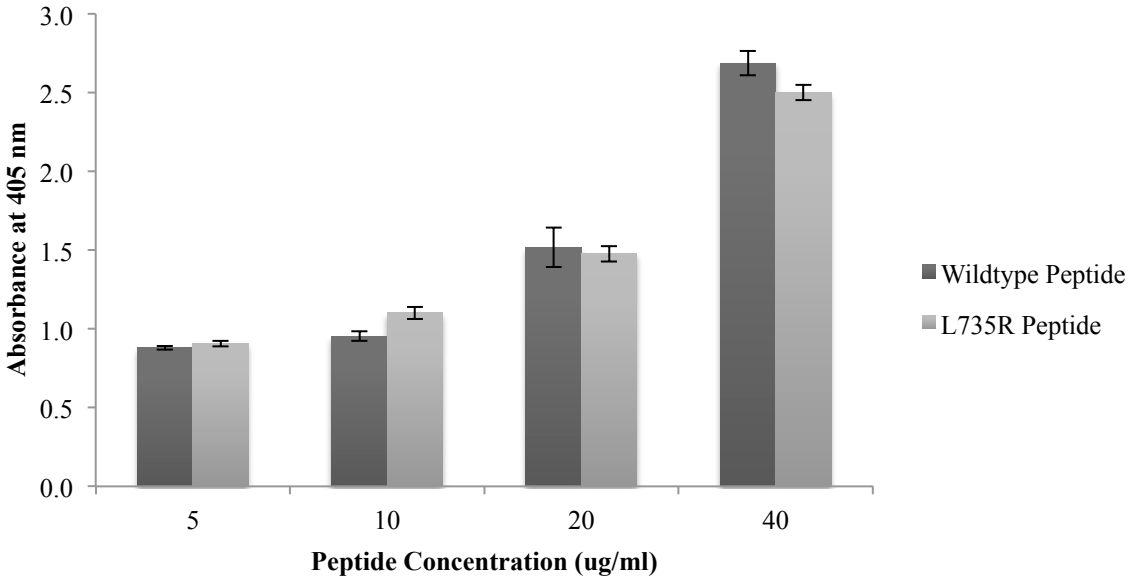
3.0
2.5
2.0
1.5
1.0
0.5
0.0
Absorbance at 405 nm
5
10
20
40
Peptide Concentration (ug/ml)
Wildtype Peptide
L735R Peptide

B)

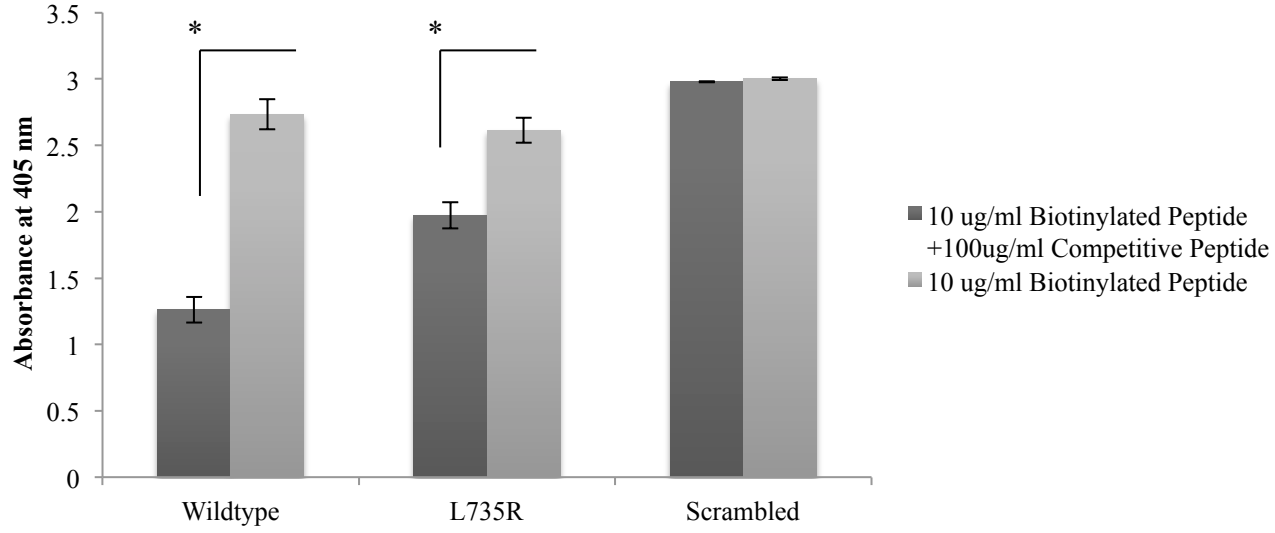
3.5
3
2.5
2
1.5
1
0.5
0
Absorbance at 405 nm
*
*
Wildtype
L735R
Scrambled
10 ug/ml Biotinylated Peptide +100ug/ml Competitive Peptide
10 ug/ml Biotinylated Peptide

Figure 3.2: Wildtype and mutant C-terminal RHAMM peptides directly bind to α-, β-tubulin heterodimers in an ELISA assay

Direct and competitive tubulin ELISA assays were performed using purified α/β-tubulin heterodimers and biotinylated C-terminal RHAMM peptides (aa 720-750) **A)** Direct binding interactions of wildtype and mutant RHAMM peptides to tubulin were detected in a concentration dependent manner **B)** Binding of biotinylated wildtype and mutant RHAMM peptides to tubulin heterodimers was competed off with excess unlabeled wildtype RHAMM peptide (aa 720-750). Scrambled peptide was not able to compete off, confirming the specificity of the C-terminal RHAMM sequence to tubulin. Bars represent mean ± S.E. of n=3 replicates; *$p<0.05$

Mutation of the leucine zipper does not affect RHAMM binding to tubulin *in vitro*

The ELISA data confirmed the specific interaction of wildtype C-terminal RHAMM peptide with tubulin heterodimers. To determine the role of the leucine zipper in this interaction, a RHAMM peptide containing mutation L735R of the leucine zipper was synthesized (Table 3.2) and its binding to tubulin was tested. A leucine zipper is a common protein-protein interaction motif that contains heptad repeats of hydrophobic leucine residues, which form amphipathic α helices used for parallel dimerization with other proteins (129). Typically, the mutation of one leucine residue disrupts leucine zipper function and thus the ELISA assay was only carried out for one mutant RHAMM form. Mutating one leucine residue, L735R, in RHAMM's leucine zipper, however, did not disrupt binding to tubulin; under these conditions the L735R peptide retained an ability to bind to tubulin in a concentration dependent manner (Figure 3.2A) and wildtype unlabeled peptide was able to compete for its binding (Figure 3.2B). These results demonstrate that although the C-terminal RHAMM sequence contained within this peptide mediates direct binding to tubulin heterodimers, these interactions were not through the leucine zipper dimerization motif, as disruption of its function did not abolish binding to tubulin.

3.2 Objective 2: Assessing the role of RHAMM$^{\Delta 163}$ in mitotic spindle functions and tumorigenesis

Overexpression of wildtype and mutant RHAMM$^{\Delta 163}$ in fibroblasts does not promote cell proliferation to similar extents

Our *in vitro* data confirmed that RHAMM binds directly to tubulin via its carboxy terminal domain and that the leucine zipper motif does not mediate this binding. To determine if this interaction was retained in cell culture and if leucine zipper mutations abolished RHAMM/mitotic spindle interactions, GFP-tagged RHAMM$^{\Delta 163}$, both wildtype and mutant forms, were expressed in 10T1/2 cell lines. Interestingly, expression of GFP fusion proteins under a strong CMV promoter resulted in cell death; hence we were unable to obtain stable transfectants. GFP fusion proteins were thus expressed under the β-actin promoter to reduce deleteriously high RHAMM expression. Stable transfectants were selected for with G418, however, under selection pressure few G418-resistant colonies showed any detectable green fluorescence and expression rapidly declined. As an alternate approach, transient expression of GFP- RHAMM$^{\Delta 163}$ was used, however, this resulted in too low of an expression to be useful. Thus assessing the direct effects of mutant RHAMM$^{\Delta 163}$ expression on mitotic spindle interactions in culture proved to be difficult using this approach.

As an alternative method, cellular events that are relevant to mitotic spindle formation were used as surrogate markers to indirectly assess if RHAMM/mitotic spindle interactions were perturbed. Based on previous publications, we assumed that leucine

zipper mutations would abolish RHAMM/mitotic spindle interactions and that cellular events including cell proliferation, cell cycle progression, and apoptosis would be altered.

Overexpression of RHAMM mRNA and protein levels was first confirmed in established stably transfected 10T1/2 cell lines by qPCR and western blot analysis, respectively. 10T1/2 parental MEFs express low levels of endogenous RHAMM forms, including $RHAMM^{\Delta 163}$ and full-length RHAMM ($RHAMM^{FL}$). RHAMM mRNA expression in 10T1/2- $RHAMM^{\Delta 163}$, 10T1/2- $RHAMM^{\Delta 163}$-L735R, and 10T1/2- $RHAMM^{\Delta 163}$-L728A/L735R cells were significantly higher than parental 10T1/2 fibroblasts, with a ~2.6-2.8 fold increase in expression (Figure 3.3A, B**)**. Western blot analysis displayed a similar expression pattern with parental 10T1/2 fibroblasts displaying low levels of endogenous $RHAMM^{\Delta 163}$ compared to wildtype and mutant 10T1/2- $RHAMM^{\Delta 163}$ expressing cells, which displayed higher levels of ectopic $RHAMM^{\Delta 163}$. Levels of endogenous $RHAMM^{FL}$ served as the loading control (Figure 3.4).

A)

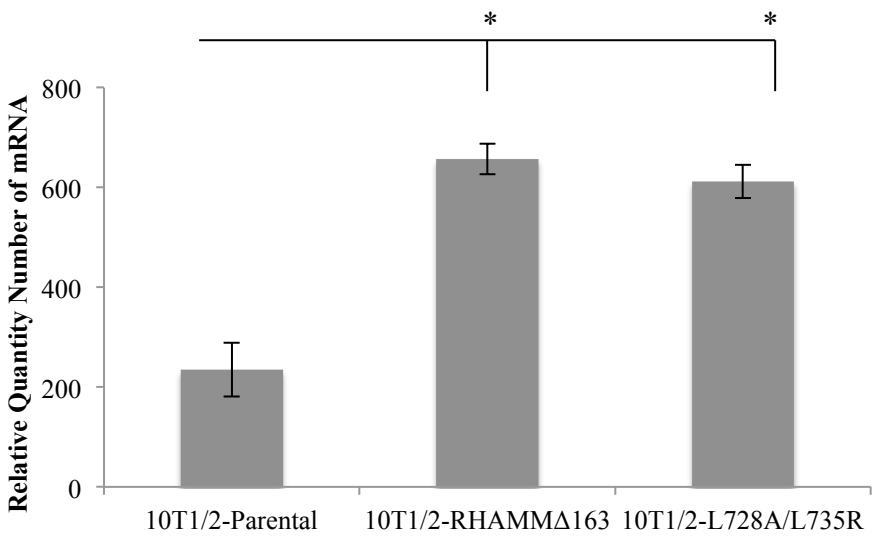
*
*
800
600
400
200
0
Relative Quantity Number of mRNA
10T1/2-Parental
10T1/2-RHAMMΔ163
10T1/2-L728A/L735R

B)

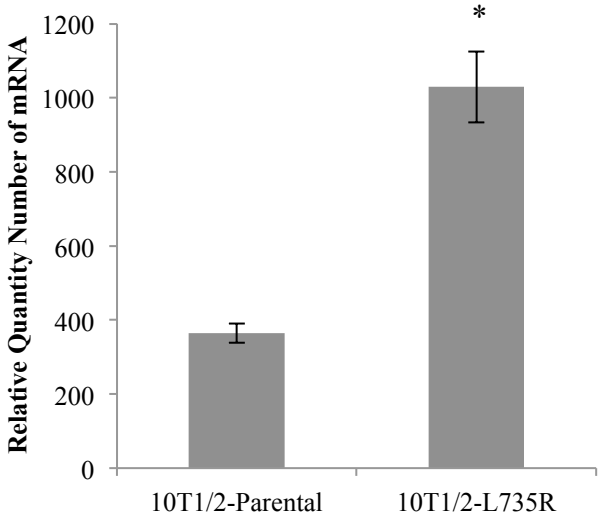
*
1200
1000
800
600
400
200
0
Relative Quantity Number of mRNA
10T1/2-Parental
10T1/2-L735R

Figure 3.3: mRNA expression levels of RHAMM in 10T1/2 MEFs

10T1/2 MEFs were transfected with RHAMM$^{\Delta 163}$, RHAMM$^{\Delta 163}$-L735A, or RHAMM$^{\Delta 163}$-L728A/L735R, and a mixed pool of transfectants were selected for using G418. cDNA from parental 10T1/2 MEFs and 10T1/2 MEFs stably expressing wildtype or mutant RHAMM$^{\Delta 163}$ were analyzed by qRT-PCR using RHAMM specific primers. Relative expression levels of the RHAMM gene were determined using the standard curve method with expression normalized to 28S mRNA. **A)** 10T1/2 MEFs expressing RHAMM$^{\Delta 163}$ and L728A/L735R showed a 2.8 and 2.6 fold increase in RHAMM expression, respectively, compared to control 10T1/2 MEFs which express low levels of endogenous RHAMM **B)** 10T1/2 MEFs expressing L735R showed a 2.8 fold increase in RHAMM expression compared to control 10T1/2 MEFs. Data represents the mean of n=3 replicates ±S.E; *$p<0.05$

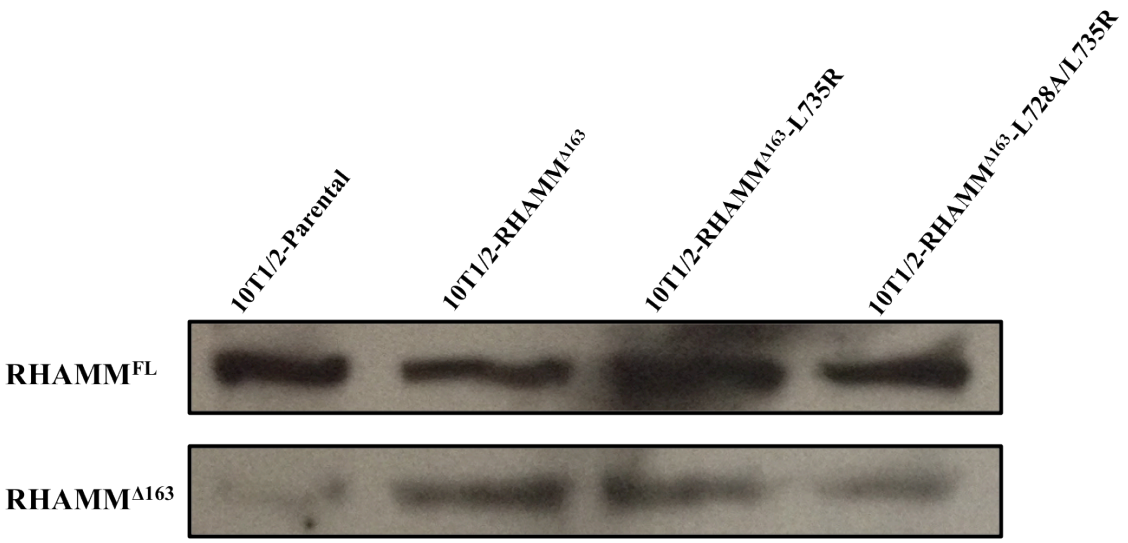

Figure 3.4: RHAMM$^{\Delta163}$ protein levels in 10T1/2 fibroblasts

10T1/2 MEFs were transfected with w RHAMM$^{\Delta163}$, RHAMM$^{\Delta163}$-L735A, or RHAMM$^{\Delta163}$-L728A/L735R, and a mixed pool of transfectants were selected for using G418. Whole cell lysates were prepared and analyzed by western blotting. RHAMM$^{\Delta163}$ protein expression was determined by hybridization with a monoclonal RHAMM antibody recognizing sequences in the N-terminus. As expected, 10T/12 parental cells express low levels of endogenous RHAMM$^{\Delta163}$ compared to ectopic overexpression of RHAMM$^{\Delta163}$ in established stable 10T1/2 cell lines. Expression of endogenous full-length RHAMM (RHAMM^{FL}) was used as a loading control as this form is detected using the same RHAMM antibody

The first aim was to determine whether ectopic overexpression of RHAMM$^{\Delta 163}$ promoted cell proliferation in 10T1/2 MEFs by using the innate reducing ability of cells to convert exogenously added alamarBlue reagent, resazurin, into a measurable fluorescent product, resorufin. Results unexpectedly showed that the proliferation of 10T1/2-RHAMM$^{\Delta 163}$ fibroblasts was significantly reduced over the duration of 96 hours compared to 10T1/2 parental MEFs. The greatest difference in proliferation was seen at 48 and 72 hours post cell plating (Figure 3.5A).

RHAMM$^{-/-}$ fibroblasts provide a cleaner system to study the effects of RHAMM$^{\Delta 163}$ on cell proliferation since they lack endogenous RHAMM. Similar to 10T1/2 MEFs, stable overexpression of RHAMM$^{\Delta 163}$ in RHAMM$^{-/-}$ cells showed a decrease in cell proliferation (Figure 3.6A).

Overexpression of RHAMM$^{\Delta 163}$-L735R or RHAMM$^{\Delta 163}$-L728A/L735R in 10T1/2 MEFs similarly decreased proliferation when compared to parental fibroblasts (Figure 3.5B). However, they did not alter proliferation when compared to RHAMM$^{\Delta 163}$; L735R growth was not significantly different from RHAMM$^{\Delta 163}$, while L728A/L735R expressing fibroblasts showed a subtle, yet significant, increase in proliferation at 24, 48, and 72 hours, though the significance of these results were variable between experiments **(**Figure 3.5C). Furthermore, expression of L735R mutant in RHAMM$^{-/-}$ (KO) cells showed significant, yet minor affects on cell proliferation compared to RHAMM$^{\Delta 163}$ expressing cells (Figure 3.6B).

Collectively, these results demonstrate that overexpression of RHAMM$^{\Delta 163}$ inhibits rather than stimulates proliferation of 10T1/2 and RHAMM$^{-/-}$ fibroblasts and disrupting the

leucine zipper does not further affect this function. However, expression of RHAMM$^{\Delta 163}$-L728A/L735R significantly increased proliferation compared to RHAMM$^{\Delta 163}$ suggesting a plausible role for specific leucine residues, but not a leucine zipper function in RHAMM effects on proliferation.

A)

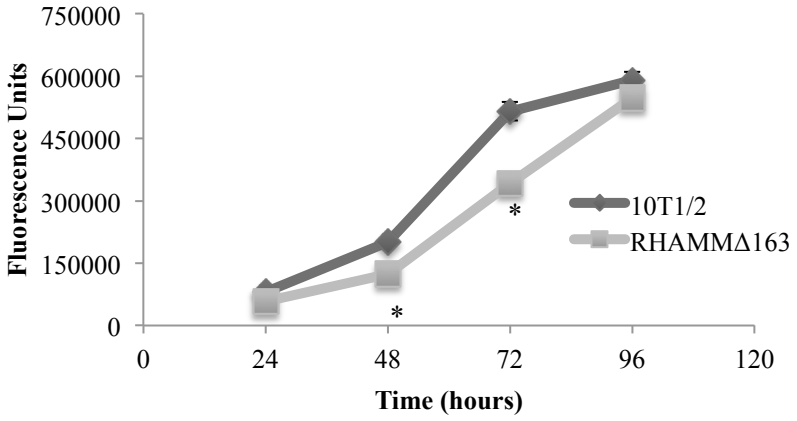
750000
600000
450000
300000
150000
0
Fluorescence Units
0
24
48
72
96
120
Time (hours)
10T1/2
RHAMMΔ163
*
*

B)

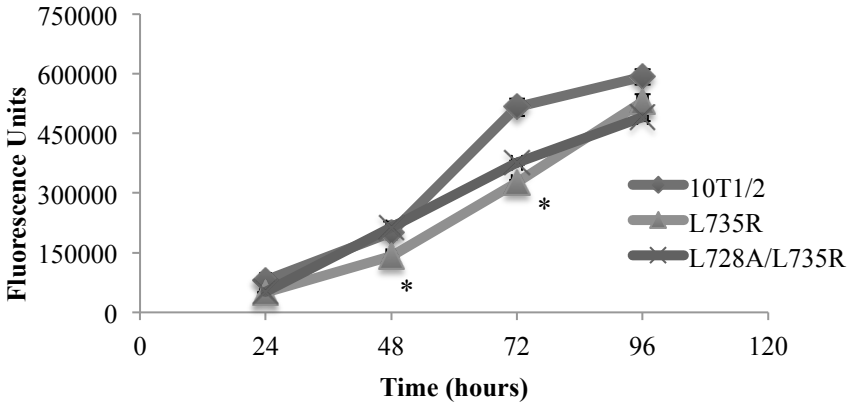
750000
600000
450000
300000
150000
0
Fluorescence Units
0
24
48
72
96
120
Time (hours)
10T1/2
L735R
L728A/L735R
*
*

C)

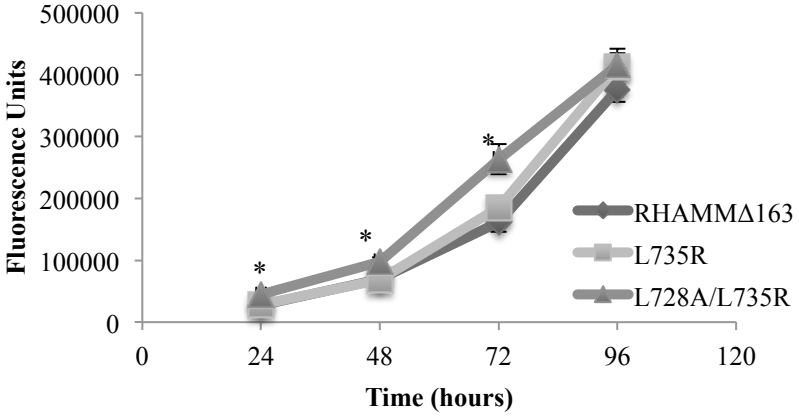
500000
400000
300000
200000
100000
0
Fluorescence Units
0
24
48
72
96
120
Time (hours)
RHAMMΔ163
L735R
L728A/L735R
*
*
*

Figure 3.5: Overexpression of wildtype and mutant RHAMM$^{\Delta 163}$ in 10T1/2 fibroblasts does not promote cell proliferation

Cell proliferation of parental 10T1/2 MEFs and 10T1/2 fibroblasts expressing RHAMM$^{\Delta 163}$, RHAMM$^{\Delta 163}$-L735R, and RHAMM$^{\Delta 163}$-L728A/L735R was assessed by alamarBlue reagent. **A)** Overexpression of RHAMM$^{\Delta 163}$ in 10T1/2 MEFs decreases cell proliferation over the course of 96 hours. **B)** Expression of RHAMM$^{\Delta 163}$-L735R or RHAMM$^{\Delta 163}$-L728A/L735R, in 10T1/2 MEFs similarly decreases cell proliferation. **C)** Overexpression of RHAMM$^{\Delta 163}$-L735R has subtle affects on cell proliferation compared to RHAMM$^{\Delta 163}$. The results represent mean fluorescence units ±S.E of n=9 replicates. * $p<0.05$

A)

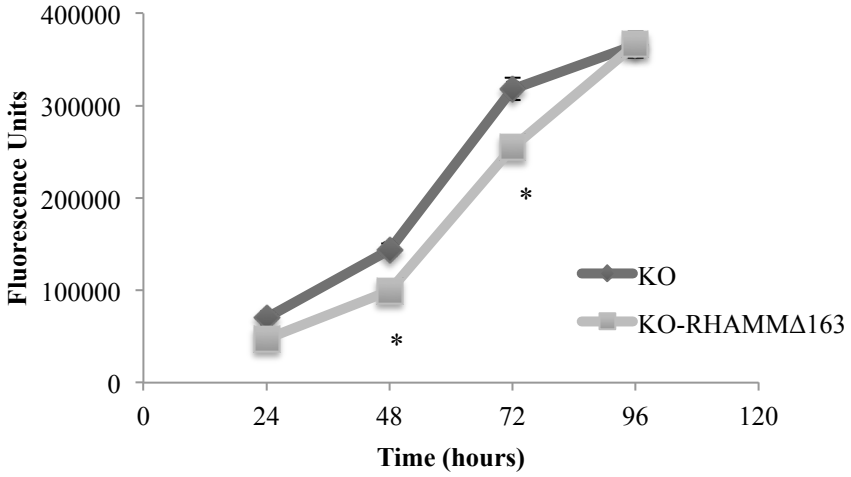
400000
300000
200000
100000
0
Fluorescence Units
0
24
48
72
96
120
Time (hours)
KO
KO-RHAMMΔ163
*
*

B)

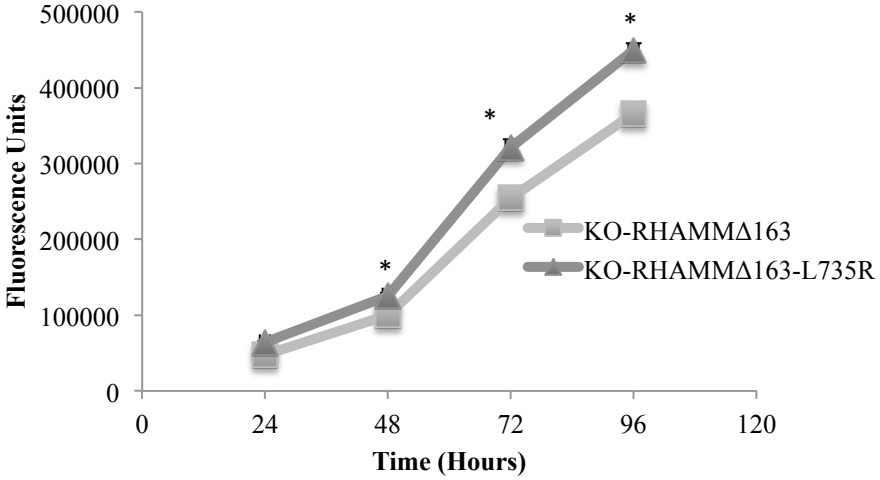
500000
400000
300000
200000
100000
0
Fluorescence Units
0
24
48
72
96
120
Time (Hours)
KO-RHAMMΔ163
KO-RHAMMΔ163-L735R
*
*
*

Figure 3.6: Expressing RHAMM$^{\Delta 163}$ –L735R in RHAMM$^{-/-}$ fibroblasts does not drastically alter cell proliferation

Cell proliferation of KO- RHAMM$^{\Delta 163}$ and KO- RHAMM$^{\Delta 163}$–L735R cells were assessed using alamarBlue reagent. **A)** Overexpression of RHAMM$^{\Delta 163}$ in RHAMM$^{-/-}$ fibroblasts results in a decrease in cell proliferation over 96 hours. **B)** Overexpression of RHAMM$^{\Delta 163}$-L735R has subtle affects on cell proliferation. The results represent mean fluorescence units of n=9 replicates per cell per cell line ±SE *$p<0.05$

Overexpression of wildtype or mutant RHAMM$^{\Delta 163}$ does not alter cell cycle progression when expressed in 10T1/2 MEFs

RHAMM expression is tightly regulated during the cell cycle and levels of RHAMM peak at G2/M. Mutating the mitotic spindle-binding region of RHAMM would thus be expected to impact cell cycle progression. Previous studies have shown that overexpression of RHAMM isoforms in certain cell lines results in a mitotic arrest at G2/M (19). We therefore first determined if overexpression of RHAMM$^{\Delta 163}$, in 10T1/2 mouse embryonic fibroblasts similarly blocked cell cycle progression.

Cell cycle profiles of asynchronous 10T1/2- RHAMM$^{\Delta 163}$ MEFs, as demonstrated by DNA content using PI staining and subsequent flow cytometry, revealed similar profiles with distinct G1, S, and G2/M peaks as parental 10T1/2 MEFs at 24 hours post culturing (Figure 3.7A,B**)**. The percentage of cells in each stage of the cell cycle did not differ significantly between the two populations (Figure 3.7C). Results suggest that a 2.8 fold increase in RHAMM mRNA expression was not sufficient to arrest the cells in mitosis.

Likewise, expression of RHAMM$^{\Delta 163}$-L735R or RHAMM$^{\Delta 163}$-L728A/L735R did not significantly alter 10T1/2 cell cycle progression when compared to either parental cells or RHAMM$^{\Delta 163}$ expressing fibroblasts. The percentages of cells in the different stages of the cell cycle—G1, S and G2/M—were not significantly different between the different populations (Figure 3.7C), suggesting leucine zipper mutations do not impact cell cycle progression.

A)

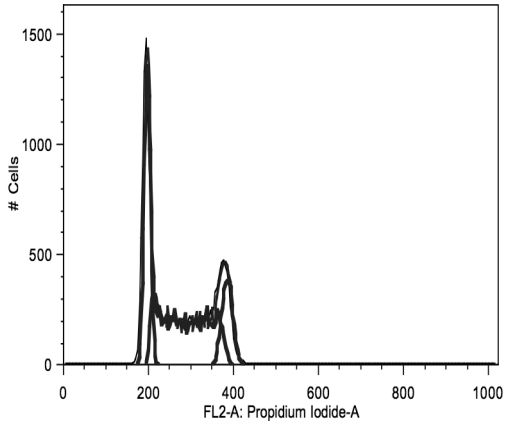

10T1/2 Parental

B)

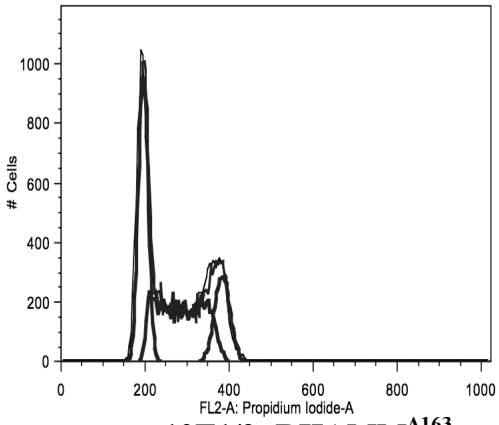

10T1/2- RHAMM$^{\Delta 163}$

C)

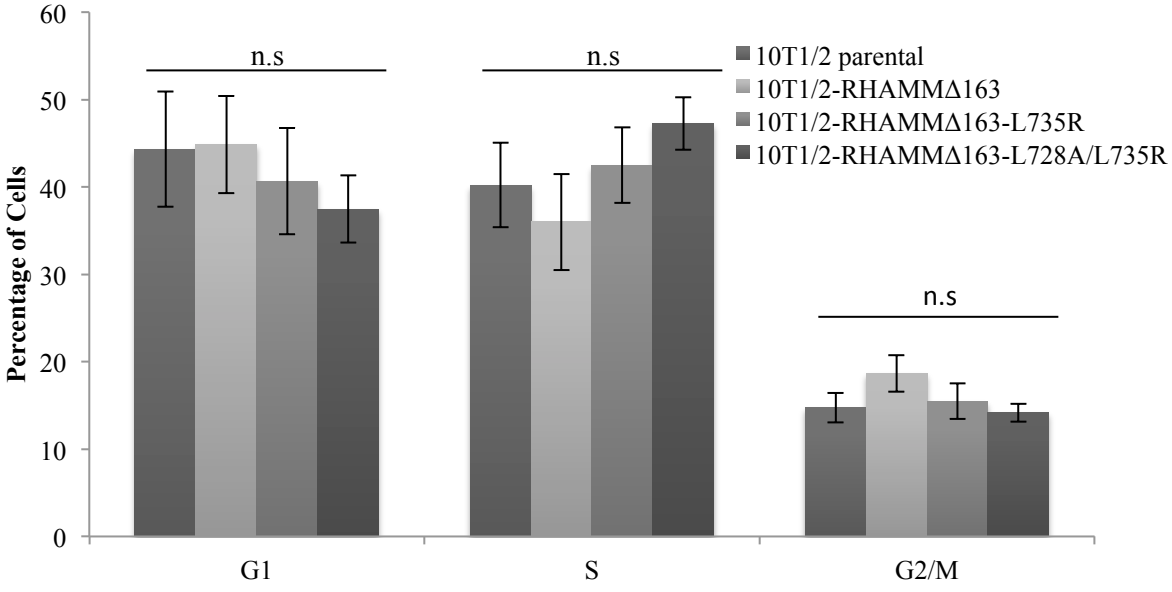

Figure 3.7: Overexpression of wildtype or mutant RHAMM$^{\Delta 163}$ in asynchronous 10T1/2 fibroblasts does not alter cell cycle progression

DNA content of asynchronous 10T1/2 parental and 10T1/2- RHAMM$^{\Delta 163}$ cells, both wildtype and mutant (L735R or L728A/L735R), was stained with propidium iodide and analyzed by flow cytometry. Representative histograms of DNA content during the cell cycle of **A)** 10T1/2 parental cells and **B)** 10T/12- RHAMM$^{\Delta 163}$ transfected cells. Grey outline of each graph represents the Watson-Pragmatic model of cell cycle analysis **C)** Cell cycle distribution of 10T1/2 parental and 10T1/2 cells expressing RHAMM$^{\Delta 163}$, RHAMM$^{\Delta 163}$-L735R, and RHAMM$^{\Delta 163}$-L728A/L735R expressed as a percent obtained via the Watson Pragmatic model. Overexpression of RHAMM$^{\Delta 163}$ –L735R or RHAMM$^{\Delta 163}$ –L735R/L728A/L735R had no effect on cell cycle progression. Each column represents the mean of n=4 independent experiments ± S.E; n.s indicates no statistical significance between 10T1/2 parental cells or 10T1/2- RHAMM$^{\Delta 163}$ cells in the same phases of the cell cycle, $p>0.05$

Expression of mutant RHAMM$^{\Delta 163}$ forms in 10T1/2 MEFs does not affect cell apoptosis

Since RHAMM is known to play a role in mitotic spindle integrity, we speculated that mutations in the putative mitotic spindle-binding region would contribute to aberrations during spindle assembly. Consequently, an accumulation of defects in mitotic spindle assembly has the potential to trigger the apoptotic machinery. To assess if mutations made in the leucine zipper of RHAMM would alter the number of apoptotic cells, levels of apoptosis of 10T1/2 MEFs stably expressing RHAMM$^{\Delta 163}$, L735R or L28A/L735R were assessed. The presence of cytoplasmic histone-associated DNA fragments that were present after cell death was quantified from cell lysates of both wildtype and mutant 10T1/2-RHAMM$^{\Delta 163}$ cells using ELISA. Expression of L735R or L728A/L735R RHAMM$^{\Delta 163}$ did not induce changes in apoptosis when compared to RHAMM$^{\Delta 163}$ expressing MEFs (Figure 3.8**)**. This suggests that mutations in the leucine zipper sequence of RHAMM do not have an effect on cell death.

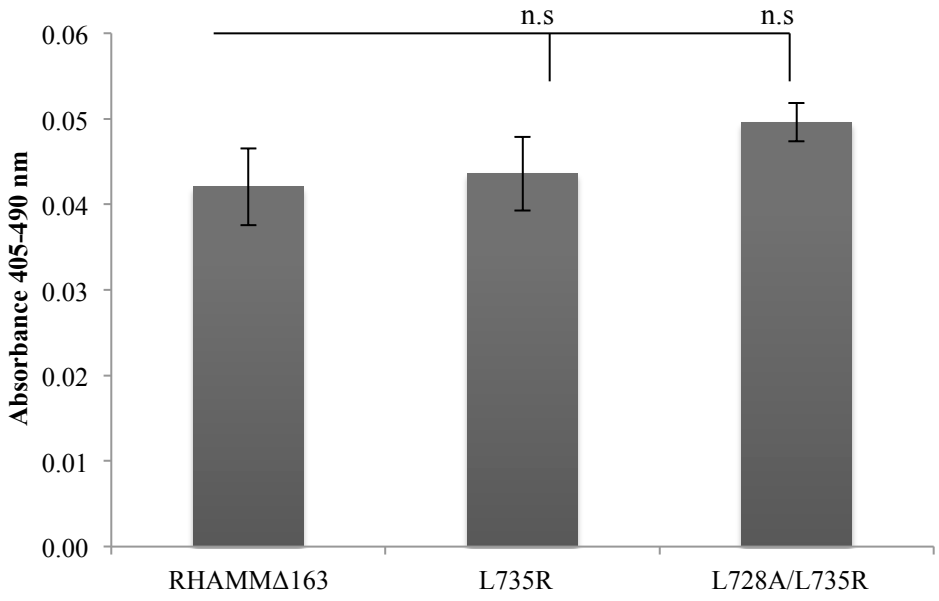

Figure 3.8: Expression of mutant RHAMM$^{\Delta 163}$ forms in 10T1/2 MEFs does not affect apoptosis

Lysates of 10T1/2-RHAMM$^{\Delta 163}$, 10T1/2- RHAMM$^{\Delta 163}$ -L735R and 10T1/2-RHAMM$^{\Delta 163}$ -L728A/L735R fibroblasts were analyzed 24 hours post seeding to determine levels of apoptosis. Cell death was assessed using an ELISA assay detecting mono- and oligonucleosomes using anti-histone and anti-DNA antibodies. Each column represents the mean absorbance of n=4 replicates ± S.E; n.s indicates no statistical significance from RHAMM$^{\Delta 163}$, $p>0.05$

Mutant 10T1/2- RHAMM$^{\Delta 163}$ expressing fibroblasts retain the ability to form tumor xenografts in immune compromised mice

Our lab has shown that overexpression of RHAMM$^{\Delta 163}$ in 10T1/2 mouse embryonic fibroblasts results in cell transformation as shown by tumor formation in immune compromised mice (95) and this ability has been linked to genomic instability generated by aberrant mitosis in multiple myeloma (81). Cell transformation was used as a surrogate marker to assess a change in tumor formation if RHAMM/mitotic spindle interactions were altered. To determine whether mutant RHAMM$^{\Delta 163}$ retains oncogenic effects and in turn to assess if a mutated leucine zipper affects the transforming potential, 10T1/2 MEFs expressing RHAMM$^{\Delta 163}$, RHAMM$^{\Delta 163}$ -L735R or RHAMM$^{\Delta 163}$ -L728A/L735R were subcutaneously injected in the flank of NSG mice and tumor growth was monitored. Both 10T1/2- RHAMM$^{\Delta 163}$-L735R and 10T1/2- RHAMM$^{\Delta 163}$-L728A/L735R retain their ability to form tumor xenografts (Table 3.3). Tumors were excised and their wet weights determined (see Appendix A). The differences in tumor weights, however, could not be compared as tumor-forming capabilities varied between experiments. These results suggest that disruption of the leucine zipper does not have strong effects on tumorigenesis as mutant RHAMM$^{\Delta 163}$ forms still formed tumor xenografts in immune compromised mice.

Table 3.3: Summary of transforming abilities of 10T1/2 fibroblasts

Cell Type	Transforming?
10T parental MEFs	NO
10T Empty Vector	NO
10T RHAMM$^{\Delta 163}$ MEFs	YES
10T RHAMM$^{\Delta 163}$ –L735R MEFs	YES
10T RHAMM$^{\Delta 163}$ –L728A/L735R MEFs	YES

10T1/2 parental and RHAMM$^{\Delta 163}$ expressing (wildtype or mutant) fibroblasts were subcutaneously injected in the flank of NSG mice and tumor growth was monitored over 6 weeks. L735R and L728A/L735R fibroblasts retain the ability to transform cells and form tumors in mice. Ability to transform is based on tumor formation seen in triplicate mice per cell line injected. 10T1/2 parental and 10T1/2 empty vector cells serve as the negative controls, while 10T1/2 RHAMM$^{\Delta 163}$ served as the positive control

3.3 Objective 3: Assessing the role of RHAMM $^{\Delta 163}$ in directed cell migration

Mutant RHAMM$^{\Delta 163}$ expression in RHAMM$^{-/-}$ MEFs causes defects in cell migration due to loss of directionality

Tight control of centrosomal function is essential not only for proper cell division, but also for directed cell migration. Defects in the function, structure, number, or position of centrosomes can contribute to aberrant cell migration and division due to loss of polarity.

The carboxy terminal leucine zipper of RHAMM is known to function in binding to and modulating the position of centrosomes (19, 84). RHAMM also plays an essential role during cell migration and its genetic deletion results in an inability of cells to resurface scratch wounds with a concomitant decrease in motility rate, which can be rescued by RHAMM expression. To determine the effects of L735R-RHAMM$^{\Delta 163}$ expression on directed cell migration and if these cells were able to rescue the motility defects in RHAMM$^{-/-}$ MEFs, we conducted scratch wound assays on RHAMM$^{-/-}$ cells stably expressing RHAMM$^{\Delta 163}$ or RHAMM$^{\Delta 163}$-L735R. This assay assesses the ability of cells to move into a cell-free area created by scraping the center of a confluent monolayer of cells. Time-lapse analysis of the scratch-wounds revealed significantly fewer mutant RHAMM$^{\Delta 163}$-L735R cells present in the scratches compared to RHAMM$^{\Delta 163}$ cells (Figure 3.9A-C). The differences seen in cell migration were not due to differences in cell growth, as expression of RHAMM$^{\Delta 163}$-L735R in RHAMM$^{-/-}$ cells did not inhibit cell proliferation (Figure 3.6B). These results suggest that a mutation in the leucine zipper of RHAMM$^{\Delta 163}$ (L735R) impacts the ability to recover scratch wounds.

A)

KO-RHAMM$^{\Delta 163}$

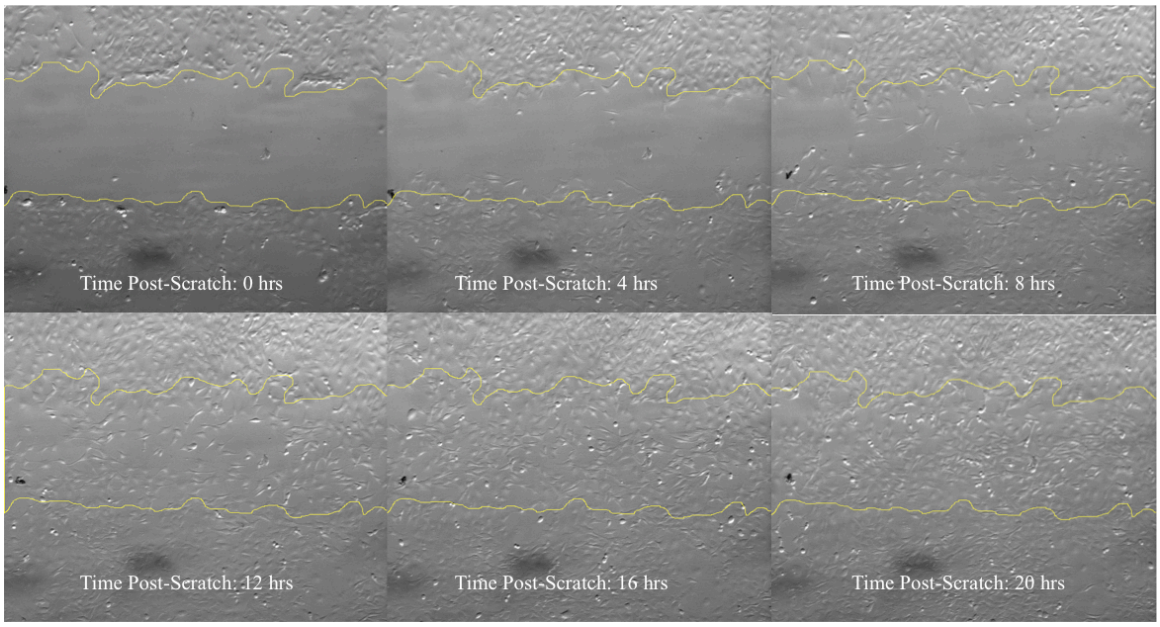

B)

KO- RHAMM$^{\Delta 163}$ –L735R

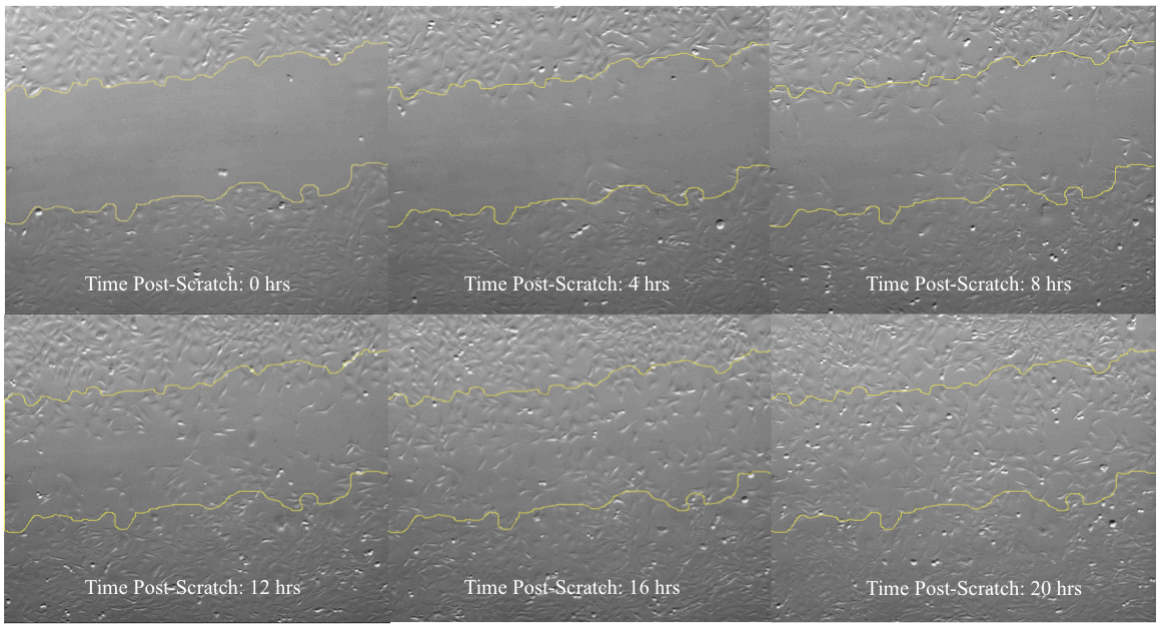

C)

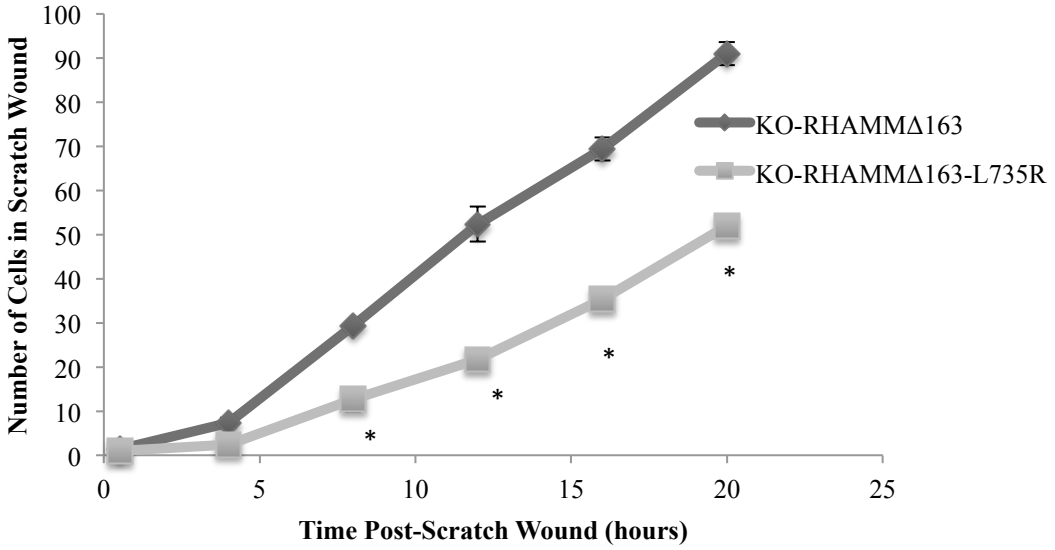

Figure 3.9: RHAMM$^{\Delta 163}$ –L735R expression in RHAMM$^{-/-}$ MEFs causes defects in cell migration

Confluent monolayers of RHAMM$^{-/-}$ (KO) MEFs stably expressing RHAMM$^{\Delta 163}$or RHAMM$^{\Delta 163}$-L735R were cultured overnight and subsequently scratched using a sterile pipette tip. Wound closure was assessed by time-lapse microscopy at the indicated time points at 4x magnification. Images from a representative experiment of **A)** KO-RHAMM$^{\Delta 163}$ and **B)** KO-RHAMM$^{\Delta 163}$–L735R at different time points are shown. **C**) Fewer number of KO-RHAMM$^{\Delta 163}$–L735R cells migrated into the scratch wound. Data represents the mean of three randomized areas of the scratched wound with error bars representing standard error. * $p<0.05$

Furthermore, the defects in migration could account for a reduced rate of motility or altered directional movement. To identify if RHAMM$^{\Delta 163}$-L735R fails to promote speed or direction of movement, the motility of individual cells from the scratch wound assays were tracked using vector analysis. Results show that RHAMM$^{\Delta 163}$-cells migrated further distances away from the cell origin compared to RHAMM$^{\Delta 163}$-L735R expressing cells (Figure 3.10A-C). Whereas RHAMM$^{\Delta 163}$ cells migrated into the wound, the directionality was disturbed in RHAMM$^{\Delta 163}$-L735R cells, which traveled back into the monolayer resulting in a decrease in distance migrated from the cell origin (Figure 3.10C). The L735R mutant did not affect overall distance travelled by the cells and therefore did not have a significant impact on rate of motility (Figure 3.10D). Note that RHAMM-/- fibroblasts are directionally and speed impaired and these defects are rescued by RHAMM$^{\Delta 163}$ expression. Thus, mutating the leucine zipper of RHAMM$^{\Delta 163}$ rescued speed, but did not rescue the directionality defects of RHAMM$^{-/-}$ fibroblasts.

A) **KO- RHAMM$^{\Delta 163}$**

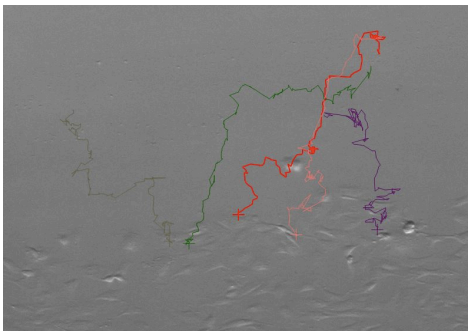

B) **KO- RHAMM$^{\Delta 163}$-L735R**

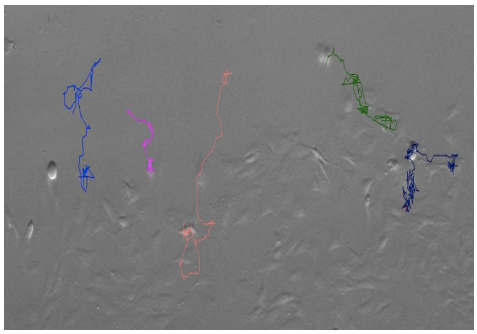

C)

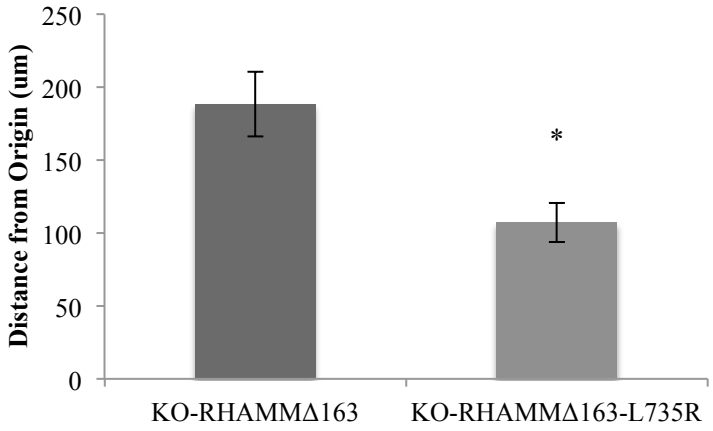

D)

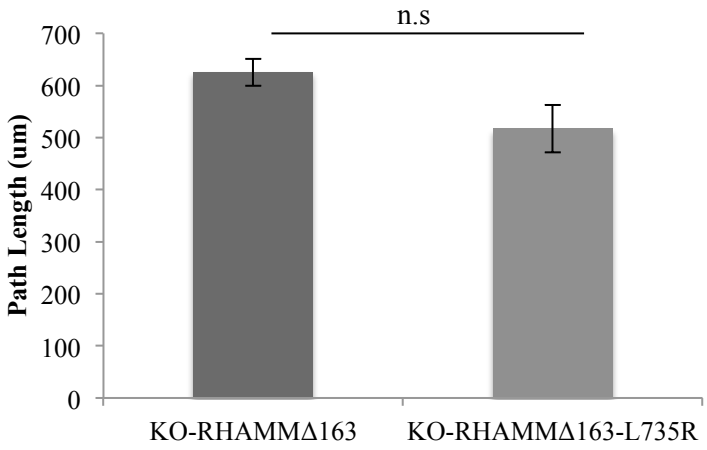

Figure 3.10: KO-RHAMM$^{\Delta 163}$-L735R fibroblasts migrate shorter distances from the cell origin

Confluent monolayers of RHAMM$^{-/-}$ (KO) MEFs stably expressing RHAMM$^{\Delta 163}$or RHAMM$^{\Delta 163}$-L735R were cultured overnight and subsequently scratched using a sterile pipette tip. Wound closure was assessed by time-lapse microscopy overnight at 4x magnification. The motility of individual cells was tracked using NIS Elements imaging software. Representative images of the path of individual **A)** KO-RHAMM$^{\Delta 163}$ and **B)** KO-RHAMM$^{\Delta 163}$-L735R- fibroblasts as they migrate into the scratch wounds **C)** Average distance of cells at the wound edge as they travel from cell origin **D)** Average path length fibroblasts traveled from wound edge Mean ±SE, n=10, *$p<0.05$

Percentage of KO-RHAMM$^{\Delta 163}$-L735R cells with n>1 centrosome was greater than KO- RHAMM$^{\Delta 163}$ –rescued cells

Our results suggested that there was a migration defect when expressing RHAMM$^{\Delta 163}$ mutated in the leucine zipper region. Since this region is known to bind to centrosomes and regulates their structure/function, we next determined if centrosome number or location within the RHAMM$^{\Delta 163}$ –L735R expressing cells was altered.

KO, KO-RHAMM$^{\Delta 163}$, and KO-RHAMM$^{\Delta 163}$-L735R expressing cells were seeded on coverslips and confluent monolayers were scratched and allowed to recover before staining the cells with a centrosome marker, pericentrin, and DAPI to stain the nucleus. Cells at the wound edge were imaged (Figure 3.11A-D) and the number and location of centrosomes were quantified. The percentage of non-dividing cells with more than one centrosome was greatest in KO- RHAMM$^{\Delta 163}$-L735R cells **(**Figure 3.11E). Additionally, the location of the centrosome with respect to the cell nucleus was altered in KO-RHAMM$^{\Delta 163}$-L735R cells in that there were a greater percentage of cells with centrosomes behind the nucleus; however, it was not significantly different from KO-RHAMM$^{\Delta 163}$ or KO cells (Figure 3.11F). These results suggest that RHAMM leucine zipper may play a functional role in regulating centrosome number, but not in centrosome placement/position.

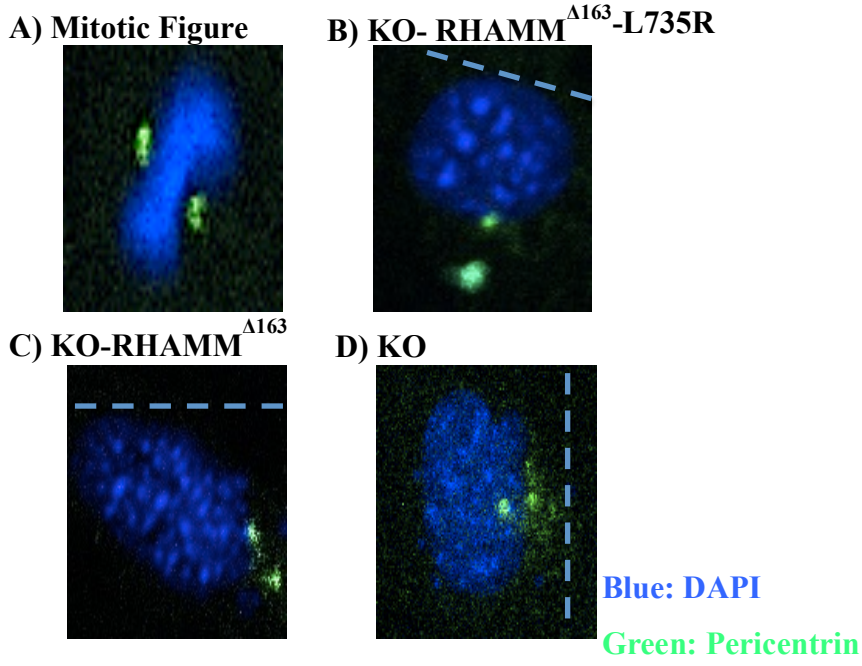
A) Mitotic Figure
B) KO- RHAMM$^{\Delta 163}$-L735R
C) KO-RHAMM$^{\Delta 163}$
D) KO
Blue: DAPI
Green: Pericentrin

E)

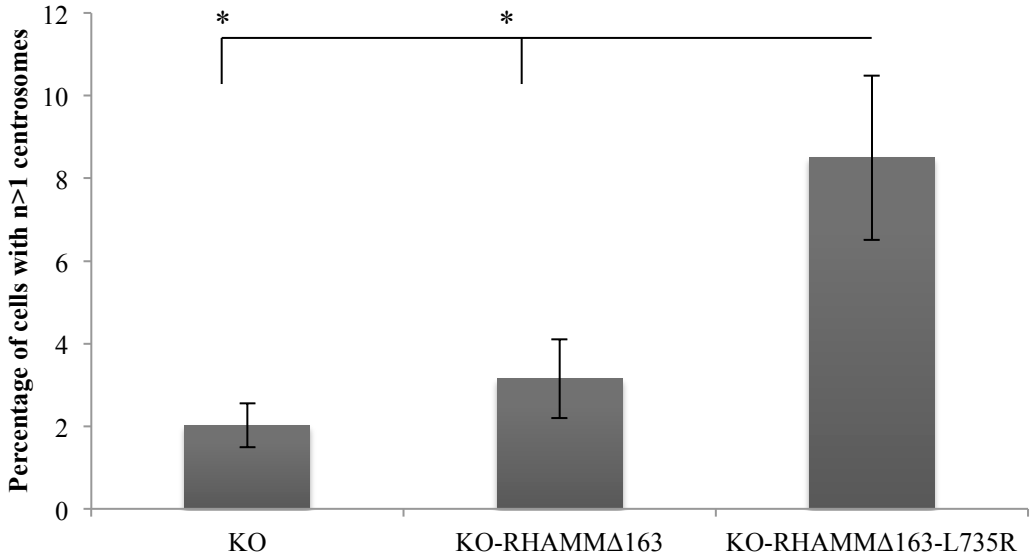
Percentage of cells with n>1 centrosomes
12
10
8
6
4
2
0
*
*
KO
KO-RHAMMΔ163
KO-RHAMMΔ163-L735R

F)

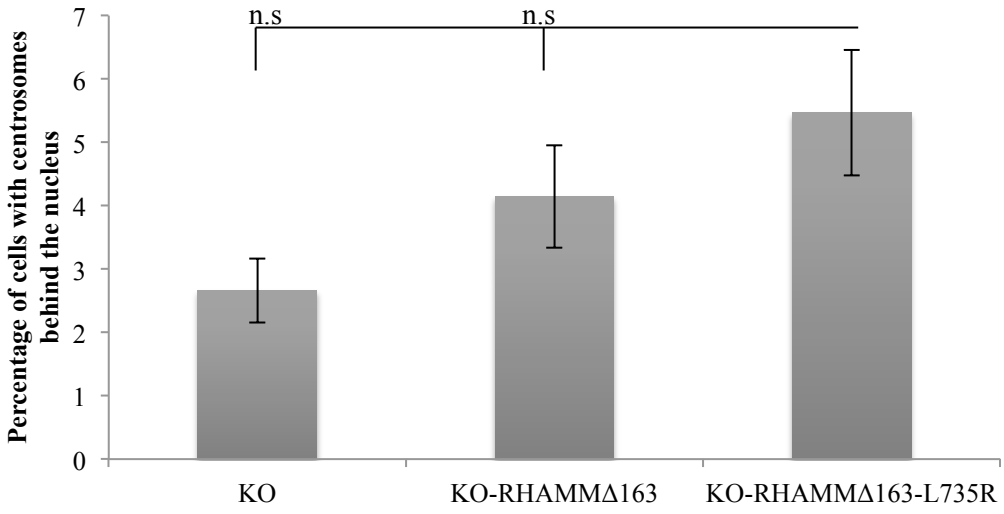

Figure 3.11: The percentage of cells with n>1 centrosome is greatest in KO-RHAMM$^{\Delta 163}$-L735R

KO, KO- RHAMM$^{\Delta 163}$, and KO- RHAMM$^{\Delta 163}$-L735R expressing fibroblasts were grown to confluency overnight and subsequently scratched using a sterile pipette tip. Cells were fixed and stained with the centrosome marker, pericentrin, and DAPI to visualize the nucleus. Cells at the wound edge were imaged at 20x magnification and analyzed. Representative immunofluorescent images of **A)** mitotic figures that were not included in the analysis, **B)** KO- RHAMM$^{\Delta 163}$-L735R, **C)** KO- RHAMM$^{\Delta 163}$ and **D)** KO parental cells, where green represents pericentrin staining, blue represents DAPI staining, and the dashed line represents the wound edge **E)** The percentage of cells with n>1 centrosome was greatest in KO- RHAMM$^{\Delta 163}$-L735R cells compared to KO or KO- RHAMM$^{\Delta 163}$ cells. **F)** The orientation of the centrosome with respect to the cell nucleus was not altered in KO- RHAMM$^{\Delta 163}$–L735R expressing cells compared to either KO-RHAMM$^{\Delta 163}$ or parental KO cells. Data represents the percentage of the average number

of counted cells: 517 KO, 488 KO- RHAMM$^{\Delta 163}$, and 483 KO- RHAMM$^{\Delta 163}$-L735R; *$p<0.05$, n.s indicates no statistical significance compared to KO or KO- RHAMM$^{\Delta 163}$ where $p>0.05$.

Chapter 4

4 General Discussion

4.1 Role of RHAMM in mitotic functions

Several reports have established a role for RHAMM in binding to and regulating mitotic spindle integrity (19, 20, 73). During the mitotic phase of the cell cycle, RHAMM localizes to the mitotic spindle along the length of microtubules and is particularly concentrated at the spindle poles (20, 69, 74). Genetic deletion or inhibition of endogenous RHAMM forms results in abnormal mitotic figures with multi-polar mitotic spindles (19, 20, 74). Silencing of RHAMM also impacts the kinetics of mitosis and results in a delay in spindle assembly and in mitotic completion (100), suggesting a role for RHAMM in mediating microtubule assembly. Further experiments reveal that RHAMM also impacts positioning of the mitotic spindle and thus helps establish an oriented bipolar spindle (93, 100).

Consistent with RHAMM's role in regulating mitotic spindle functions, the RHAMM gene is cell cycle regulated and its expression increases during G2/M, a stage in the cell cycle where a cell prepares for and subsequently undergoes mitosis (4, 111). Blocking cell surface or knockdown of intracellular RHAMM forms results in a slower progression of cells through G2/M and a fewer percentage of cells at G2/M, respectively (91, 109).

Previous literature utilizing deletion constructs of carboxyl terminal RHAMM fragments have narrowed down the last 100 amino acid residues containing a leucine zipper motif to be essential in localizing RHAMM to mitotic spindles (19). Mutational analysis of the leucine residues in the leucine zipper to arginines further revealed that this particular region serves a functional role in proper aster spindle formation in *Xenopus* egg extracts and was thus required for mitotic spindle integrity (20, 73, 100). The latter study made use of a C-terminal RHAMM peptide corresponding to the leucine zipper that when present in excess disrupts aster spindle formation. When mutated in the leucine zipper motif, however, the peptide does not display defects in spindle assembly. The effects of this regulation were dependent on the presence of BRCA1/BARD1 complex, whose role was predicted to safeguard the formation of a bipolar mitotic spindle (73, 78). The authors of the study concluded that the leucine zipper motif is therefore functionally important in regulating spindle integrity. Results from this study and other works showing that deletion of RHAMM has a similar effect on spindle integrity indicates that RHAMM levels must be tightly regulated throughout the cell cycle, since its deletion or forced high expression results in abnormal mitosis

The mechanism by which RHAMM mediates spindle pole assembly and regulation is complex, involves numerous factors, and not fully understood. The literature, however, highlights an important role for the leucine zipper motif within RHAMM's carboxyl terminus in mediating direct and indirect effects via its binding partners.

Work in our lab has demonstrated a putative mechanism by which the carboxyl terminal of RHAMM directly regulates the mitotic spindle and this is through its direct

interactions with tubulin heterodimers [microtubules] as this interaction can be competed off using a synthesized peptide containing the leucine zipper sequence (20).

Additionally, several reports have established that RHAMM/centrosome interactions, also mediated through the leucine zipper, are essential for mitotic spindle integrity in a variety of cell types (19, 84). Mutational analysis of the centrosomal binding region of RHAMM not only results in less RHAMM localized around centrosomes, but also spindle pole defects characterized by tetrapolar mitotic figures (84).

Furthermore, recent work has identified a role of RHAMM leucine zipper to be essential, although not sufficient, in mediating interactions with the spindle assembly protein factor, TPX2. This study also proposed that the major effect of RHAMM on mitotic spindle function was mediated by TPX2, which binds to the leucine residues of the leucine zipper (73, 100). RHAMM/TPX2 interactions are seen in several cell types and are important for proper microtubule and spindle assembly (100). Mutation of the three conserved leucine amino acids of the leucine zipper sequence in RHAMM to arginines disrupted TPX2 localization at the spindle poles and consequently proper activation of AURKA kinase activity(100). AURKA is an important regulator of the cell cycle and is essential for progression through mitosis (17).

Collectively, previous data suggests that RHAMM mediates binding to microtubule structures, centrosomes, and the spindle assembly protein factor TPX2 through its carboxyl terminal leucine zipper sequence and these interactions play a role in the regulation of the mitotic spindle. Although these studies established a critical role for leucine zipper sequence, they did not assess a role for its dimerization function; the

consequences of mutating only one leucine residue, which would have compromised the dimerization motif of a leucine zipper, was not reported in these studies.

With this in mind, this study first aimed to assess if RHAMM/microtubule interactions were mediated through a leucine zipper function and to ascertain if an intact leucine zipper was required for mitotic spindle integrity. The experimental approach that was taken was to disrupt the leucine zipper by site mutating single leucine residues. In doing so, we could assess if the leucine zipper function of dimerization was responsible for interactions with microtubules and the mitotic spindle.

RHAMM interactions with microtubules [tubulin heterodimers], *in vitro*, were first assessed using synthesized RHAMM peptides containing the leucine zipper, both mutated and wildtype sequences. The consequences of a mutated leucine zipper on mitotic spindle assembly in culture were not directly assessed due to the difficulty in expressing GFP-tagged RHAMM$^{\Delta 163}$. The effects of the leucine zipper mutations on RHAMM/mitotic spindle integrity were therefore examined indirectly using cell proliferation, cell cycle progression, and apoptosis as surrogate markers. Based on previous literature, it was predicted that RHAMM's interactions with microtubules and the mitotic spindle would be disrupted and that alterations in key cellular events would be evident.

Studies confirmed that RHAMM/tubulin interactions occur directly through RHAMM's carboxyl terminus, but most importantly showed that this binding was not mediated by the leucine zipper motif. Under the conditions of this study, the ability of the L735R mutant to bind to tubulin was not compromised since it bound in similar amounts as

wildtype and since wildtype RHAMM peptide retained an ability to compete with L735R for binding to tubulin. RHAMM/tubulin interactions therefore do not require dimerization through a leucine zipper; however, the C-terminal RHAMM peptide used in this assay contains a site for microtubule binding.

Furthermore, studies showed that disruption of the leucine zipper motif did not appear to have significant effects on mitotic spindle functions as assessed using the surrogate markers of cell proliferation, cell cycle progression and apoptosis.

A minor inhibition of proliferation was seen in RHAMM$^{\Delta 163}$ –transfected cells, however, the differences in proliferation between RHAMM$^{\Delta 163}$-L735R, RHAMM$^{\Delta 163}$-L728A/L735R, and RHAMM$^{\Delta 163}$ –expressing fibroblasts were very subtle in both 10T1/2 and RHAMM$^{-/-}$ cell backgrounds. There were, however, slight differences observed in cell growth between L735R- and L728A/L735R-RHAMM$^{\Delta 163}$ forms. These disparities, combined with our studies showing the apparent reversion of the third leucine in the leucine zipper region under selection pressure, predict a functional role of individual leucine residues as opposed to a leucine zipper function during cellular processes. The leucine zipper domain partially overlaps with the ERK docking site and the HA binding region and thus mutation of specific residues could impact on these functions, as RHAMM dependent ERK activation and RHAMM-HA interactions are known to mediate cell proliferation in numerous cell backgrounds (67, 109, 130, 131).

In addition, RHAMM$^{\Delta 163}$ did not alter 10T1/2 cell cycle progression compared to parental cells and disrupting the leucine zipper via expression of L735R or L728A/L735R did not modify the percentage of cells in each stage of the cell cycle. Given that

RHAMM is tightly regulated throughout the cell cycle and peaks at G2/M, if mitotic spindle assembly were compromised due to disrupted RHAMM/mitotic spindle interactions, a block in the mitotic phase of the cell cycle would be evident. Cells would be expected to arrest at G2/M, however this did not seem likely given our data. Furthermore, while we did not look at the cell cycle profile of synchronized cells, it is possible that these mutations impact the rate of cell cycle progression in a minor way, which has been shown to be RHAMM regulated (100).

Data presented here further suggests that mutations in the leucine zipper motif do not impact apoptosis since levels of cell death did not differ between wildtype and mutant RHAMM$^{\Delta 163}$-transfected 10T1/2 cells. Defects in mitotic spindle assembly or regulation have the potential to trigger the apoptotic machinery (84), but this did not appear likely in these studies.

The conflicting data in the literature pertaining to RHAMM's role during cell proliferation and cell cycle progression could partially be attributed to the levels of RHAMM protein expression and to the numerous RHAMM isoforms present in cell lines and in human cancers. The levels of spindle assembly protein factors must be finely tuned since abundance or inhibition can abrogate their function and regulation of the mitotic spindle (132). Certainly, RHAMM protein levels could contribute to the differences between the work presented here and previous studies showing that cells arrest at G2/M when RHAMM was ectopically overexpressed. For example, this study showed that 2.8-fold overexpression of RHAMM does not have an impact on the percentage of cells in different stages of the cell cycle, whereas other studies show that a 5-fold overexpression of RHAMM arrests cells in G2/M (19).

Although the mechanism underlying the expression pattern or presence of the different RHAMM isoforms is not well established, studies predict that specific forms are generated during particular responses, localize to distinctive subcellular compartments and the effects they exert are often context-dependent and cell-type specific (69, 92, 94). Additionally, previous works often fail to indicate which RHAMM isoform is being studied/investigated, thus making it difficult to establish the specific functions of each RHAMM form and to elucidate the effects they have during particular cell processes.

The discrepancy in cell proliferation seen in this study and previous work showing RHAMM either promotes or has no effect on cell proliferation may largely be due to differences in cell backgrounds. Studies showing no effect on cell proliferation when RHAMM expression is downregulated do, however, show that cell migration and invasion is inhibited in invasive breast cancer cell lines (133).

The proliferation data on fibroblasts in this study, however, are consistent with previous literature suggesting that RHAMM overexpression does not promote cell growth and may even have an inhibitory effect on proliferation (117). This effect is quite surprising and unexpected given that overexpression of wildtype and mutant RHAMM$^{\Delta 163}$ forms transformed 10T1/2 fibroblast cell lines and formed tumors when cells were injected in NOG immune compromised mice. While this was not the major focus of this study, these results suggest that the effect of RHAMM$^{\Delta 163}$ isoform on 10T1/2 cell transformation is therefore unrelated mechanistically to cell proliferation. To our knowledge, this is the first study relating the tumorigenic properties of RHAMM$^{\Delta 163}$ isoform in 10T1/2 MEFs to cell proliferation.

4.2 Functions of RHAMM in directed cell migration

RHAMM also plays an essential role during cell migration. Given that RHAMM binds to centrosomes via the leucine zipper motif and that an intact centrosome is required for proper cell migration (19, 42), the second aim of this thesis was to determine if RHAMM mutated in the leucine zipper impacts directed cell motility. An underlying defect seen in RHAMM$^{-/-}$ fibroblasts is their inability to resurface scratch wounds due to their decreased rate of motility compared to wildtype or RHAMM rescued counterparts (64). The defects seen in migration are known to be due to aberrant activation of ERK1,2, but also were hypothesized to be a result of defects in centrosome function (64). Centrosomes are the main constituents of the MTOC and play an integral role during directed cell migration by polarizing the cell and positioning the MTOC in the direction of migration relative to the cell nucleus (124). RHAMM has been shown to not only regulate the position and function of centrosomes, but also cell polarization during migration (124).

RHAMM$^{\Delta 163}$-L735R-transfected RHAMM$^{-/-}$ fibroblasts showed a defect in cell migration that was characterized by fewer migrating cells into the scratch wounds and that was not attributed to a difference in cell proliferation. The alteration in migration could account for a reduced cell motility rate or aberrant directional cell migration. Tracking the motility of individual cells at the wound edge established that L735R- RHAMM$^{\Delta 163}$ transfected fibroblasts traveled shorter distances from the cell origin, with decreased, yet comparable motility rates as RHAMM$^{\Delta 163}$ expressing cells. Whereas RHAMM$^{\Delta 163}$ – rescued cells moved into the scratch wounds, a portion of L735R- RHAMM$^{\Delta 163}$ expressing cells were directionally impaired as these cells traveled back into the

monolayer before moving into the scratch wound space. Interestingly, expression of L735R mutant resulted in the appearance of a small subset of cells with polycentrosomes during interphase. While a number of RHAMM$^{\Delta 163}$ expressing cells also had more than one centrosome, the percentages were not different from RHAMM$^{-/-}$ parental fibroblasts. Previous studies had established a role for RHAMM in regulating centrosome volume in multiple myeloma plasma cells, but not centrosome number (81). Data from this study was based on experiments showing that centrosome number was not altered when RHAMM levels were overexpressed (81). This is consistent with work presented here in that overexpression of RHAMM$^{\Delta 163}$ did not show an impact on centrosome number in RHAMM$^{-/-}$ cells, however, when mutating the centrosome binding region (i.e. leucine zipper) we saw an increase in the number of centrosomes per cell, suggesting a functional role of the leucine zipper in centrosome regulation, perhaps affecting centriolar replication. RHAMM is a known constituent of the pericentriolar material surrounding centrioles in the MTOC and regulation of PCM proteins is essential during centrosome duplication and separation; slight differences in the levels and function of PCM components have been shown to impact cell polarity (134, 135). Whether RHAMM plays a role in centrosome replication remains to be determined, but results here hypothesize that it is likely contributing and thus affecting cell directionality.

Furthermore, while the majority of L735R- RHAMM$^{\Delta 163}$ fibroblasts were front-polarized, there was a trend for a greater number of cells that were rear-polarized (i.e. centrosome behind the nucleus), however, the percentages were not drastically different from RHAMM$^{\Delta 163}$ or parental RHAMM$^{-/-}$ cells. This trend is consistent with RHAMM's

role in regulating the position of centrosomes (84) and also suggests that this regulation partially depends on an intact leucine zipper motif.

While the work presented here showed that expression of RHAMM$^{\Delta 163}$-L735R in RHAMM$^{-/-}$ increases the number of polycentrosome cells, it did not establish whether this defect is associated to the directional defects seen in cell migration. Given that centrosomes help polarize and direct the cell during migration, we predict that the centrosome defect in L735R- RHAMM$^{\Delta 163}$ cells may account for a defect in directional migration. Collectively, these results and hypothesis are supported by data showing that disrupted centrosomes in an epithelial cell line migrate at slower rates, though not significantly different from control cells, and in a disoriented direction away from the scratch wound, due to loss of polarity (42).

It is well established that polycentrosomic cells contribute to defects in spindle pole assembly during mitosis (84, 135). However, the effects of polycentrosomes during interphase on non-mitotic functions are not well known. Recent work has identified that supernumery centrosomes impact directed cell migration of endothelial cells (135). Excess centrosomes, even one extra, resulted in altered directed cell migration with reduced distance traveled from cell origin into a scratch wound. Centrosome positioning was perturbed and centrosomes were more scattered; these defects could be partially rescued by ablating excess centrosomes and were shown to be independent of mitotic functions(135).

This seemingly contradictory data suggests that polycentrome cells would result in multi-pole mitotic spindles, though it doesn't appear likely from our data. It is important to

note, however, that mitotic spindle and migration studies were investigated in 10T1/2 and RHAMM$^{-/-}$ fibroblasts, respectively. The distinctive cell backgrounds could contribute to the difference in results but warrants further investigation.

An alternate interpretation for our results is that the defect in RHAMM's regulation of centrosomes via its leucine zipper motif could have subtle affects on rate of cell cycle progression. Centrosomes begin replication during the S phase of the cell cycle, alongside DNA replication, and begin to separate during prophase of mitosis to initiate a bipolar mitotic spindle. A minor defect in the replication/separation of centrosomes could account for the presence of numerous cells with more than one centrosome. Future work will aim to investigate the contributing factors to migration defects and to elucidate RHAMM's regulation of centrosome replication during mitosis and migration.

Taken together, the data here suggests that the leucine zipper motif is critical for directed cell migration in fibroblasts. Despite mutations in the leucine zipper, expression of L735R- RHAMM$^{\Delta 163}$ was able to rescue the rate of motility defect, though not directionality of RHAMM$^{-/-}$ fibroblasts. Further studies are needed to reveal a mechanism for RHAMM leucine zipper and centrosome interaction in directed cell migration and polarity. Previous work in our lab has established a role of RHAMM in random and directed motility that is dependent on RHAMM regulated ERK activation and subcellular localization (64). Future work will examine the impact of and the levels of ERK activation in mutant RHAMM$^{\Delta 163}$-expressing fibroblasts.

4.3 Summary and future studies

Our work suggests that the mechanism by which RHAMM regulates mitotic spindle integrity is very complex and involves multiple regulatory factors. To our knowledge, this is the first RHAMM study directly assessing a role for its leucine zipper dimerization motif on mitotic spindle functions and migration. While previous literature has no doubt established a vital role for leucine zipper sequence of RHAMM in maintaining mitotic spindle integrity, results here suggest that the leucine zipper isn't functioning as a classic dimerization motif in mitotic spindle regulation. In previous studies, mutations of leucine residues to large arginine residues within this region may have altered the conformation of RHAMM protein and thus disrupted binding sites that may or may not overlap the leucine zipper region. Results presented here demonstrate that site mutating single leucine residues establish a role for the leucine zipper dimerization motif in directed cell migration.

Recent work has identified a role of the leucines in the leucine zipper region of RHAMM in TPX2 interactions and for its proper localization and activation of AURKA (100). The consequence of TPX2/AURKA mislocalization has been shown to result in abnormal mitosis, characterized by shortened/compressed mitotic spindles giving rise to mitotic failure (100, 136). As proper positioning and alignment of the spindle poles relative to each other determine spindle length (137), it is likely that RHAMM's role in maintaining spindle orientation is partially through its interactions with TPX2. Furthermore, TPX2 has functions in mitotic spindle integrity that are independent of AURKA(11) and these functions may be in part mediated through RHAMM activity. Although it is assumed,

these studies have not established whether the leucine zipper is functioning as a dimerization motif in TPX2 interactions or if it is specific to leucine residues or overlapping binding sites. It is therefore difficult to predict whether our mutations, L735R or L728A/L735R, will contribute to TPX2 mislocalization and future studies will need to address this.

Whether TPX2 is in fact regulating the major effect of RHAMM on mitotic spindles, has yet to be examined. Work in our lab has also shown that RHAMM's effect on mitotic spindle assembly is indirectly through MEK1 activity since mutant active MEK1 has the ability to rescue mitotic defects seen in RHAMM$^{-/-}$ fibroblasts.

Our studies also revealed an important role of the leucine zipper in directed cell motility, and thus future studies will need to address the role of RHAMM/TPX2 interactions on cell migration. The role of TPX2 in cell migration is an understudied area of research, but has been shown to regulate migration and invasion of colon cancer cell lines (138). A mechanism linking TPX2 and ERK, if any, with regards to mitotic spindle functions and migration will need to be elucidated. A full understanding of how RHAMM regulates these cell processes including mitosis and migration can provide insight on RHAMM's role during cancer initiation and progression.

Conclusions

Results of this study show that RHAMM directly binds tubulin heterodimers in vitro via a carboxyl terminal sequence and further, that this interaction is not mediated by the

leucine zipper dimerization motif. Evidence presented in this study suggests that disrupting the leucine zipper by site mutating single leucine residues does not affect the binding of RHAMM to tubulin and importantly has no detectable effects on mitotic spindle integrity as assessed using the surrogate markers of cell cycle progression, cell proliferation, and apoptosis. However, ablating the leucine zipper function did aberrantly increase centrosome number in interphase cells and disrupted directed cell migration, which is a centrosome function. Our results, combined with previous work, suggest a model wherein extracellular RHAMM/ERK impacts rate of motility, while intracellular RHAMM interacts with centrosomes to control directed cell migration (Figure 4.1).

Limitations

Although this study provided data based on using a surrogate approach to assess whether RHAMM/mitotic spindle interactions were abolished, studies are needed to confirm direct effects in cell culture. Surrogate markers can provide insight albeit not definite results. Furthermore, while in vitro studies displayed that point mutations in the leucine zipper region do not disrupt binding to tubulin heterodimers, in vitro, we need to confirm it in cell culture. The lack of reliable RHAMM antibodies for immunofluorescence makes it challenging since expression of GFP tagged-RHAMM in cell lines is difficult.

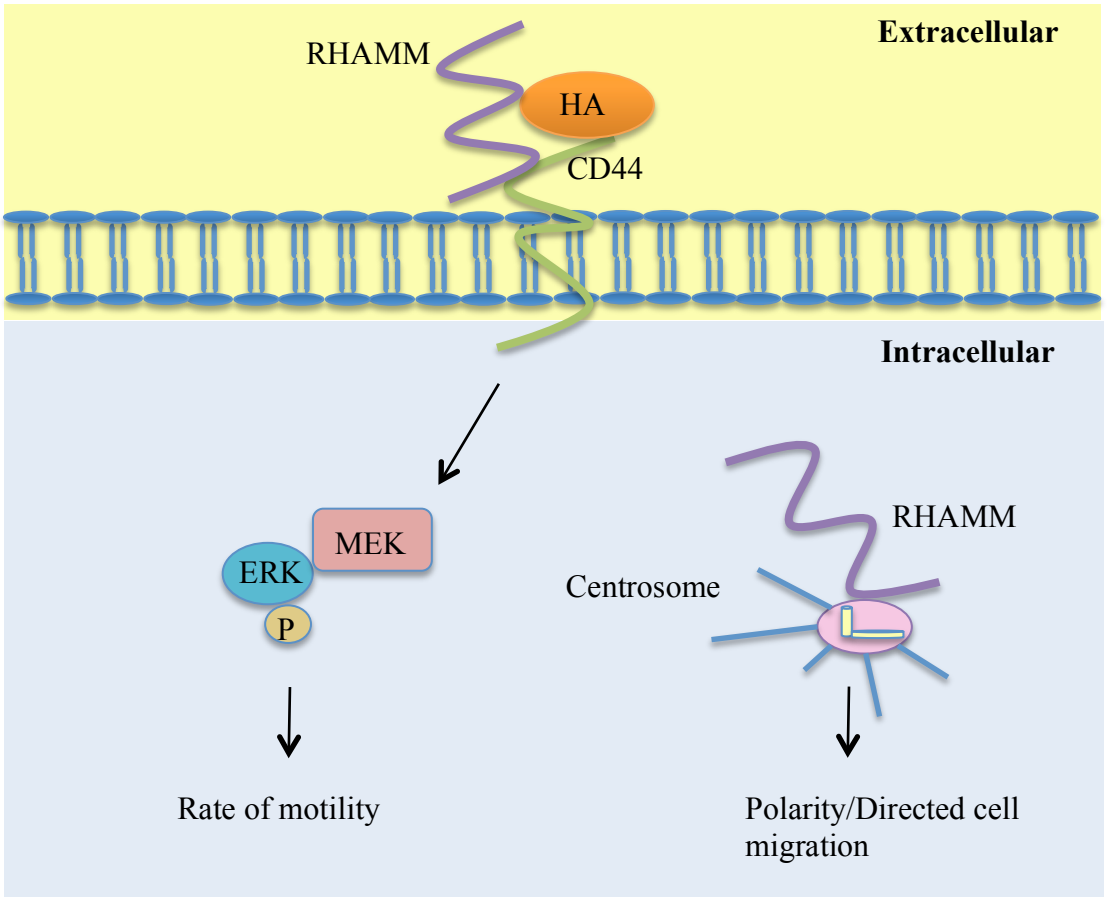

Figure 4.1: Proposed model for RHAMM-regulated cell migration

Cell surface RHAMM regulates ERK activation, which impacts rate of cell motility, while intracellular RHAMM forms interact with centrosome structures and affect polarity and directed cell migration

References

1. Jorgensen, P., and Tyers, M. (2004) How cells coordinate growth and division. *Curr.Biol.* **14,** R1014-27

2. Cotter, T.G. (2009) Apoptosis and cancer: the genesis of a research field. *Nat.Rev.Cancer.* **9,** 501-507

3. Manchado, E., Guillamot, M., and Malumbres, M. (2012) Killing cells by targeting mitosis. *Cell Death Differ.* **19,** 369-377

4. Vermeulen, K., Van Bockstaele, D.R., and Berneman, Z.N. (2003) The cell cycle: a review of regulation, deregulation and therapeutic targets in cancer. *Cell Prolif.* **36,** 131-149

5. Kramer, A., Neben, K., and Ho, A.D. (2002) Centrosome replication, genomic instability and cancer. *Leukemia.* **16,** 767-775

6. Azimzadeh, J., and Bornens, M. (2007) Structure and duplication of the centrosome. *J.Cell.Sci.* **120,** 2139-2142

7. Quintyne, N.J., and Schroer, T.A. (2002) Distinct cell cycle-dependent roles for dynactin and dynein at centrosomes. *J.Cell Biol.* **159,** 245-254

8. Firat-Karalar, E.N., and Stearns, T. (2014) The centriole duplication cycle. *Philos.Trans.R.Soc.Lond.B.Biol.Sci.* **369,** 20130460

9. Nigg, E.A., and Stearns, T. (2011) The centrosome cycle: Centriole biogenesis, duplication and inherent asymmetries. *Nat.Cell Biol.* **13,** 1154-1160

10. Schmidt, S., Essmann, F., Cirstea, I.C., Kuck, F., Thakur, H.C., Singh, M., Kletke, A., Janicke, R.U., Wiek, C., Hanenberg, H., Ahmadian, M.R., Schulze-Osthoff, K., Nurnberg, B., and Piekorz, R.P. (2010) The centrosome and mitotic spindle apparatus in cancer and senescence. *Cell.Cycle.* **9,** 4469-4473

11. Bird, A.W., and Hyman, A.A. (2008) Building a spindle of the correct length in human cells requires the interaction between TPX2 and Aurora A. *J.Cell Biol.* **182,** 289-300

12. Nousiainen, M., Sillje, H.H., Sauer, G., Nigg, E.A., and Korner, R. (2006) Phosphoproteome analysis of the human mitotic spindle. *Proc.Natl.Acad.Sci.U.S.A.* **103,** 5391-5396

13. O'Connell, C.B., and Khodjakov, A.L. (2007) Cooperative mechanisms of mitotic spindle formation. *J.Cell.Sci.* **120,** 1717-1722

14. Xia, F., Lee, C.W., and Altieri, D.C. (2008) Tumor cell dependence on Ran-GTP-directed mitosis. *Cancer Res.* **68,** 1826-1833

15. Carazo-Salas, R.E., Gruss, O.J., Mattaj, I.W., and Karsenti, E. (2001) Ran-GTP coordinates regulation of microtubule nucleation and dynamics during mitotic-spindle assembly. *Nat.Cell Biol.* **3,** 228-234

16. Schatz, C.A., Santarella, R., Hoenger, A., Karsenti, E., Mattaj, I.W., Gruss, O.J., and Carazo-Salas, R.E. (2003) Importin ?-regulated nucleation of microtubules by TPX2. *EMBO J.* **22,** 2060-2070

17. Fu, J., Bian, M., Jiang, Q., and Zhang, C. (2007) Roles of Aurora kinases in mitosis and tumorigenesis. *Mol.Cancer.Res.* **5,** 1-10

18. Xia, F., Lee, C.W., and Altieri, D.C. (2008) Tumor cell dependence on Ran-GTP-directed mitosis. *Cancer Res.* **68,** 1826-1833

19. Maxwell, C.A., Keats, J.J., Crainie, M., Sun, X., Yen, T., Shibuya, E., Hendzel, M., Chan, G., and Pilarski, L.M. (2003) RHAMM is a centrosomal protein that interacts with dynein and maintains spindle pole stability. *Mol.Biol.Cell.* **14,** 2262-2276

20. Tolg, C., Hamilton, S.R., Morningstar, L., Zhang, J., Zhang, S., Esguerra, K.V., Telmer, P.G., Luyt, L.G., Harrison, R., McCarthy, J.B., and Turley, E.A. (2010)

RHAMM promotes interphase microtubule instability and mitotic spindle integrity through MEK1/ERK1/2 activity. *J.Biol.Chem.* **285,** 26461-26474

21. Foley, E.A., and Kapoor, T.M. (2013) Microtubule attachment and spindle assembly checkpoint signalling at the kinetochore. *Nat.Rev.Mol.Cell Biol.* **14,** 25-37

22. Lara-Gonzalez, P., Westhorpe, F.G., and Taylor, S.S. (2012) The spindle assembly checkpoint. *Curr.Biol.* **22,** R966-80

23. Zhou, J., Yao, J., and Joshi, H.C. (2002) Attachment and tension in the spindle assembly checkpoint. *J.Cell.Sci.* **115,** 3547-3555

24. Bishop, J.M. (1991) Molecular themes in oncogenesis. *Cell.* **64,** 235-248

25. Croce, C.M. (2008) Oncogenes and cancer. *N.Engl.J.Med.* **358,** 502-511

26. Hanahan, D., and Weinberg, R.A. (2000) The hallmarks of cancer. *Cell.* **100,** 57-70

27. Giehl, K. (2005) Oncogenic Ras in tumour progression and metastasis. *Biol.Chem.* **386,** 193-205

28. Sherr, C.J. (2004) Principles of tumor suppression. *Cell.* **116,** 235-246

29. Sherr, C.J., and McCormick, F. (2002) The RB and p53 pathways in cancer. *Cancer.Cell.* **2,** 103-112

30. Burkhart, D.L., and Sage, J. (2008) Cellular mechanisms of tumour suppression by the retinoblastoma gene. *Nat.Rev.Cancer.* **8,** 671-682

31. Jiang, M., and Milner, J. (2003) Bcl-2 constitutively suppresses p53-dependent apoptosis in colorectal cancer cells. *Genes Dev.* **17,** 832-837

32. Valastyan, S., and Weinberg, R.A. (2011) Tumor metastasis: molecular insights and evolving paradigms. *Cell.* **147,** 275-292

33. Watanabe, T., Noritake, J., and Kaibuchi, K. (2005) Regulation of microtubules in cell migration. *Trends Cell Biol.* **15,** 76-83

34. Raftopoulou, M., and Hall, A. (2004) Cell migration: Rho GTPases lead the way. *Dev.Biol.* **265,** 23-32

35. Ridley, A.J., Schwartz, M.A., Burridge, K., Firtel, R.A., Ginsberg, M.H., Borisy, G., Parsons, J.T., and Horwitz, A.R. (2003) Cell migration: integrating signals from front to back. *Science.* **302,** 1704-1709

36. Horwitz, R., and Webb, D. (2003) Cell migration. *Curr.Biol.* **13,** R756-9

37. Hanahan, D., and Weinberg, R.A. (2011) Hallmarks of cancer: the next generation. *Cell.* **144,** 646-674

38. Petrie, R.J., Doyle, A.D., and Yamada, K.M. (2009) Random versus directionally persistent cell migration. *Nat.Rev.Mol.Cell Biol.* **10,** 538-549

39. Iden, S., and Collard, J.G. (2008) Crosstalk between small GTPases and polarity proteins in cell polarization. *Nat.Rev.Mol.Cell Biol.* **9,** 846-859

40. Ganguly, A., Yang, H., Sharma, R., Patel, K.D., and Cabral, F. (2012) The role of microtubules and their dynamics in cell migration. *J.Biol.Chem.* **287,** 43359-43369

41. Harrison, R.E., and Turley, E.A. (2001) Active erk regulates microtubule stability in H-ras-transformed cells. *Neoplasia.* **3,** 385-394

42. Wakida, N.M., Botvinick, E.L., Lin, J., and Berns, M.W. (2010) An intact centrosome is required for the maintenance of polarization during directional cell migration. *PLoS One.* **5,** e15462

43. Yamaguchi, H., Wyckoff, J., and Condeelis, J. (2005) Cell migration in tumors. *Curr.Opin.Cell Biol.* **17,** 559-564

44. Wang, W., Goswami, S., Sahai, E., Wyckoff, J.B., Segall, J.E., and Condeelis, J.S. (2005) Tumor cells caught in the act of invading: their strategy for enhanced cell motility. *Trends Cell Biol.* **15,** 138-145

45. Frantz, C., Stewart, K.M., and Weaver, V.M. (2010) The extracellular matrix at a glance. *J.Cell.Sci.* **123,** 4195-4200

46. Heino, J., and Kapyla, J. (2009) Cellular receptors of extracellular matrix molecules. *Curr.Pharm.Des.* **15,** 1309-1317

47. Kim, S.H., Turnbull, J., and Guimond, S. (2011) Extracellular matrix and cell signalling: the dynamic cooperation of integrin, proteoglycan and growth factor receptor. *J.Endocrinol.* **209,** 139-151

48. Nikitovic, D., Kouvidi, K., Karamanos, N.K., and Tzanakakis, G.N. (2013) The roles of hyaluronan/RHAMM/CD44 and their respective interactions along the insidious pathways of fibrosarcoma progression. *Biomed.Res.Int.* **2013,** 929531

49. Lu, P., Weaver, V.M., and Werb, Z. (2012) The extracellular matrix: a dynamic niche in cancer progression. *J.Cell Biol.* **196,** 395-406

50. Cirri, P., and Chiarugi, P. (2012) Cancer-associated-fibroblasts and tumour cells: a diabolic liaison driving cancer progression. *Cancer Metastasis Rev.* **31,** 195-208

51. Bhowmick, N.A., Neilson, E.G., and Moses, H.L. (2004) Stromal fibroblasts in cancer initiation and progression. *Nature.* **432,** 332-337

52. Heldin, P., Basu, K., Olofsson, B., Porsch, H., Kozlova, I., and Kahata, K. (2013) Deregulation of hyaluronan synthesis, degradation and binding promotes breast cancer. *J.Biochem.* **154,** 395-408

53. Fraser, J.R., Laurent, T.C., and Laurent, U.B. (1997) Hyaluronan: its nature, distribution, functions and turnover. *J.Intern.Med.* **242,** 27-33

54. Laurent, T.C., and Fraser, J.R. (1992) Hyaluronan. *FASEB J.* **6,** 2397-2404

55. Jacobson, A., Rahmanian, M., Rubin, K., and Heldin, P. (2002) Expression of hyaluronan synthase 2 or hyaluronidase 1 differentially affect the growth rate of transplantable colon carcinoma cell tumors. *Int.J.Cancer.* **102,** 212-219

56. Li, Y., and Heldin, P. (2001) Hyaluronan production increases the malignant properties of mesothelioma cells. *Br.J.Cancer.* **85,** 600-607

57. Udabage, L., Brownlee, G.R., Nilsson, S.K., and Brown, T.J. (2005) The over-expression of HAS2, Hyal-2 and CD44 is implicated in the invasiveness of breast cancer. *Exp.Cell Res.* **310,** 205-217

58. Bertrand, P., Girard, N., Duval, C., d'Anjou, J., Chauzy, C., Menard, J.F., and Delpech, B. (1997) Increased hyaluronidase levels in breast tumor metastases. *Int.J.Cancer.* **73,** 327-331

59. Tan, J.X., Wang, X.Y., Li, H.Y., Su, X.L., Wang, L., Ran, L., Zheng, K., and Ren, G.S. (2011) HYAL1 overexpression is correlated with the malignant behavior of human breast cancer. *Int.J.Cancer.* **128,** 1303-1315

60. McKee, C.M., Penno, M.B., Cowman, M., Burdick, M.D., Strieter, R.M., Bao, C., and Noble, P.W. (1996) Hyaluronan (HA) fragments induce chemokine gene expression in alveolar macrophages. The role of HA size and CD44. *J.Clin.Invest.* **98,** 2403-2413

61. McKee, C.M., Lowenstein, C.J., Horton, M.R., Wu, J., Bao, C., Chin, B.Y., Choi, A.M., and Noble, P.W. (1997) Hyaluronan fragments induce nitric-oxide synthase in murine macrophages through a nuclear factor kappaB-dependent mechanism. *J.Biol.Chem.* **272,** 8013-8018

62. West, D.C., Hampson, I.N., Arnold, F., and Kumar, S. (1985) Angiogenesis induced by degradation products of hyaluronic acid. *Science.* **228,** 1324-1326

63. Day, A.J., and Prestwich, G.D. (2002) Hyaluronan-binding proteins: tying up the giant. *J.Biol.Chem.* **277,** 4585-4588

64. Tolg, C., Hamilton, S.R., Nakrieko, K.A., Kooshesh, F., Walton, P., McCarthy, J.B., Bissell, M.J., and Turley, E.A. (2006) Rhamm-/- fibroblasts are defective in CD44-mediated ERK1,2 motogenic signaling, leading to defective skin wound repair. *J.Cell Biol.* **175,** 1017-1028

65. Turley, E.A., Noble, P.W., and Bourguignon, L.Y. (2002) Signaling properties of hyaluronan receptors. *J.Biol.Chem.* **277,** 4589-4592

66. Turley, E.A. (1982) Purification of a hyaluronate-binding protein fraction that modifies cell social behavior. *Biochem.Biophys.Res.Commun.* **108,** 1016-1024

67. Turley, E.A., Noble, P.W., and Bourguignon, L.Y. (2002) Signaling properties of hyaluronan receptors. *J.Biol.Chem.* **277,** 4589-4592

68. Hardwick, C., Hoare, K., Owens, R., Hohn, H.P., Hook, M., Moore, D., Cripps, V., Austen, L., Nance, D.M., and Turley, E.A. (1992) Molecular cloning of a novel hyaluronan receptor that mediates tumor cell motility. *J.Cell Biol.* **117,** 1343-1350

69. Assmann, V., Jenkinson, D., Marshall, J.F., and Hart, I.R. (1999) The intracellular hyaluronan receptor RHAMM/IHABP interacts with microtubules and actin filaments. *J.Cell.Sci.* **112 (Pt 22),** 3943-3954

70. Yang, B., Yang, B.L., Savani, R.C., and Turley, E.A. (1994) Identification of a common hyaluronan binding motif in the hyaluronan binding proteins RHAMM, CD44 and link protein. *EMBO J.* **13,** 286-296

71. Yang, B., Zhang, L., and Turley, E.A. (1993) Identification of two hyaluronan-binding domains in the hyaluronan receptor RHAMM. *J.Biol.Chem.* **268,** 8617-8623

72. Lynn, B.D., Li, X., Cattini, P.A., Turley, E.A., and Nagy, J.I. (2001) Identification of sequence, protein isoforms, and distribution of the hyaluronan-binding protein RHAMM in adult and developing rat brain. *J.Comp.Neurol.* **439,** 315-330

73. Joukov, V., Groen, A.C., Prokhorova, T., Gerson, R., White, E., Rodriguez, A., Walter, J.C., and Livingston, D.M. (2006) The BRCA1/BARD1 heterodimer modulates ran-dependent mitotic spindle assembly. *Cell.* **127,** 539-552

74. Groen, A.C., Cameron, L.A., Coughlin, M., Miyamoto, D.T., Mitchison, T.J., and Ohi, R. (2004) XRHAMM functions in ran-dependent microtubule nucleation and pole formation during anastral spindle assembly. *Curr.Biol.* **14,** 1801-1811

75. Wang, C., Entwistle, J., Hou, G., Li, Q., and Turley, E.A. (1996) The characterization of a human RHAMM cDNA: conservation of the hyaluronan-binding domains. *Gene.* **174,** 299-306

76. Tolg, C., Poon, R., Fodde, R., Turley, E.A., and Alman, B.A. (2003) Genetic deletion of receptor for hyaluronan-mediated motility (Rhamm) attenuates the formation of aggressive fibromatosis (desmoid tumor). *Oncogene.* **22,** 6873-6882

77. Nedvetzki, S., Gonen, E., Assayag, N., Reich, R., Williams, R.O., Thurmond, R.L., Huang, J.F., Neudecker, B.A., Wang, F.S., Turley, E.A., and Naor, D. (2004) RHAMM, a receptor for hyaluronan-mediated motility, compensates for CD44 in inflamed CD44-knockout mice: a different interpretation of redundancy. *Proc.Natl.Acad.Sci.U.S.A.* **101,** 18081-18086

78. Pujana, M.A., Han, J.D., Starita, L.M., Stevens, K.N., Tewari, M., Ahn, J.S., Rennert, G., Moreno, V., Kirchhoff, T., Gold, B., Assmann, V., Elshamy, W.M., Rual, J.F., Levine, D., Rozek, L.S., Gelman, R.S., Gunsalus, K.C., Greenberg, R.A., Sobhian, B., Bertin, N., Venkatesan, K., Ayivi-Guedehoussou, N., Sole, X., Hernandez, P., Lazaro, C., Nathanson, K.L., Weber, B.L., Cusick, M.E., Hill, D.E., Offit, K., Livingston, D.M., Gruber, S.B., Parvin, J.D., and Vidal, M. (2007) Network modeling links breast cancer susceptibility and centrosome dysfunction. *Nat.Genet.* **39,** 1338-1349

79. Yang, C.W., Su, J.Y., Tsou, A.P., Chau, G.Y., Liu, H.L., Chen, C.H., Chien, C.Y., and Chou, C.K. (2005) Integrative genomics based identification of potential human hepatocarcinogenesis-associated cell cycle regulators: RHAMM as an example. *Biochem.Biophys.Res.Commun.* **330,** 489-497

80. Assmann, V., Marshall, J.F., Fieber, C., Hofmann, M., and Hart, I.R. (1998) The human hyaluronan receptor RHAMM is expressed as an intracellular protein in breast cancer cells. *J.Cell.Sci.* **111 (Pt 12),** 1685-1694

81. Maxwell, C.A., Keats, J.J., Belch, A.R., Pilarski, L.M., and Reiman, T. (2005) Receptor for hyaluronan-mediated motility correlates with centrosome abnormalities in multiple myeloma and maintains mitotic integrity. *Cancer Res.* **65,** 850-860

82. Pilarski, L.M., Miszta, H., and Turley, E.A. (1993) Regulated expression of a receptor for hyaluronan-mediated motility on human thymocytes and T cells. *J.Immunol.* **150,** 4292-4302

83. Savani, R.C., Cao, G., Pooler, P.M., Zaman, A., Zhou, Z., and DeLisser, H.M. (2001) Differential involvement of the hyaluronan (HA) receptors CD44 and receptor for HA-mediated motility in endothelial cell function and angiogenesis. *J.Biol.Chem.* **276,** 36770-36778

84. Silverman-Gavrila, R., Silverman-Gavrila, L., and Bendeck, M.P. (2013) Cell division fidelity is altered during the vascular response to injury: its novel role in atherosclerosis progression. *Am.J.Pathol.* **182,** 628-639

85. Maxwell, C.A., McCarthy, J., and Turley, E. (2008) Cell-surface and mitotic-spindle RHAMM: moonlighting or dual oncogenic functions?. *J.Cell.Sci.* **121,** 925-932

86. Adamia, S., Maxwell, C.A., and Pilarski, L.M. (2005) Hyaluronan and hyaluronan synthases: potential therapeutic targets in cancer. *Curr.Drug Targets Cardiovasc.Haematol.Disord.* **5,** 3-14

87. Savani, R.C., Wang, C., Yang, B., Zhang, S., Kinsella, M.G., Wight, T.N., Stern, R., Nance, D.M., and Turley, E.A. (1995) Migration of bovine aortic smooth muscle cells after wounding injury. The role of hyaluronan and RHAMM. *J.Clin.Invest.* **95,** 1158-1168

88. Zhang, S., Chang, M.C., Zylka, D., Turley, S., Harrison, R., and Turley, E.A. (1998) The hyaluronan receptor RHAMM regulates extracellular-regulated kinase. *J.Biol.Chem.* **273,** 11342-11348

89. Park, D., Kim, Y., Kim, H., Kim, K., Lee, Y.S., Choe, J., Hahn, J.H., Lee, H., Jeon, J., Choi, C., Kim, Y.M., and Jeoung, D. (2012) Hyaluronic acid promotes angiogenesis by inducing RHAMM-TGFbeta receptor interaction via CD44-PKCdelta. *Mol.Cells.* **33,** 563-574

90. Manzanares, D., Monzon, M.E., Savani, R.C., and Salathe, M. (2007) Apical oxidative hyaluronan degradation stimulates airway ciliary beating via RHAMM and RON. *Am.J.Respir.Cell Mol.Biol.* **37,** 160-168

91. Mohapatra, S., Yang, X., Wright, J.A., Turley, E.A., and Greenberg, A.H. (1996) Soluble hyaluronan receptor RHAMM induces mitotic arrest by suppressing Cdc2 and cyclin B1 expression. *J.Exp.Med.* **183,** 1663-1668

92. Maxwell, C.A., Rasmussen, E., Zhan, F., Keats, J.J., Adamia, S., Strachan, E., Crainie, M., Walker, R., Belch, A.R., Pilarski, L.M., Barlogie, B., Shaughnessy, J.,Jr, and Reiman, T. (2004) RHAMM expression and isoform balance predict aggressive disease and poor survival in multiple myeloma. *Blood.* **104,** 1151-1158

93. Dunsch, A.K., Hammond, D., Lloyd, J., Schermelleh, L., Gruneberg, U., and Barr, F.A. (2012) Dynein light chain 1 and a spindle-associated adaptor promote dynein asymmetry and spindle orientation. *J.Cell Biol.* **198,** 1039-1054

94. Hamilton, S.R., Fard, S.F., Paiwand, F.F., Tolg, C., Veiseh, M., Wang, C., McCarthy, J.B., Bissell, M.J., Koropatnick, J., and Turley, E.A. (2007) The hyaluronan receptors CD44 and Rhamm (CD168) form complexes with ERK1,2 that sustain high basal motility in breast cancer cells. *J.Biol.Chem.* **282,** 16667-16680

95. Hall, C.L., Yang, B., Yang, X., Zhang, S., Turley, M., Samuel, S., Lange, L.A., Wang, C., Curpen, G.D., Savani, R.C., Greenberg, A.H., and Turley, E.A. (1995) Overexpression of the hyaluronan receptor RHAMM is transforming and is also required for H-ras transformation. *Cell.* **82,** 19-26

96. Liska, A.J., Popov, A.V., Sunyaev, S., Coughlin, P., Habermann, B., Shevchenko, A., Bork, P., Karsenti, E., and Shevchenko, A. (2004) Homology-based functional proteomics by mass spectrometry: application to the Xenopus microtubule-associated proteome. *Proteomics.* **4,** 2707-2721

97. Fang, Z., Takizawa, N., Wilson, K.A., Smith, T.C., Delprato, A., Davidson, M.W., Lambright, D.G., and Luna, E.J. (2010) The membrane-associated protein, supervillin,

accelerates F-actin-dependent rapid integrin recycling and cell motility. *Traffic.* **11,** 782-799

98. Smith, T.C., Fang, Z., and Luna, E.J. (2010) Novel interactors and a role for supervillin in early cytokinesis. *Cytoskeleton (Hoboken).* **67,** 346-364

99. Smith, T.C., Fridy, P.C., Li, Y., Basil, S., Arjun, S., Friesen, R.M., Leszyk, J., Chait, B.T., Rout, M.P., and Luna, E.J. (2013) Supervillin binding to myosin II and synergism with anillin are required for cytokinesis. *Mol.Biol.Cell.* **24,** 3603-3619

100. Chen, H., Mohan, P., Jiang, J., Nemirovsky, O., He, D., Fleisch, M.C., Niederacher, D., Pilarski, L.M., Lim, C.J., and Maxwell, C.A. (2014) Spatial regulation of Aurora A activity during mitotic spindle assembly requires RHAMM to correctly localize TPX2. *Cell.Cycle.* **13,**

101. Evanko, S.P., Parks, W.T., and Wight, T.N. (2004) Intracellular hyaluronan in arterial smooth muscle cells: association with microtubules, RHAMM, and the mitotic spindle. *J.Histochem.Cytochem.* **52,** 1525-1535

102. Evanko, S.P., and Wight, T.N. (1999) Intracellular localization of hyaluronan in proliferating cells. *J.Histochem.Cytochem.* **47,** 1331-1342

103. Lokeshwar, V.B., Lopez, L.E., Munoz, D., Chi, A., Shirodkar, S.P., Lokeshwar, S.D., Escudero, D.O., Dhir, N., and Altman, N. (2010) Antitumor activity of hyaluronic acid synthesis inhibitor 4-methylumbelliferone in prostate cancer cells. *Cancer Res.* **70,** 2613-2623

104. Verlhac, M.H., de Pennart, H., Maro, B., Cobb, M.H., and Clarke, H.J. (1993) MAP kinase becomes stably activated at metaphase and is associated with microtubule-organizing centers during meiotic maturation of mouse oocytes. *Dev.Biol.* **158,** 330-340

105. Reszka, A.A., Seger, R., Diltz, C.D., Krebs, E.G., and Fischer, E.H. (1995) Association of mitogen-activated protein kinase with the microtubule cytoskeleton. *Proc.Natl.Acad.Sci.U.S.A.* **92,** 8881-8885

106. Roskoski, R.,Jr (2012) ERK1/2 MAP kinases: structure, function, and regulation. *Pharmacol.Res.* **66,** 105-143

107. Telmer, P.G., Tolg, C., McCarthy, J.B., and Turley, E.A. (2011) How does a protein with dual mitotic spindle and extracellular matrix receptor functions affect tumor susceptibility and progression?. *Commun.Integr.Biol.* **4,** 182-185

108. Wittmann, T., Boleti, H., Antony, C., Karsenti, E., and Vernos, I. (1998) Localization of the kinesin-like protein Xklp2 to spindle poles requires a leucine zipper, a microtubule-associated protein, and dynein. *J.Cell Biol.* **143,** 673-685

109. Hatano, H., Shigeishi, H., Kudo, Y., Higashikawa, K., Tobiume, K., Takata, T., and Kamata, N. (2011) RHAMM/ERK interaction induces proliferative activities of cementifying fibroma cells through a mechanism based on the CD44-EGFR. *Lab.Invest.* **91,** 379-391

110. Gruss, O.J., Wittmann, M., Yokoyama, H., Pepperkok, R., Kufer, T., Sillje, H., Karsenti, E., Mattaj, I.W., and Vernos, I. (2002) Chromosome-induced microtubule assembly mediated by TPX2 is required for spindle formation in HeLa cells. *Nat.Cell Biol.* **4,** 871-879

111. Sohr, S., and Engeland, K. (2008) RHAMM is differentially expressed in the cell cycle and downregulated by the tumor suppressor p53. *Cell.Cycle.* **7,** 3448-3460

112. Teixeira, L.K., and Reed, S.I. (2013) Ubiquitin ligases and cell cycle control. *Annu.Rev.Biochem.* **82,** 387-414

113. Song, L., and Rape, M. (2010) Regulated degradation of spindle assembly factors by the anaphase-promoting complex. *Mol.Cell.* **38,** 369-382

114. Hatano, H., Shigeishi, H., Kudo, Y., Higashikawa, K., Tobiume, K., Takata, T., and Kamata, N. (2012) Overexpression of receptor for hyaluronan-mediated motility (RHAMM) in MC3T3-E1 cells induces proliferation and differentiation through phosphorylation of ERK1/2. *J.Bone Miner.Metab.* **30,** 293-303

115. Niedworok, C., Kretschmer, I., Rock, K., Vom Dorp, F., Szarvas, T., Hess, J., Freudenberger, T., Melchior-Becker, A., Rubben, H., and Fischer, J.W. (2013) The impact of the receptor of hyaluronan-mediated motility (RHAMM) on human urothelial transitional cell cancer of the bladder. *PLoS One.* **8,** e75681

116. Lompardia, S.L., Papademetrio, D.L., Mascaro, M., Alvarez, E.M., and Hajos, S.E. (2013) Human leukemic cell lines synthesize hyaluronan to avoid senescence and resist chemotherapy. *Glycobiology.* **23,** 1463-1476

117. Du, Y.C., Chou, C.K., Klimstra, D.S., and Varmus, H. (2011) Receptor for hyaluronan-mediated motility isoform B promotes liver metastasis in a mouse model of multistep tumorigenesis and a tail vein assay for metastasis. *Proc.Natl.Acad.Sci.U.S.A.* **108,** 16753-16758

118. Wang, C., Thor, A.D., Moore, D.H.,2nd, Zhao, Y., Kerschmann, R., Stern, R., Watson, P.H., and Turley, E.A. (1998) The overexpression of RHAMM, a hyaluronan-binding protein that regulates ras signaling, correlates with overexpression of mitogen-activated protein kinase and is a significant parameter in breast cancer progression. *Clin.Cancer Res.* **4,** 567-576

119. Wang, Z., Wu, Y., Wang, H., Zhang, Y., Mei, L., Fang, X., Zhang, X., Zhang, F., Chen, H., Liu, Y., Jiang, Y., Sun, S., Zheng, Y., Li, N., and Huang, L. (2014) Interplay of mevalonate and Hippo pathways regulates RHAMM transcription via YAP to modulate breast cancer cell motility. *Proc.Natl.Acad.Sci.U.S.A.* **111,** E89-98

120. Mohan, P., Castellsague, J., Jiang, J., Allen, K., Chen, H., Nemirovsky, O., Spyra, M., Hu, K., Kluwe, L., Pujana, M.A., Villanueva, A., Mautner, V.F., Keats, J.J., Dunn, S.E., Lazaro, C., and Maxwell, C.A. (2013) Genomic imbalance of HMMR/RHAMM regulates the sensitivity and response of malignant peripheral nerve sheath tumour cells to aurora kinase inhibition. *Oncotarget.* **4,** 80-93

121. Mendoza, M.C., Emrah, E., Zhang, W., Ballif, B.A., Elliott, H.L., Danuser, G., and Blenis, J. (2011) ERK-MAPK Drives Lamellipodia Protrusion by Activating the WAVE2 Regulatory Complex. *Mol.Cell.* **41,** 661-671

122. Collis, L., Hall, C., Lange, L., Ziebell, M., Prestwich, R., and Turley, E.A. (1998) Rapid hyaluronan uptake is associated with enhanced motility: implications for an intracellular mode of action. *FEBS Lett.* **440,** 444-449

123. Goueffic, Y., Guilluy, C., Guerin, P., Patra, P., Pacaud, P., and Loirand, G. (2006) Hyaluronan induces vascular smooth muscle cell migration through RHAMM-mediated PI3K-dependent Rac activation. *Cardiovasc.Res.* **72,** 339-348

124. Silverman-Gavrila, R., Silverman-Gavrila, L., Hou, G., Zhang, M., Charlton, M., and Bendeck, M.P. (2011) Rear polarization of the microtubule-organizing center in neointimal smooth muscle cells depends on PKCalpha, ARPC5, and RHAMM. *Am.J.Pathol.* **178,** 895-910

125. Casalegno-Garduno, R., Meier, C., Schmitt, A., Spitschak, A., Hilgendorf, I., Rohde, S., Hirt, C., Freund, M., Putzer, B.M., and Schmitt, M. (2012) Immune responses to RHAMM in patients with acute myeloid leukemia after chemotherapy and allogeneic stem cell transplantation. *Clin.Dev.Immunol.* **2012,** 146463

126. Kalmyrzaev, B., Pharoah, P.D., Easton, D.F., Ponder, B.A., Dunning, A.M., and SEARCH Team (2008) Hyaluronan-mediated motility receptor gene single nucleotide polymorphisms and risk of breast cancer. *Cancer Epidemiol.Biomarkers Prev.* **17,** 3618-3620

127. Gust, K.M., Hofer, M.D., Perner, S.R., Kim, R., Chinnaiyan, A.M., Varambally, S., Moller, P., Rinnab, L., Rubin, M.A., Greiner, J., Schmitt, M., Kuefer, R., and Ringhoffer, M. (2009) RHAMM (CD168) is overexpressed at the protein level and may constitute an immunogenic antigen in advanced prostate cancer disease. *Neoplasia.* **11,** 956-963

128. Duval, A., Rolland, S., Compoint, A., Tubacher, E., Iacopetta, B., Thomas, G., and Hamelin, R. (2001) Evolution of instability at coding and non-coding repeat sequences in human MSI-H colorectal cancers. *Hum.Mol.Genet.* **10,** 513-518

129. Pu, W.T., and Struhl, K. (1991) The leucine zipper symmetrically positions the adjacent basic regions for specific DNA binding. *Proc.Natl.Acad.Sci.U.S.A.* **88,** 6901-6905

130. Aitken, K., and Bagl, D.J. (2001) Stretch-induced bladder smooth muscle cell (SMC) proliferation is mediated by RHAMM-dependent extracellular-regulated kinase (erk) signaling. *Urology.* **57,** 109

131. Lompardia, S.L., Papademetrio, D.L., Mascaro, M., Alvarez, E.M., and Hajos, S.E. (2013) Human leukemic cell lines synthesize hyaluronan to avoid senescence and resist chemotherapy. *Glycobiology.* **23,** 1463-1476

132. Heinrich, S., Geissen, E.M., Kamenz, J., Trautmann, S., Widmer, C., Drewe, P., Knop, M., Radde, N., Hasenauer, J., and Hauf, S. (2013) Determinants of robustness in spindle assembly checkpoint signalling. *Nat.Cell Biol.* **15,** 1328-1339

133. Wang, Z., Wu, Y., Wang, H., Zhang, Y., Mei, L., Fang, X., Zhang, X., Zhang, F., Chen, H., Liu, Y., Jiang, Y., Sun, S., Zheng, Y., Li, N., and Huang, L. (2014) Interplay of mevalonate and Hippo pathways regulates RHAMM transcription via YAP to modulate breast cancer cell motility. *Proc.Natl.Acad.Sci.U.S.A.* **111,** E89-98

134. Kim, S., Kim, S., and Rhee, K. (2011) NEK7 is essential for centriole duplication and centrosomal accumulation of pericentriolar material proteins in interphase cells. *J.Cell.Sci.* **124,** 3760-3770

135. Kushner, E.J., Ferro, L.S., Liu, J.Y., Durrant, J.R., Rogers, S.L., Dudley, A.C., and Bautch, V.L. (2014) Excess centrosomes disrupt endothelial cell migration via centrosome scattering. *J.Cell Biol.* **206,** 257-272

136. Ozlu, N., Srayko, M., Kinoshita, K., Habermann, B., O'toole, E.T., Muller-Reichert, T., Schmalz, N., Desai, A., and Hyman, A.A. (2005) An essential function of the C. elegans ortholog of TPX2 is to localize activated aurora A kinase to mitotic spindles. *Dev.Cell.* **9,** 237-248

137. Dumont, S., and Mitchison, T.J. (2009) Compression regulates mitotic spindle length by a mechanochemical switch at the poles. *Curr.Biol.* **19,** 1086-1095

138. Wei, P., Zhang, N., Xu, Y., Li, X., Shi, D., Wang, Y., Li, D., and Cai, S. (2013) TPX2 is a novel prognostic marker for the growth and metastasis of colon cancer. *J.Transl.Med.* **11,** 313-5876-11-313

Appendices

A) Experiment 1: Xenograft tumor formation summary

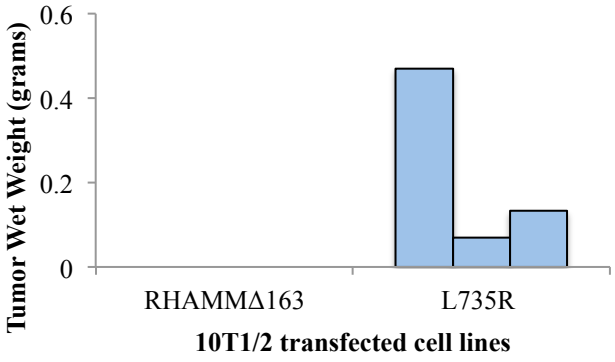

B) Experiment 2: Xenograft tumor formation summary

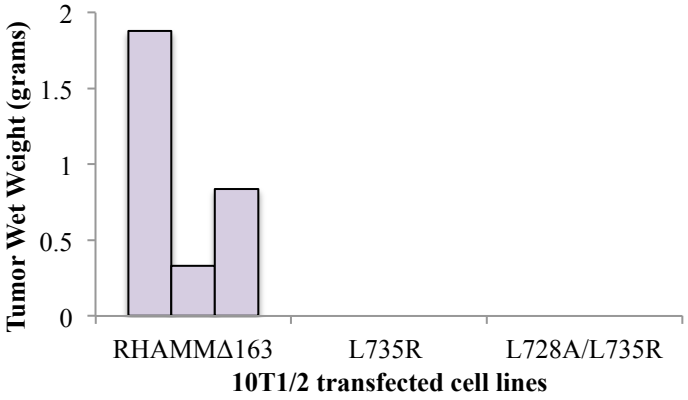

C) Experiment 3: Xenograft tumor formation summary

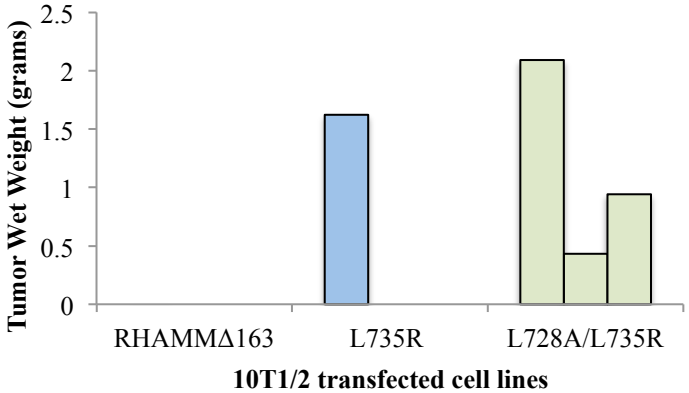

Appendix A Wet weights of wildtype and mutant 10T1/2-RHAMM$^{\Delta 163}$ xenograft tumors

10T1/2 RHAMM$^{\Delta 163}$ expressing, wildtype or mutant, fibroblasts were subcutaneously injected in the flank of NSG immune compromised mice and tumor growth was monitored over 6 weeks. Mice that developed tumors were sacrificed and tumor wet weights were measured. Three separate experiments were carried out (A), B), and C)) with n=3 mice per cell line injected per experiment. Each bar under a given cell line represents the wet weight of a single tumor formed from an individual mouse from each experiment. Lack of bars or less than 3 bars under a given cell line identify that tumors did not form or that tumors did not form in all experimental mice, respectively. The differences in tumor weights between cell lines could not be compared as tumor-forming capabilities varied between experiments. Studies in our lab are currently underway to investigate the discrepancies in this data.